Ca' Foscari
University
of Venice

Master's Degree

in Chemistry and Sustainable Technologies
(LM-54)

Final Thesis

Fishery waste valorization: chitin pulping using ionic liquids

Supervisor
Ch. Prof. Alvise Perosa

Assistant supervisor
Ch. Prof. Maurizio Selva

Graduand
Ilaria Bertuol
Matriculation Number
858684

Academic Year
2020 / 2021

ABSTRACT

The aim of the research described in this thesis was the valorization of fishery waste biomass to obtain chitin with a sustainable and green approach using ionic liquids (ILs). In particular, attention was focused on the development of an extraction protocol for chitin from Spider Crab (*Maja squinado)* carapace, with a "waste to wealth" idea to obtain high added-value products. Chitin, in fact, finds various applications in different fields due to its intrinsic biocompatibility and biodegradability, ecological safety, low toxicity and biological activity such as antimicrobial and low immunogenicity. The key step of this work was the improvement of a one-step extraction procedure using ILs as both extracting agents and solvents, as opposed to the traditional chemical extraction which involves two steps using strong and hazardous acids and bases.

The one-pot pulping-based method was investigated, using simple, readily-available ILs such as hydroxyl-ammonium acetate, ammonium acetate and ammonium formate. Each extraction was performed in two ways: by using the neat IL as solid salt or by synthesizing it *in-situ* as an aqueous solution. The study of different reaction temperatures and the influence of different mesh sizes was performed to optimize the extraction conditions. The pulped-chitin was fully characterized by FT-IR and NMR spectroscopy, XRD, ICP-OES to define the acetylation degree, and purity of the products. The so obtain pulped chitin was further deacetylated to chitosan, and MW and polydispersity of were determined by GPC analysis.

INDEX

1 INTRODUCTION

1.1 The oceans: an essential source

Covering 70% of our planet, oceans are the source of half of the oxygen and are responsible for 17% of animal protein production. In addition, they are an essential resource for global sustenance and economy, providing reliable sources of food, tourism, and jobs. Therefore, it is mandatory to preserve the marine aquatic ecosystem that, especially in recent years, is threatened by incorrect management and resources exploitation, pollution, and climate change. In addition to these fundamental aspects, which are threatening the abundance and natural biodiversity of marine life, there is also the major issue of disposal of fish waste. For example, returning it to the marine environment can reduce the oxygen level in seawater and introduce diseases and foreign species in the aquatic ecosystem.[1]

From 1990 to 2018, there was a 122% rise in total fish products consumption, propelling a 14% and 527% increase in fish capture and aquaculture, respectively (figure 1.1). It is estimated that in 2018 global fish production has reached about 179 million tons, with a total first sale of 82 million tons coming from aquaculture. Of the overall total, 156 million tonnes were used for human consumption and the remaining quantity was destined for non-food uses, mainly to produce fishmeal and fish oil.

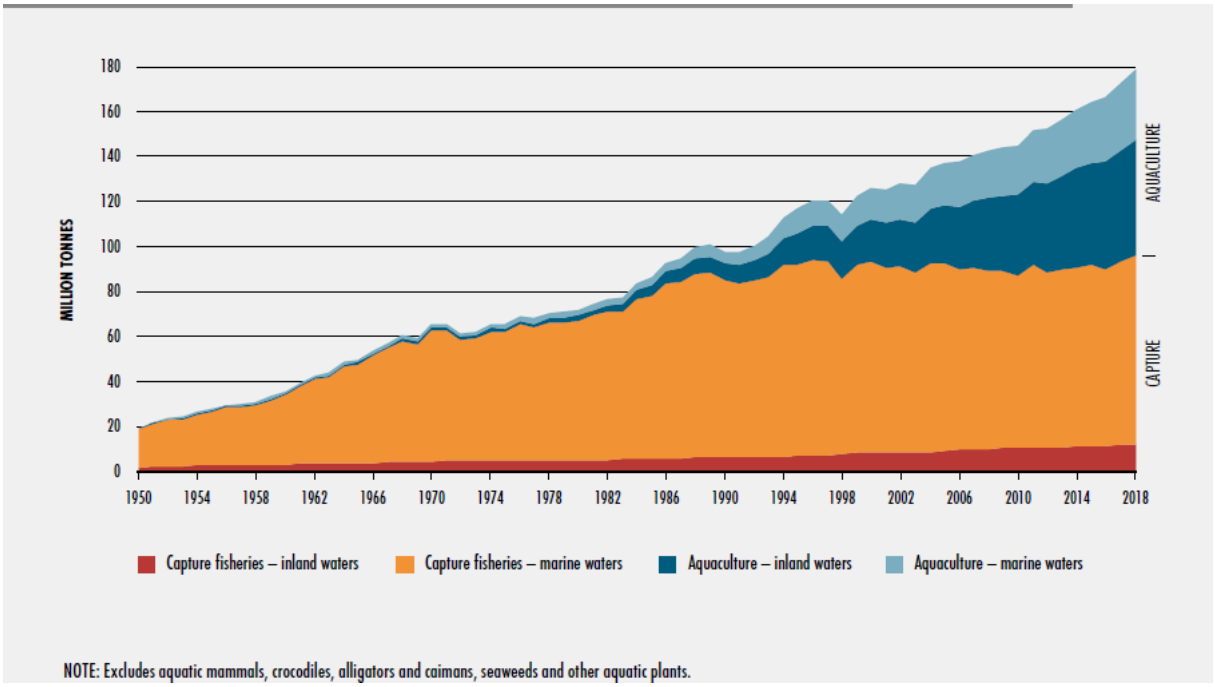

Figure 1.1: World capture fisheries and aquaculture production[2].

China is still the major fish producer, accounting for 35% of global fish production in 2018. Other major fish producers in 2018 were Asia (excluding China, 34%), followed by the Americas (14%), Europe (10%), Africa (7%) and Oceania (1%). Except for Europe and the Americas, the total fish production has seen an extensive increasing trend during the last decades, as can be seen in figure 1.2 [2].

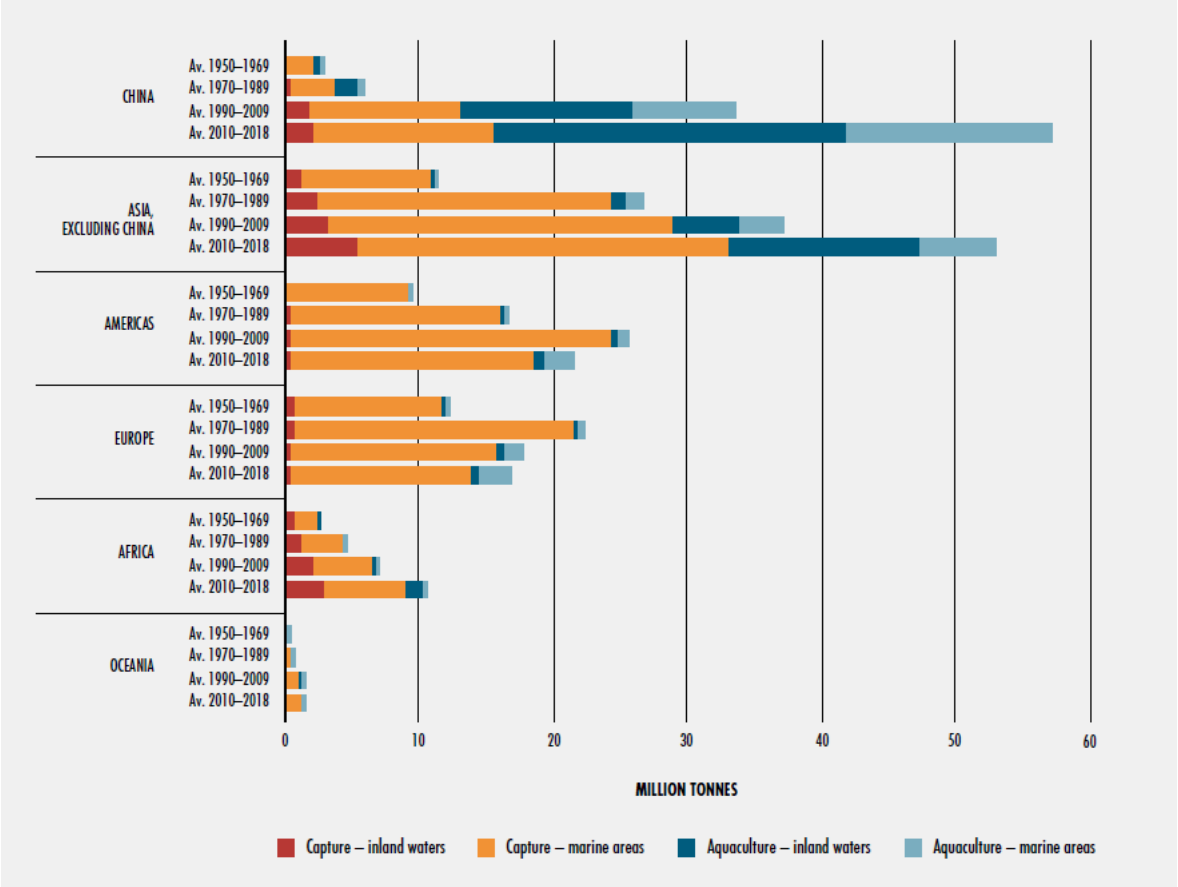

Figure 1.2:Regional contribution to world fisheries and aquaculture production[2].

As a percentage of total landed weight, only 40% of prawns, 39% of crustaceans, 14% of mussels, 32% of crabs, 35% of brown shrimp and 35–45% of catfish harvested are destined for human consumption, the remaining mass being discarded as waste[3]. In general, about 50% of the seafood mass is discarded depending on the type of fish, product and processing techniques. Fishery waste mainly consists of whole waste fish, head, viscera, skin, bones, blood, frames liver, gonads, guts, some muscle tissue, *etc*. The corresponding composition varies according to the species, sex, age, nutritional status, time of the year and health of the fish[4]. Both liquid (effluent) and solid wastes are generated by most seafood processing. The almost universal treatment of the effluents removes from them most settleable solids, namely offal, skin, and bones, which are collected for disposal or reprocessing into fishmeal. The remaining suspended and dissolved solids are discharged in the

effluents[5]. However, fishery waste can be a sustainable source of high valuable molecules; therefore, development of extraction methods for the upgrading of these biowaste is desirable with a view to the economic and environmental sustainability of the process. The application of the principles of green chemistry for the valorization and reuse of fishery waste, can pave the way towards the reduction of the environmental impact associated with fishing industry and aquaculture[1].

1.2 Green chemistry and blue economy

1.2.1 Green chemistry: principles and fundamental concepts

Green chemistry has been defined as the design of chemical products and processes to avoid the use and generation of hazardous substances and prevent pollution at the molecular level. This innovative area recognizes that during the design of any chemical synthesis, product, or process, it is mandatory to minimize the use of hazardous chemicals[6]. Advances in green chemistry address hazards derived from processes, energy production, availability of a safe and adequate water supply, food production, and the presence of toxic substances in the environment. The design of any procedure should be guided by the twelve Principles of Green Chemistry, a classification of the theoretical approach taken to achieve the green chemistry goals of harmless products and processes[7]. Green chemistry considers the entire life cycle of materials and energy processes, from the origin of feedstocks, through manufacturing and product design, to disposal at the end of commercial life[8]. Its fundamental notions are substantial components of sustainability and represent the intersection of three major crossroads: environmental integrity, social responsibility and economic viability[9] (figure 1.3). Producing sustainable and cost-effective products is probably the biggest challenge facing green chemistry nowadays.

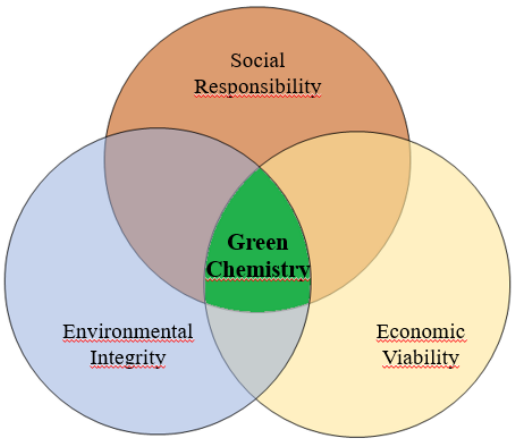

Figure 1.3:Green chemistry intersects environmental integrity, social responsibility, and economic viability.

Adapted from[9].

1.2.2 Blue Economy: toward biorefineries and sustainable marine industries

Although the use of the green chemistry principles has provided an enormous contribution toward sustainable production systems, much needs to be done to safeguard the aquatic biodiversity and ecosystems. Oceans are still seriously under-protected: just over 1% of the ocean surface is designated as protected areas, compared to nearly 15% of inlands[10]. This difference is quite surprising, especially considering that green chemistry principles were initially designed to protect our water resources. Considering these aspects and the increase of global warming, which is causing severe acidification and deoxygenation of the marine environment, the safeguard of the oceans is now a matter of primary concern. For this purpose, in 2012, during the Rio + 20UN Conference on Sustainable Development, the term "blue economy" was introduced to extend the substantial aspects of the green economy to marine activities. Different definitions of blue economy have been proposed by the major organizations all over the world, and they all agree that it is a concept related to the sustainable exploitation of the oceans and to the preservation of their resources. A representative definition by Conservation International is here reported to describe the purposes and basis in this context: "'*Blue economy' refers to the range of economic uses of ocean and coastal resources — such as energy, shipping, fisheries, aquaculture, mining, and tourism. It also includes economic benefits that may not be marketed, such as carbon storage, coastal protection, cultural values and biodiversity*"[11]. Recently have also been established traditional Blue Economy activities, that include: marine living resources, marine non-living resources, marine renewable energy, ports activities, shipbuilding and repair, maritime transport and coastal tourism[10]. It is clear that all these activities must devote primary consideration to the protection and safeguard of the marine environment, and also that synergy between blue and green economies will be based on the development of an integrated biorefinery scheme able to maximize the use of biomass and waste. Biorefining is one of the key strategies towards the circular economy, and its primary purpose is the development of biomass-based materials and chemicals as valid alternatives to petrol-based ones. Similarly, to petrochemical refineries, where crude oil is converted into added value compounds that can serve as building blocks for consumers goods, biomass can be fractionated into its major components and converted into useful materials. A proper valorization of these widespread residues would decrease ocean contamination, improve marine resource management, and increase sector competitiveness.

1.3 Spider crab (*Maja Squinado)*: occurrence and description

The Mediterranean spider crab *Maja squinado* (Herbst, 1788)[12], also known as European spider crab, spinous spider crab or granseola, is one of the biggest crabs of European coasts and its geographical range goes from the north-eastern Atlantic to the Mediterranean sea [13]. FAO[14] reported that the total annual catches of *M. squinado* from 2001 to 2011 ranged from a minimum of 5,168 tons registered in 2005 to a maximum of 6,957 in 2006. As reported in table 1.1 the main producer is France, which contributed to more than 67% of the total catch in 2011.

Table 1.1: Catches list of Maja Squinado species in European coasts from 2001 to 2011. Adapted from[14].

Country	Fishing Area	2001 (t)	2002 (t)	2003 (t)	2004 (t)	2005 (t)	2006 (t)	2007 (t)	2008 (t)	2009 (t)	2010 (t)	2011 (t)
United Kingdom (Channel Islands)	Atlantic, Northeast	428	406	379	323	242	194	165	265	257	246	184
Croatia	Mediterranean and Black Sea	21	61	54	113	110	69	244	246	19	22	29
Denmark	Atlantic, Northeast	2	2	2	1	2	1	1	0	1	0	0
France	Atlantic, Northeast	4,807	4,134	4,440	4,017	3,917	4,542	4,695	4,166	4,965	4,537	3,758
France	Mediterranean and Black Sea	1	2	2	2	3	2	0	0	2	8	7
Ireland	Atlantic, Northeast	264	330	222	180	25	153	60	153	443	415	306
Morocco	Atlantic, Eastern Central	0	168	175	108	18	1	1	0	1	4	2
Morocco	Mediterranean and Black Sea	0	0	5	4	3	0	0	0	1	0	0
Portugal	Atlantic, Northeast	51	49	59	53	48	67	56	26	37	37	26
Portugal	Atlantic, Eastern Central	0	0	0	0	0	0	1	0	0	0	0
Serbia and Montenegro	Mediterranean and Black Sea	0	1	0	2	0	0	0	0	0	0	0
Spain	Atlantic, Northeast	108	114	128	196	298	379	288	333	375	295	314
Spain	Mediterranean and Black Sea	5	3	2	2	4	6	5	2	5	5	6
United Kingdom	Atlantic, Northeast	1,199	1,171	1,027	623	498	1,568	1,441	1,023	865	769	940
Yugoslavia SFR	Mediterranean and Black Sea	0	0	0	0	0	0	0	0	0	0	0
	Total:	**6,886**	**6,441**	**6,495**	**5,624**	**5,168**	**6,982**	**6,957**	**6,214**	**6,971**	**6,338**	**5,572**

Nowadays, *Maja squinado* (figure 1.4) represents a resource for smaller-scale fisheries and is included in the list of species whose exploitation is regulated under Annex III of the Barcelona Convention Protocol (1976).

Figure 1.4: Photograph of Maja Squinado species.

Maja squinado is characterized by a reddish-brown to yellowish-brown carapace with an average length of 13 cm and a width of 18 cm, though it can reach a maximum length of 25 cm[15]. It inhabits rocky or sandy bottoms at depths up to 10 m.

1.4 Chitin

Chitin was first reported in 1811 by the French professor Henri Braconnot, who carried out some reactions on raw material isolated from different species of fungi, under the name of "fungine"[16]. After cellulose, chitin (poly β-(1-4)-N-acetyl-D-glucosamine) is the second most abundant natural polysaccharide[17,18] (see figure 1.5). In chitin, the degree of acetylation (DA), defined as the ratio of 2-acetamido-2-deoxy-D-glucopyranose to 2-amino-2-deoxy-D-glucopyranose units, varies typically between 0.80 and 0.95 depending on the source[19], indicating the presence of a certain degree of free amino groups[20].

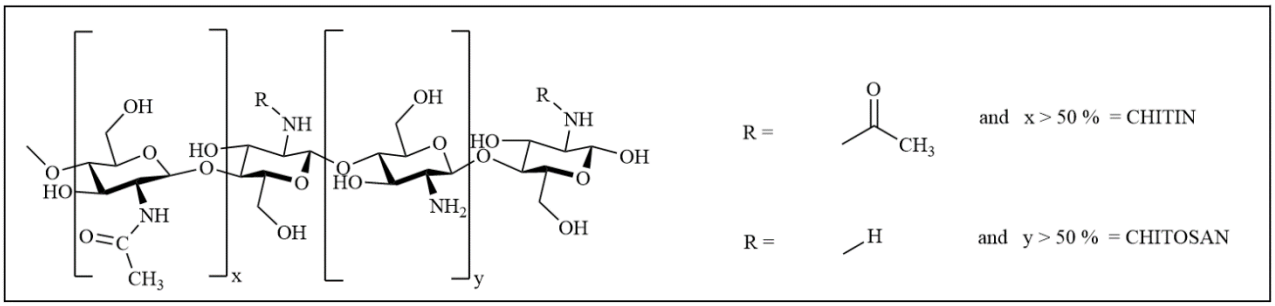

Figure 1.5: Repeating residues for chitin and chitosan. Chitin is composed predominantly of N-acetyl glucosamine (GlcNAc, x) units; Chitosan is mainly composed of glucosamine (GlcN, y) units.

Chitosan is known as the partially deacetylated derivative of chitin, and different definitions are available in the literature. Most sources mention a deacetylation degree (DD), representing the reverse of DA, of at least 50%[21] as a criterion for defining the molecule as chitosan. Others report a deacetylation degree of at least 60% or 75% for chitosan, implying that more than 60% consist of D-glucosamine monomers[22,23].

1.4.1 Production and relative sources

Chitin is present globally, and a reasonable estimate for both annual production and the steady state amount of chitin in the biosphere is of the order of 10^{12}-10^{14} kg [24]. Marine organisms are the principal source of chitin since it is a constituent of the exoskeleton of arthropods such as crustaceans (crab, lobsters and shrimps) and the endoskeleton of mollusks[25]. However, it is also produced by several other living organisms in the lower plant and animal kingdoms, serving in many functions where reinforcement and support properties are required[26].

The total annual chitin production from arthropods was estimated to be 2.8×10^{12} kg for freshwater ecosystems and 1.3×10^{12} kg for marine ecosystems[27]. The relatively laborious isolation process has led to a limited attention toward chitin and its derivatives in contrast to cellulose[28]. In addition, it has long been regarded just as a structural material without notable biological activity or functions while now it is known for interesting properties, e.g. antibacterial and analgesic.

1.4.2 Structure

Chitin exists in three polymorphic forms: α-, β-, and γ-chitin (figure 1.6)[29]. The most common form, α-chitin, obtained from the shell of crustaceans, is tightly compacted, characterized by a crystalline orthorhombic form where the polymer chains are arranged in an antiparallel conformation, allowing

maximum hydrogen bonding[18]. β-chitin is associated with protein in squid pens[30] or in tubes of pogonophoran worms[31] and has a monoclinic form with a parallel disposition of the chains. Compared to the α- and β- chitins, γ-chitin is less common. It is considered a mixture (or an intermediate) of the previous two forms[32], where chitin chains are randomly arranged in parallel and antiparallel directions.

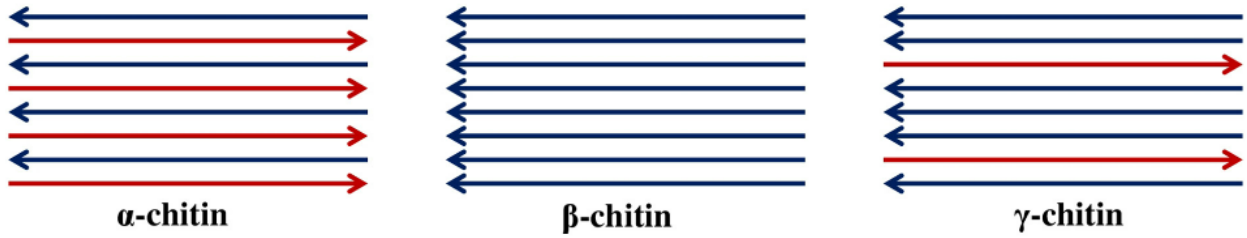

Figure 1.6:Polymorphic forms of chitin and relative disposition of chains.

In α- and β-chitin, the polymer chains are organized in sheets held together tightly by a strong network of intermolecular hydrogen bonds[26] between the amide groups ($C(2_1)NH\cdots O{=}C(7_3)$), approximately parallel to the *a-axis* (figure 1.7 **d**). In α-chitin, each chain also has a C(3')OH···OC(5) intramolecular hydrogen bond along the *c* axis (figure 1.7 **a**), like the one present in cellulose. On different chains the CH_2OH group can form hydrogen bonds in two different ways. On one hand these groups can bond with the oxygen of the amidic group of the adjacent monomer $C(6_1')OH\cdots O{=}C(7_1)$ (figure 1.7 **b**). On the other hand they can build a hydrogen bond with the CH_2OH group of the adjacent chain $C(6_1')O\cdots HOC(6_2)$ approximately along b*c* diagonal (figure 1.7 **c**). The results indicate that a 50/50 statistical mixture of CH_2OH orientations is present, equivalent to half oxygens on each residue, forming inter-and intramolecular hydrogen bonds[33]. β-Chitin is more prone to intra-crystalline swelling compared to α-chitin due to the fewer hydrogen bonds [34]. The effect of chitin structure and hydrogen-bonding network on the solubility of this biopolymer will be discussed in detail in section 1.4.3.

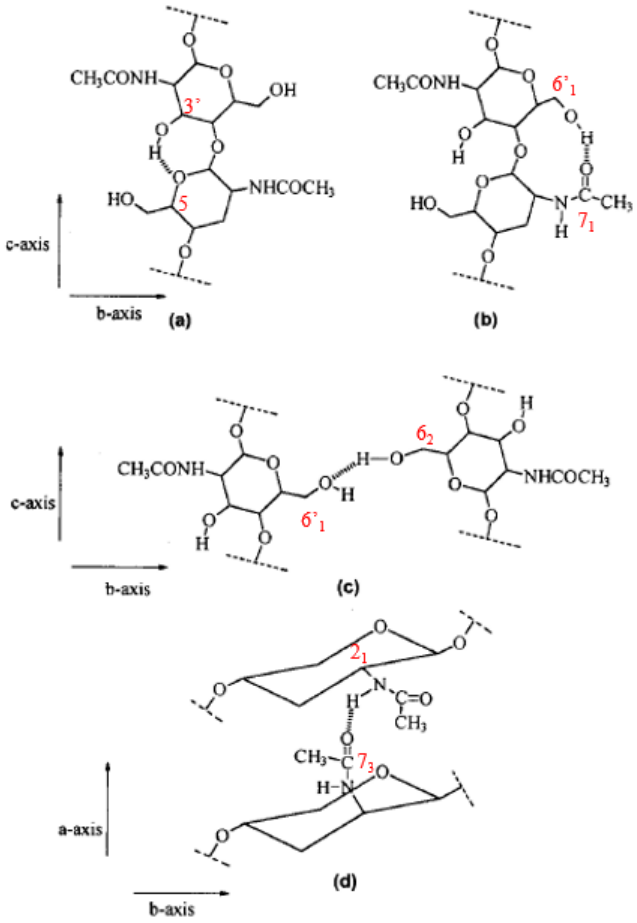

Figure 1.7: Modes of hydrogen bonding in R-chitin: (a) intrachain C(3')-OH···OC(5) bond; (b) intrachain C(6'$_1$)OH···O═C(7$_1$) bond; (c) interchain C(6'$_1$)O···HOC(6$_2$) bond; (d) interchain C(2$_1$)NH···O═C(7$_3$) bond. Adapted from[18].

In living systems chitin chains aggregate to form microfibrils that are cross-linked with other sugars, proteins, glycoproteins and proteoglycans [35]. In particular, in fungal cell walls chitin is covalently bonded to glucans , either directly or via peptide bridges[36]. In insects and other invertebrates, instead, chitin is always associated with specific proteins, with both covalent and noncovalent bonding, to produce ordered structures (see figure 1.8).

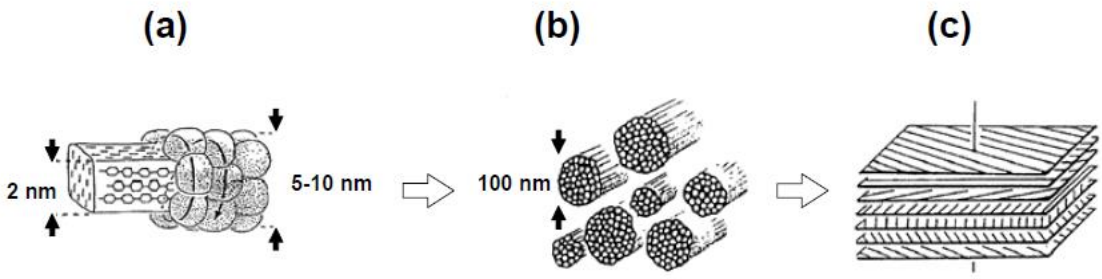

Figure 1.8: Hierarchical levels in the chitin-protein matrix in crustacean cuticles. **(a)** chitin crystals surrounded by proteins. **(b)** Chitin-protein fibrils. **(c)** Schematic representation of fibrils lying horizontal and parallel in successive planes.

1.4.3 Solubility

Due to the high crystallinity and the strong intermolecular hydrogen bonding, chitin is not soluble in water, dilute acidic and basic solutions and many common organic solvents. Austin[45] and Rutherford conducted the first extensive study on chitin solubility in 1976 when they discovered the potential of lithium chloride-tertiaryamide solvent systems would yield at least 5% chitin solutions. Chitin is coordinated with LiCl through the acetyl carbonyl group, forming a chitin-LiCl complex, which is soluble in dimethylacetamide (DMAc) and N-methyl-2-pyrrolidone (NMP). Austin also determined the solubility parameters of chitin in various solvents, including the previously cited LiCl/NMP and LiCl/DMAc mixtures and strong carboxylic acids, such as dichloroacetic acid and trichloroacetic acid[37]. Recently new solvent systems based on methanol saturated with calcium chloride, as well as highly acidic and polar fluorinated solvents such as hexafluoroisopropyl alcohol, hexafluoroacetone sesquihydrate[38] have been described.

Despite its abundance, low cost and availability, the variability of chitin solubility still limits product development and market access in large volumes. In fact, batch-to-batch variability, non-precise characterization, and randomly distributed acetyl groups can result in bad reproducibility of chitin solubility. Even if some exceptions and other solvent systems have been proposed in the literature, these solvents are usually toxic, volatile, corrosive, or degradative. In this context, attention has been given to converting chitin into more soluble derivatives. Various chemical modifications that can disrupt inter- and intra-molecular hydrogen bonds without glycosidic linkages cleavage are effective in making chitin soluble in water or other solvents. The most straightforward modification is the N-deacetylation to transforms chitin to chitosan[39].

1.4.4 Deacetylation to Chitosan

Charge density, pH, DD, and the distribution of acetylated monomers in the chitosan polymer chain strongly influence its solubility. Due to the basicity imparted to chitosan by its amino groups (pKa = 6.3) [20], this biopolymer can generally be dissolved in acidic solutions at pH < 6.0[40].

The alkaline deacetylation reaction of chitin to chitosan consists of a pseudo-first-order[41], two-step nucleophilic substitution reaction. The first step involves the addition of hydroxide to the amide carbonyl, followed in the second step by carbon-nitrogen bond cleavage that yield the free amine (chitosan) and acetate.

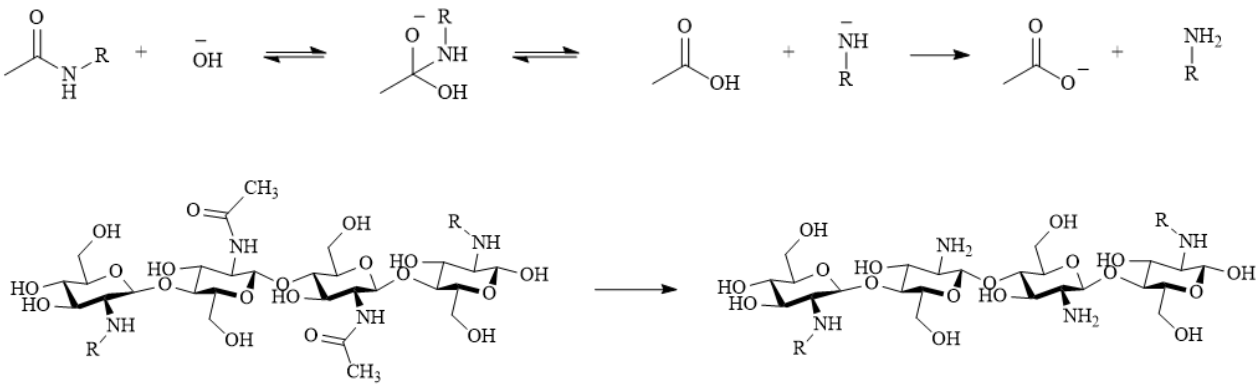

Figure 1.9: Reaction mechanism of deacetylation promoted by strong alkali reagents (top) that convert chitin to chitosan (bottom). R: amine or acetamide groups.

Thermal treatment with strong aqueous alkali (sodium or potassium hydroxides 30-50% w/v, T = 100 °C) is therefore needed to obtain chitosan with DA < 30%. The most common methods for chitosan production are the Broussignac[42] and Kurita[43] processes that involve deacetylation of chitin via alkali treatment under heterogeneous and homogeneous conditions, respectively. The first deacetylation procedure involves a mixture of solid potassium hydroxide (50%, w/w), 96% ethanol (25%, w/w) and mono ethylene glycol (25%, w/w). The dissolution is exothermic, and the temperature of the mixture may increase up to 90°C during this step. In the method applied by Kurita and co-workers, on the other hand, a suspension of chitin is treated with 40% aqueous sodium hydroxide and heated at 80 °C under a nitrogen stream for three hours[43]. Both methods have been extensively compared. The results show that different reaction parameters such as chitin source, extraction conditions, temperature, and repeated alkali treatment strongly influence final product MW and DD. When the same temperature was applied in both processes (80 °C), the molecular weight was equivalent, but better deacetylation was obtained by using the Kurita process. Moreover, it was observed that, after two repeated alkaline steps, the final acetylation degree was obtained; increasing the number of reaction steps only led to depolymerization. To get the same degree of acetylation with the Broussignac process, it was necessary to increase the reaction temperature to 120 °C. Still, in these conditions, important depolymerization was observed (MW of 126,000 g/mol instead of more than 600,000 g/mol)[44]. In conclusion, Kurita's process is functional to obtain chitosan with high MWs and with a disperse range of DA while Broussignac's process is faster and leads to chitosan with low DA and MWs.

In this context, many deacetylation conditions have been reported in literature. However, deacetylation of chitin under heterogeneous conditions remains the most widely used method at present to achieve an effective reaction. Under these conditions, *N*-deacetylation takes place preferentially in the amorphous region of chitin and then proceeds from the edge to the inside of the

crystalline region. Regarding the effect of temperature on rate of deacetylation, it was found that higher temperature increased the percentage of deacetylation but reduced molecular size[45]. The effect of alkali concentration and treatment time were also extensively studied. It was demonstrated that deacetylation proceeds during the first minutes of alkali treatment and progresses only gradually after this. Akali concentration strongly affect the DD all samples, thus higher concentrations led to higher DD and increasing rate constants. Furthermore, alkali treatment beyond a certain time (depending on alkali concentration) does not deacetylate significantly but serves only to degrade the molecular chain. However, if conditions are too mild, the resulting product will be insoluble in weak acid. Rigby (1936) earlier showed that free access of oxygen to chitin during deacetylation had a substantial degrading effect on the chitosan product and deacetylation in an atmosphere of nitrogen yielded chitosans of higher viscosity and molecular-weight distributions than did deacetylation in air. The degradative effect of air became more pronounced with increased deacetylation time.

1.4.5 Properties and applications of chitin and chitosan

Chitin and chitosan have interesting characteristics that make them suitable in many fields and applications. In this paragraph, the most important properties and related uses will be discussed in detail, other than the mechanism of action and influences of physicochemical characteristics of chitin/chitosan biomaterials that play a crucial role in the exploitation of biological properties.

Both chitin and chitosan are biocompatible, to a degree that depends on the characteristics of the sample (i.e. source, DA and MW)[22]. Chitosan has been studied more than chitin due to its biological properties, easier dissolution, and processability.

Clinical tests on chitosan-based biomaterials demonstrated that, under normal conditions, no inflammatory or allergic response after implantation, injection, local dermal application or ingestion were observed[46]. *In vitro* and *in vivo* studies established its high cytocompatibility, and that the DA plays a crucial role in cell adhesion and proliferation. Chitosan is more cytocompatible *in vitro* than chitin thanks to the higher number of positive charges that enhance the interaction with the cells[47].

Chitin and chitosan can be degraded *in vivo* by several proteases, like lysozyme, pepsin, and papain. Lysozyme is a non-specific protease present in all mammalian tissues, and it possesses the ability to hydrolyze l-4 glycosidic linkages of chitin and certain bacterial cell-wall peptidoglycans[48]. By this process, non-toxic oligosaccharides of various lengths are produced and excreted by the organism or incorporated into glycoproteins or glycosaminoglycans. The degradation kinetics have been extensively studied, highlighting the inverse proportionality between the degradation rate, the degree of crystallinity[49] and deacetylation degree. The distribution of acetyl groups also influences the

biodegradability, as demonstrated by Aiba[23] in 1992: chitosan with a block-type distribution of acetyl groups was degraded four times more rapidly than a sample with the same DA but a random-type distribution of acetyl groups.
The biodegradability makes chitin and chitosan-based materials suitable for applications such as drug delivery and tissue regeneration.
Chitin and chitosan possess analgesic properties, and many reports assess that they provide a cool and pleasant soothing effect when applied topically over open wounds. The mechanism of action is different for the two polymers: as reported by Okamoto and co-workers[50] chitosan accomplishes analgesic effect by absorbing proton ions released in the inflammatory site, while chitin absorbs bradykinin, one of the main substances related to pain.

Chitosan and sulphated chitosan oligomers have been tested also for their anticoagulant activity as a safer alternative to the traditional heparin. Their anticoagulant activity has been shown to be due to the interaction of the positively charged chitosan polymer with receptors on the cell surface[51]. For this reason, chitosan is more effective than chitin and high DD are preferable.

One of the better known and applied characteristics of chitosan is its antimicrobial activity on Gram-negative bacteria. Two different modes of action have been proposed in the literature: one involving the binding of the cationic chitosan to the anionic cell surface resulting in changes in permeability[52], and the other involving the inhibition of DNA transcription[53]. For both mechanisms, however, the physicochemical properties of the polymer (MW and DD), its concentration, and pH of the medium influenced its performances.

Beyond all these fundamental properties, chitin and chitosan have demonstrated antioxidant and radical scavenging, anticholesterolemic, and antitumoral activities, and in all cases the DD and MW of chitosan substrate strongly influenced their applicability and performances. Due to these diverse properties, these biopolymers, especially chitosan, have been exploited in many different applications such as in biomedicine, as food preservatives, as excipients in cosmetics, in antimicrobial packaging, and in biocatalysis. Some general recommendations, particularly related to the DD and MWs, and relative application fields are reported below in table 1.2.

Table 1.2: General Recommendations for the Use of chitin and chitosan in several applications. Adapted from[22].

Application	General Recommendations
Wound healing	High DD chitosan preferred over chitin Low MW samples (oligomers)
Drug delivery systems	High DD High MW
Gene Delivery	DD ≤ 80 Low MW (around 10 kDa)
Scaffolds (tissue engineering)	DD about 85 (good proliferation and structure) High MW (prolonged biodegradation)
Cell immobilization	Chitosan preferred over chitin (high DD)
Enzyme immobilization	Depend on the enzyme, immobilization method and reaction media Low ash content β-chitin preferred over α-chitin in organic reaction media
Dietary ingredient	High DD; high MW (viscosity) Fine particle
Food preservative	High DD Medium-low MW (5-80 kDa)
Emulsifying agent	Low DD for emulsion stability High viscosity
Wastewater treatment	Depend on pollutant and water conditions (pH, ionic strength) In general, chitosan preferred over chitin. High DD Low crystallinity
Molecular imprinting	Not yet tested High DD is expected to improve crosslinking In general, low MW chitosan is used
Metal reduction	Metal reduction depends on chitosan characteristics (not yet fully tested) High DD and low MW seems to stabilize the nanoparticles

1.5 Chitin isolation

As seen in the previous section, chitin present in biomass is strongly connected to other biomolecules. In particular, the main components of crustacean shells are – on a dry weight basis and depending on the species and season – 30%–40% protein, 30%–50% minerals, 13%–42% chitin and other minor components such as lipids, pigments and other metal salts. The chemical composition of the shells of *Maja Squinado* species has been scarcely investigated. To our knowledge, only Pires and co-workers[54] in 2017 reported the chemical composition of this biomass substrate, and the results are

described in table 1.3.

Table 1.3:Chemical composition of spider crab shells of Maja Squinado species. Data obtained from [54].

Chitin [%]	Protein [%]	Ash [%]	Total carotenoids[µg/g]
16	19-20	62.9	< 3

The remaining part is constituted by lipids, trace elements like rubidium, iron, copper, zinc and bromine, and contaminants, such as cadmium, arsenic and lead.

The process to isolate and purify chitin from biomass includes a series of consecutive steps: biomass pre-treatment, deproteinization (DP), demineralization (DM), decolouration and post-treatment processes (figure xx). Depending on the biomass source and composition, the order of these steps may change or even not be required. In addition, the DA, degree of crystallinity and molecular weight (MW) of the final product may also vary with the source and be altered during the isolation process[55].

Figure 1.10: Process steps to isolate and purify chitin from biomass.

1.5.1 Conventional chemical method

The pre-treatment process includes all the manipulation necessary to prepare the biomass sample for chitin extraction like the removal of soft tissues by scraping or boiling. The substrate is then dried and reduced in size.

The three or four upper layers of crustaceans cuticle are mineralized, with $CaCO_3$ precipitated into the twisted lamellar structure of the chitin–protein matrix[56]. DM is generally performed by acid treatment using hydrochloric acid (HCl), nitric acid (HNO_3), sulphuric acid (H_2SO_4), acetic acid (CH_3COOH) or formic acid (HCOOH)[36]. Among these, HCl is preferred because it allows almost complete removal of calcium carbonate and other organic salts. Performing demineralization at room temperature or lower can minimize the depolymerization of chitin chains[57]. However, reaction conditions and the number of repeats may vary significantly depending on the source[58].

It is generally agreed that the processing conditions strongly affect the MW and DA of chitin: as the acidic conditions for demineralization (pH, time, and temperature) become harsher, the molecular weight of the obtained products decreases. Indeed, being chitin an acid-sensitive material, it can be degraded by several pathways: hydrolytic depolymerization, deacetylation, and heat degradation leading to a significant change of its physical properties[57]. The reaction mechanism for acidic depolymerization and deacetylation of chitin are schematized in figure 1.11.

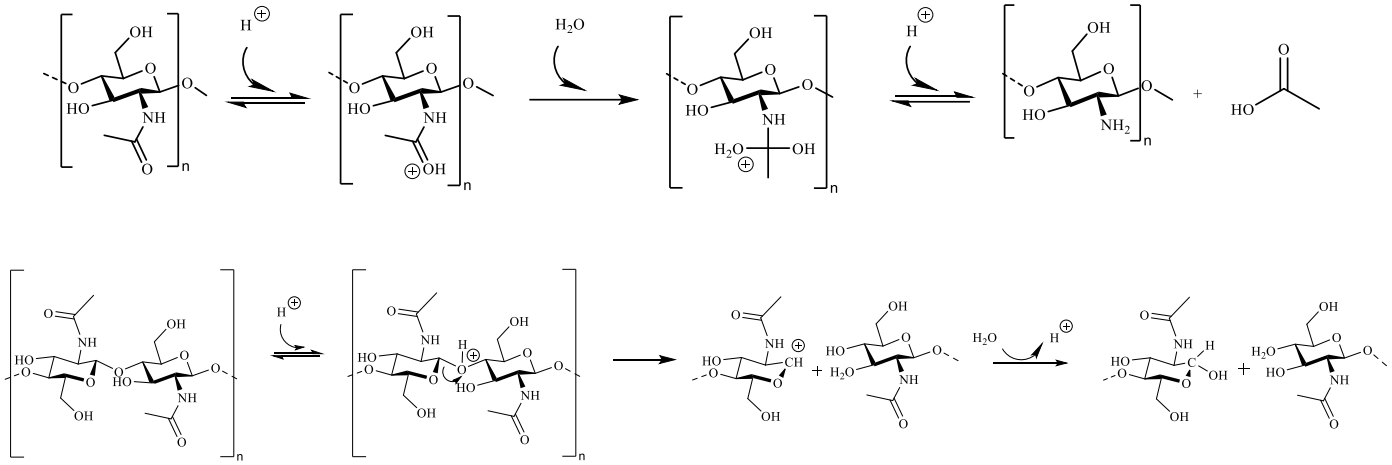

Figure 1.11: Reaction mechanism of deacetylation (top) and depolymerization (bottom) promoted by acidic treatment.

Due to the strong nature of the hydrogen and covalent bonding between chitin and protein, harsh process conditions are required for deproteinization. This step is traditionally performed using alkali solutions, and the effectiveness depends on the process temperature, alkali concentration, and the ratio of its solution to the biomass[59]. Some old literature works[60] claimed the use of a wide range of agents for this step, including NaOH, Na_2CO_3, $NaHCO_3$, KOH, K_2CO_3, $Ca(OH)_2$, $NaHSO_3$, $CaHSO_3$, Na_3PO_4, but NaOH is the most efficient agent employed. Typically, raw chitin is treated with approximately 1 M aqueous solutions of NaOH for 1-72 h at temperatures between 65 and 100 °C [36]. When necessary, a decolouration step can be introduced to remove pigment traces, like carotenoids. The most-reported processes employ mild oxidizing agents like potassium permanganate[61] or hydrogen peroxide[62] and alternatively extraction with organic solvents such as acetone[63], or chloroform, methanol and water (v/v 1:2:4) mixture[64].

Some post-treatment steps, such as neutralization, drying and milling, may be required at the end of the extraction procedure.

1.6 Chitin extraction by alternative methods

While pre-treatment, decolouration, and post-treatment procedures are general and applied for all chitin-contained substrates, alternative methods for deproteinization and demineralization have been extensively studied. According to previously reported work, the traditional method involving strong acids makes the process ecologically aggressive, energy-intensive and a source of pollution[65]. Chemical treatments also create a disposal problem for the large quantity of wastewater produced since decontamination and neutralization are necessary[66].

From an applicative point of view, the quality of the final product, which is a function of the average MW (and polydispersity) and the DA[67] is of primary concern. Although the harsh conditions used in chemical extraction adversely affect the chemical and physical properties of the extract, it is still the most commonly applied method on an industrial and commercial scale.

1.6.1 Biological methods

Taking into account the above-mentioned disadvantages, biological techniques for the processing of chitin have gained particular interest[65]in this field. They consist in the utilization of lactic acid and protease producing bacteria for DM and DP of crustacean shells, respectively. These processes can be carried out simultaneously or by successive fermentations or co-fermentation of microorganisms. Various studies showed the potential of fermentation for the production of chitin with superior physicochemical characteristics compared to the one obtained by chemical methods. These biological methods also allow the recovery of side products, such as proteins, pigments and mineral salts, that remain in the liquor fraction, providing an additional source of profit along with its ecological management[65].

1.6.2 Ionic Liquids as green alternatives for chitin processing

Ionic Liquids (ILs) are organic salts that are liquid at temperatures below 100 °C. Given their peculiar proprieties such as thermal stability, outstanding solvation potential and negligible vapour pressure, they constitute a valid alternative to traditional volatile organic solvents. Based on their cationic portion, the most commonly employed ILs can be classified into four groups: ammonium-, *N*,*N*'-dialkylimmidazolium-, phosphonium and *N*-alkylpyridinium- based ILs.

However, there is still a degree of uncertainty regarding their greenness, as their toxicity and biodegradability have not been completely assessed, particularly since the number of cation-anion combinations is basically unlimited. Each ion shows its own proprieties, and the overall effect of the ions may be different from the cation/anion individual properties, therefore an empirical evaluation of the properties of every single ionic liquid is necessary. Despite the complex assessment of both biological and toxicological aspects, it is accepted that ILs can be a valid green alternative to traditional solvents.

Isolation of chitin from biomass with ILs has gained interest recently. In this context, chitin can be either "extracted" or "pulped" from a specific source. Extraction methods consist in chitin dissolution in ILs, while in pulping methods the biomass shell matrix, which mainly consists of minerals and proteins, is removed, and chitin remains in the solid state. In this thesis work, we focused only on pulping-based protocols. To overcome the disadvantages and problems associated with chemical extraction this thesis describes pulping methods, where both the basic sites (responsible for deproteinization) and the acidic ones (responsible for demineralization) are incorporated into a single IL.

Examples of such ILs are hydroxylammonium acetate ($[NH_3OH][OAc]$) and hydroxyethylammonium acetate ($[NH_2(CH_2)_2][OAc]$[68]. These ILs have been previously reported for the isolation of chitin from shrimp shells with a > 80% purity, high DA and high degree of crystallinity. Analogously, Tolesa and co-workers[69] recently reported production of chitin, and subsequent deacetylation to chitosan, using diisopropylethylammonium acetate or propanoate and dimethylbutylammonium acetate.

1.7 Characterization techniques

Chemical characterization of chitin and chitosan were performed using Thermogravimetric Analysis (TGA), Inductive Coupled Plasma Optical Emission Spectrometry (ICP-OES), Fourier Transformed Infrared Spectroscopy (FT-IR), proton Nuclear Magnetic Resonance (^{1}H-NMR), X-ray Diffraction (XRD) and Gel Permeation Chromatography (GPC). In this section each technique will be briefly described.

TGA

TGA analysis can provide valuable information, often quantitative, on the composition of polymeric materials. If a multicomponent material contains low - molecular - mass compounds, polymeric material, and inorganic additives, the three groups can be separated by temperature.

In the specific case of chitin, a variety of TGA experiments are reported in literature, and the characteristic temperature intervals of weight losses could be identified as follow:

- In the range 250-400 °C, a 65% weight loss is caused by depolymerisation/decomposition of the polymer chains through deacetylation and cleavage of glycosidic linkages
- At temperature higher than 400 °C a 10-15% weight loss corresponds to the thermal destruction of pyranose ring and the decomposition of the residual carbon.

The presence of impurities in chitin samples can also be studied thanks to TGA analysis: in particular, proteins (weight loss at 200-250°C) and also $CaCO_3$ (weight loss at ca. 700°C) can be observed. Inorganic additives are known to be stable in an inert atmosphere up to temperatures higher than 900 ° C, although carbonates will decompose to CO_2 between 600 ° C and 700 ° C. In particular, $CaCO_3$ will convert to CaO and CO_2 and, calculating the CO_2 mass loss is possible to quantify the amount of calcium carbonate in the initial matrix.

ICP-OES

ICP-OES is an analytical technique to determine the inorganic elemental composition of a wide variety of samples. This technique uses an optical emission spectrometer to detect and quantify the radiation emitted by the sample atoms after being excited by an argon plasma at very high temperature (between 5000 K and 10,000 K)[70]. The elements present in the sample are identified according to the emitted ray wavelengths, which are characteristic of each particular atom. The emission intensities indicate the elements concentration and are quantified using calibration standards. ICP-OES detection limit is in the ppb range for most elements, making this technique suitable for the determination of trace elements in samples. Taking into account that $CaCO_3$ is the major component of crab shells, ICP-OES measurements are useful for the quantitative estimation of calcium and magnesium salts and other metal traces. In this way the effectiveness of pulping or extraction methods in the removal of inorganic salts can be verified.

^{1}H-NMR

Another technique extensively studied in this context is NMR spectroscopy. Numerous NMR techniques has been described to determine the DA of chitin/chitosan with different accuracies. These techniques include proton nuclear magnetic resonance ^{1}H NMR, cross-polarization (CP)/magic-angle spinning (MAS) ^{13}C NMR and CP/MAS ^{15}N NMR spectroscopies[71]. The most important factor is to find a proper solvent, which should have good solubility properties towards the target material and its residual signal should not overlap the signals of the sample. The most common solvents for liquid-

state NMR spectroscopy are, D_2O/CD_3COOD, $D_2O/DCOOD$ and D_2O/DCl[72]. Different studies conducted by Einbu demonstrated that concentrated DCl is a suitable solvent for the characterization of chitin samples, and the DA can be determined with high precision. One advantage of using this solvent system is that its resonance (HDO) does not interfere with any of the carbohydrate protons, as the solvent protons resonate at 9.2 ppm (probably a weighted average of the signals from water and acid protons due to the fast exchange between the two)[35]. Figure 1.12 shows ^{1}H-NMR spectrum of commercial chitin, previously dissolved in DCl for 30 minutes at 50°C.

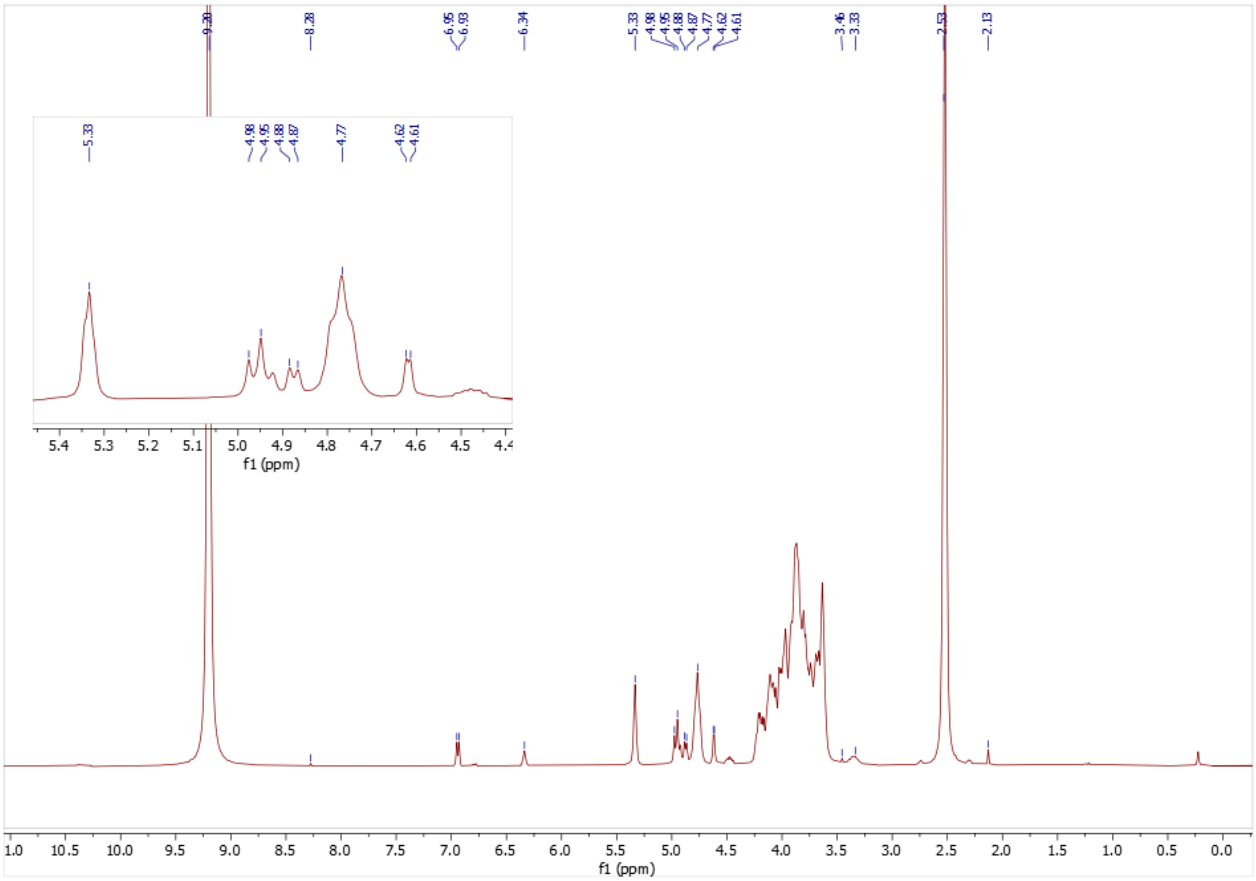

Figure 1.12: ^{1}H-NMR spectrum of commercial chitin in concentrated DCl.

The assignment of the resonances and their chemical shifts (ppm) are given in table 1.4. Figure 1.13 represent the model structures of dimeric N-acetyl glucosamine (GlcNAc) and glucosamine (GlcN)

Table 1.4: Assignments od resonances and relative chemical shifts of chitin signals.

	H-1	**H-1 (reducing end)**		**H-2**	**H-2/6**	**Acetyl-H**
GlcNAc	4.77	5.33	4.95	-	3.5-4.3	2.53
GlcN	4.98	5.55	5.11	3.33	3.5-4.3	

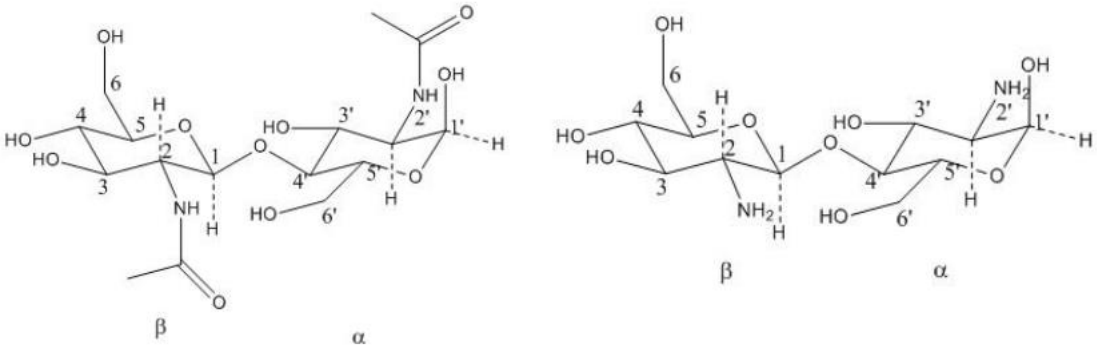

Figure 1.13: chemical structure of N-acetyl glucosamine (GlcNAc, left) and glucosamine (GlcN, right).

The spectrum shows the characteristic resonances in the anomeric region of the acetylated α- and β-anomer at 5.33 and 4.95 ppm, respectively. H-1 of internal de-*N*-acetylated units resonate at 4.98, overlapping with the β-anomeric proton at 4.95 ppm, while H-1 of internal acetylated units resonate at 4.77 ppm. H-2 of internal de-*N*-acetylated units resonate at 3.33 ppm. The remaining ring protons (H2/H6) appear between 3.5 and 4.3 ppm, while a strong signal that integrate for the three acetyl-protons is found at 2.53 ppm. The α- and β-anomer reducing end resonances from a deacetylated unit, which would be expected to appear at 5.55 ppm and 5.11 ppm, are absent, since there is no significant de-*N*-acetylation of the sample and due to the specificity of the acid hydrolysis of the glycosidic bonds. In this case only partial de-*N*-acetylation of the sample occurs after dissolution in concentrated DCl, and the resonance from the protons of acetic acid appears at 2.13 ppm. ^{1}H-NMR spectra of chitin in this solvent can also be used to give an indication of the purity of the sample, as methyl-proton resonances from protein present in the sample would appear between 1.0 and 1.5 ppm[73].

The spectrum contains additional resonances. The different relative intensities of the resonances indicate they originate from two different compounds. From previously reported NMR-data[74,75,76] it could be deduced that they are due to the presence of a glucofuranosyl oxazolinium ion existing in equilibrium with GlcNAc units in concentrated HCl (see figure 1.14).

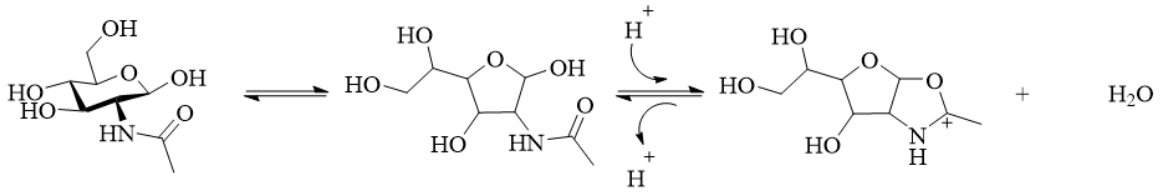

Figure 1.14: glucofuranosyl oxazolidinium ion presents in equilibrium with GlcNAc.

H-3 and H-2 of the glucofuranosyl oxazolinium ion are represent by two doublets at 4.61 ppm and 4.87 ppm respectively, while H-1 has a relatively high chemical shift at 6.94 ppm. This can be explained by deshielding of the proton by the presence of two electronegative oxygens on each side of C-1. Signals located at ca. 4.5 ppm and 6.34 ppm are associate with a second compound, that is present in lower concentrations with respect to the oxazolidinium ion. It was previously hypothesized that these resonances may derive from the protons of the open ring form of the acetylated reducing end residue of the dimer or of the monomer, since partial depolymerization of chitin chains occur in the solvent used for this analysis.

From the identification of the resonances, the DA % of chitin samples can be calculated. In this work of thesis two different equations were employed, and the respective obtained DA value compared (see equation 1 and 2 below).

$$DA\% = \frac{\left(I_{\alpha H1A} + I_{\beta H1A + H1D} + I_{H1A}\right) - I_{H2D}}{I_{\alpha H1A} + I_{\beta H1A+H1D} + I_{H1A}} \; 100$$

Equation 1.1: Formula for the calculation of the DA% based on the integrals of H-1 and H-2 signals.

$$DA\% = \frac{{}^{1}/_{3}A_{CH3}}{{}^{1}/_{3}A_{CH3} - A_{GlcN}} \; 100$$

Equation 1.2: Formula for the calculation of the DA% based on the area of the H-2 of GlcN units and of the acetyl protons of GlcNAc units.

In equation 1.1 the sum of the integrals related to the H-1 is subtracted with the integral from H-2 on deacetylated units (I_{H2D}) obtaining the integral representing only acetylated units.
In equation 1.2, A_{GlcN} represents the peak area of H-2 protons of GlcN units while A_{CH3} is the area of the peak related to acetyl protons of GlcNAc units.

FT-IR

Several studies have dealt with the description and interpretation of the infrared spectra of chitin. Because of the high crystallinity of this polymer, its IR spectra display numerous sharp absorption bands[26], and the characteristic signals are summarized in table 1.5.

Table1.5: IR bands and relative vibration mode associated with chitin[77].

α-Chitin absorption (cm^{-1})	β-Chitin absorption (cm^{-1})	Assigned
3479,3448	3479, 3426	ν_{OH}
3268	3290	ν^{as}_{NH}
3106	3102	ν^{s}_{NH}
2965	2962	$\nu^{as}_{CH_3}$
2927	2929	$\nu^{s}_{CH_2}$
2883	2880	$\nu^{as}_{CH_3}$
1660,1627	1656	$\nu_{C=O}$ (Amide I)
1558	1556	ν_{C-N} (C—N—H) + δ_{NH} (Amide II)
1422	1424	δ_{CH_2}
1376	1376	δ_{CH} + δ_{C-CH_3}
1312	1314	ν_{C-N} + δ_{NH} (Amide III)
1255	1262	δ_{NH}
1157	1155	ν^{as}_{C-O-C} (ring)
1072	1069	ν_{C-O}
1113	1111	ν_{C-O}
1021	1032	ν_{C-O}
957	948	γ_{CH_3}
896	902	γ_{CH} (C1 axial) (β bond)
746	—	ρ_{CH_2}
698	692	γ_{NH} (Amide V)
610	616	γ_{C-O}
566	—	γ_{C-C}

The α- and β-chitins can be distinguished by FTIR spectroscopy because of the different hydrogen bonds. In the region corresponding to the OH and NH groups (3600– 3000 cm^{-1}) numerous signals are present.

The more evident spectral difference is the frequency of the vibration modes of amide I in the region 1660–1620 cm^{-1}. In the α -chitin two peaks are present (1660 and 1627 cm^{-1}), while the β -chitin only one band at 1656 cm^{-1} is observed. The most accepted explanation is the existence of two types of amides: half of the carbonyl groups are bonded through hydrogen bonds to the amino group inside the same chain (C═O···HN) that is responsible for the vibration mode at 1660 cm^{-1}. The remaining carbonyl groups produce the same bond, and an additional one with the group $–CH_2OH$ from the side chain. This additional bond causes a shift of the amide I band at 1627 cm^{-1}. As previously stated, the existence of these interchain bonds is responsible for the high chemical stability of the α -chitin structure. In the β -chitin all the amide groups participate only in the first kind of hydrogen bonds and the amide I band appears at 1656 cm^{-1}. It has to be noted that amide I band occurs at similar wavelengths in polyamides and proteins, so the possible presence of impurities in the extract will affect the intensity of this absorption band.

Amide II and the NH bending of Amide III signals are present at 1558 cm^{-1} and 1312 cm^{-1} respectively. Other strong bands ascribable to complex vibrations (bending, stretching, and coupling

of these modes) of the ring structure of the polysaccharide were centred between 1021 and 1075 cm^{-1}, while the stretching vibration of the glycosidic linkage is visible at 896 cm^{-1}.

IR spectroscopy have been already proposed for quantitative determination of DA[78]. The use of IR for this purpose requires the construction of a calibration line using ratios of absorbances (A) of a probe band (PB) that changes intensity with the DA, relative to a reference band (RB), not changing intensity with the DA, against standard DA values. The absorbances of PB and RB are determined by the baseline method (BL). However, the construction of a reliable calibration line is not an easy task. On one hand, the choice of the best PB, RB and BL combinations is not obvious, and this is well illustrated by the great number of APB(BL)/ARB(BL) ratios which have been used so far. On the other hand, the choice of the best standard technique among those described in the literature is not simple because of the variability of sources, isolation and preparation procedures of chitins. Recently the different absorption band ratios, their corresponding DA ranges, and their relative advantages and disadvantages has been evaluated[78]. For the aim of this work IR will be exploited only for a qualitative analysis of pulped chitins, taking into account that numerous parameters could affect the specific calculation, such presence of protein or calcium carbonate residues in the pulped material, other than humidity traces and heterogeneity of samples.

XRD

As previously described, chitin is present in nature in three forms, depending on their crystalline structure: α-, β- and γ-chitins. X-ray diffraction is one of the most useful techniques for the analysis of crystalline structure and in general for material characterization. From X-ray diffraction patterns there are two general types of structural information that can be studied: the electronic structure (focused on valence and core electrons, which control the chemical and physical properties, among others) and geometric structure (which gives information about the locations of all or a set of atoms in a molecule at an atomic resolution)[72]. Clark and Smith[79] in 1936 were the first that reported XRD analysis on chitin and chitosan. In later works many X-ray experiments were performed with more sophisticated instrumentation and essentially they consist in slightly modified procedures from this pioneering work. In the specific case of chitin and chitosan samples, XRD enables to establish the polymorphic form, calculate the Crystallinity Index (CI) of the substrate and evaluate the water vapor sorption properties, which occurs in the amorphous domain of hydrophilic polymers. The X-ray diffraction patterns of the α-chitin samples and the corresponding hydrolysed chitosan show strong reflections at 2θ around 9–10° and 2θ of 20–21° and minor reflections at higher 2θ values (e.g., 26.4°). Different methods for CI calculation have been reported. Most studies are limited by evaluation of the index of crystallinity (CI), based on calculations of the ratio of peaks heights:

$$CI = (I_o - I_{am})/I_o$$

Equation 1.3: General formula for CI calculation generally used in literature.

where I_o is height of the crystalline peak and I_{am} is height of amorphous scattering[80,81,82].

Index of crystallinity shows the comparative content of crystalline fraction in several samples. It may indicate which of the samples has greater crystallinity, but it does not reveal the actual degree of crystallinity, express as the weight part of the crystalline fraction in the polymer[83].

In these works, CI of chitin and chitosan samples were calculated by different ways using heights of crystalline X-ray diffraction peaks from (110) or (020) planes and heights of amorphous scattering at 2θ of 12°, 12.6° or 16° with or without subtraction of the background scattering.

To determine the actual degree of crystallinity, the quantitative X-ray phase analysis should be performed, which requires the subtraction of the background, the correction of the experimental diffractogram and its separation from the scattering areas related to crystalline and non-crystalline domains. Furthermore, the area of crystalline and non-crystalline scatterings should be used to calculate the degree of crystallinity[83].

For all these reasons, in the present work of thesis this last approach has been chosen for the calculation of CI.

GPC

Gel permeation chromatography (GPC) is a technique able to monitor major changes in terms of molecular sizes (or more precisely in terms of hydrodynamic volumes). The separation process is based on the entropy decrease of the mixture due to the stationary phase made of a porous material containing fixed pore sizes. During an analysis, a mixture of molecules is sorted by size: smaller molecules will penetrate inside pores and temporally retained. In addition, one of the main challenges in GPC resides in setting a proper calibration[84]. Usually polystyrenes, polyethylene oxides (PEO) or polyethylene glycols (PEG) are used to generate a calibration curve allowing converting retention times in terms of molecular masses. The most convenient way to run GPC experiments is either to analyse known increasing size polymers corresponding to the molecules to analyse or to use the classic standards considering that the molecular masses will be an approximation. In this case, calibration was performed by PEO/PEG standards with sample weights of 601–1020000 g/mol, on the base of previous literature work[85], and commercial chitosan was used to validate the method.

Chitin can be dissolved only in a few solvents such as alkali, inorganic acids, highly concentrated formic acid, and N,N-dimethylacetamide (DMAc)-LiCl. Solubilisation of chitin in DMAc containing

5 % LiCl appears to be non-degradative[86], while acid solubilisation is accompanied by extensive simultaneous depolymerisation. However, this solvent system is notably toxic and inflammable, and its use is not advisable from a green and ecological perspectives. In the attempt of measuring MW and polydispersity of pulped chitin, its deacetylation to chitosan seems a promising alternative, producing a more soluble and easier to handle biopolymer. In this specific case 0.3 M CH_3COOH, 0.2 M $CH_3COONa + H_2O$ solvent system (pH 4.45) was used as eluent phase for GPC measurements, which have been reported in literature to be one of the best solvent systems for chitosan.

2 AIM OF THE WORK

The aim of this thesis was the development of a green one-pot method for chitin pulping using simple and readily-available ionic liquids.

Although there are several studies in this direction, the process is yet to be proven useful on an industrial scale. For this reason, it would be interesting to design alternative IL pulping methods in which we could design not only basicity (for the removal of proteins) but also acidity that would allow for the removal of the inorganic minerals such as $CaCO_3$. In essence, this study was focused on for the design of a single, inexpensive IL that would replace both the HCl and the NaOH from the industrial process to pulp crustacean shells in a single step. Four different ionic liquids, namely ammonium acetate ($[NH_4][CH_3COO]$), ammonium formate ($[NH_4][HC(O)O]$), hydroxylammonium acetate ($[NH_3OH][CH_3COO]$) and hydroxylammonium formate ($[NH_3OH][HC(O)O]$) have been tested. Each extraction was performed in two ways: using the IL as solid salt or synthesizing it *in-situ*, by sequential addition of the acid and base function or vice versa. This approach was evaluated to circumvent the need for prior synthesis of the IL and thus potentially reducing the cost, and to verify if some differences occurred with these two methods.

In a second part of the work, attention was focused on MW and polydispersity determination of the obtained pulped chitin with the best condition and IL tested previously. In order to avoid the use of hazardous and toxic solvent systems conventionally used for this purpose, pulped chitin was further deacetylated to chitosan with alkali solution under heterogeneous conditions, and GPC analysis was performed using a safer and non-toxic solvent system consisting in an aqueous solution of acetic acid (0.3M) and sodium acetate (0.2M).

3 RESULTS AND DISCUSSION

3.1 Chemical composition of crab shells

As reported in Section 1.5, in nature chitin is closely associated with proteins, minerals, lipids, and pigments that have to be quantitatively removed to achieve a high purity pulped chitin. To establish the chemical composition of our initial substrate, ash, chitin, and protein content have been evaluated.

Ash content

Ash content have been determined using the Standard Test Method for Ash in Biomass (ASTM E1755-01) described in the experimental section. This test method covers the determination of ashes, expressed as the mass percent of residue remaining after dry oxidation (oxidation at 575 ± 25°C), of pre-treated biomass with acid and alkaline solutions. In this context the ash content is an approximate measure of the mineral content and other inorganic matter in our target substrate. The measure was performed in duplicate, and for each the ash percentage was calculated by the following equation:

$$\%ash = \frac{m_{ash} - m_{cont}}{m_{ar} - m_{cont}} \times 100$$

Equation 3.1: equation used in this work for ash content determination.

Where %ash is equal to mass percent of ashes, based on 105°C oven-dried mass of the sample; m_{ash} represents the mass of ash and container (g); m_{cont} is the tare mass of container (g); m_{ar} is the initial mass of prepared biomass sample and container (g).

A representative picture of the ash residue and the obtained results are reported in Figure 3.1 and Table 3.1 respectively.

Figure 3.1: Photograph of ash residue in spider crab shell after treatment.

Table 3.1: Ash content in spider crab shells.

Sample	Ash content (%)	Mean Value (%)
1	57.3	57.5
2	57.6	

Ash content value of 57.5 % is in good agreement with literature data[54], although in this case ash amount is slightly lower. These results demonstrate that inorganic matter constitute the major component of crab shells substrate, so its effective and total removal is of primary concern in order to isolate pure chitin.

Protein content

Protein content was evaluated by performing chemical deproteinization on crab shells residue, adapting a procedure described in literature[59]. Protein percentage was extrapolated using the following formula:

$$\%proteins = 100 - (\frac{m_{residue}}{m_{\,biomass}} \times 100)$$

Equation 3.2: Equation used in this work for protein content determination.

Where $m_{residue}$ is the total dry mass of residue free of proteins and $m_{biomass}$ refers to dry mass of starting crab shells. The measure was repeated three times and the average calculated (see table 3.2).

Table 3.2: Protein content in spider crab shells.

Sample	Protein content [%]	Average protein content [%]
1	24.2	21
2	19.8	
3	19.2	

The protein content of the first product exceeds the others by ca. 5%. This may be due experimental errors or to non-homogeneous distribution of protein in the starting material. Nevertheless, these results are in agreement with literature data[54] reported for *Maja squinado* species.

Chitin content

Chitin percentage of 17 %was estimated by applying the conventional chemical extraction method to separate the totality of impurities from the chitin-containing solid fraction. To ensure the effectiveness of this method, the extract was further characterized by ^{1}H-NMR and FTIR analysis. All spectra and characterization data will be reported in the section concerning chemical extraction method (see section 3.2 Chemical extraction)

Calcium salts quantification

To perform a quantitative estimation of calcium salts content, with relation principally to calcium carbonate, ICP-OES analysis were performed on crab shells (*Maja Squinado*) residues. The results are reported in table 3.3.

Table 3.3: ICP-OES results. [a]: calculated with the hypothesis that all calcium is in form of carbonate salt.

Entry	Quantity (mg)	Ca (µg/L)	Ca (%)	$CaCO_3$ (%)[a]
crab shell (starting material)	19.53	402600	20.61	51.50

It is clear that calcium salts are the major components of spider crab shells, accounting for more than 50 wt% on dry basis. This result is also consistent with ash content analysis and shows that almost 90% of ash residue in the starting material is due to presence of calcium salts.

Lipids, carotenoids and metal traces constitute only a minor fraction of the matrix. The results of our compositional study are summarized in the pie chart reported below (see figure 3.2). The results are in agreement with previous works, focused on spider crab shells of *Maja Squinado* species. Only a slight difference can be observed, maybe likely due to experimental error while weighing the samples or by the variation occurring in the initial substrate. It is well known that chemical composition in marine sources is strongly affected by the diet of the species, seasonal variation, sex and larval stage, so these minimal changes are not surprising.

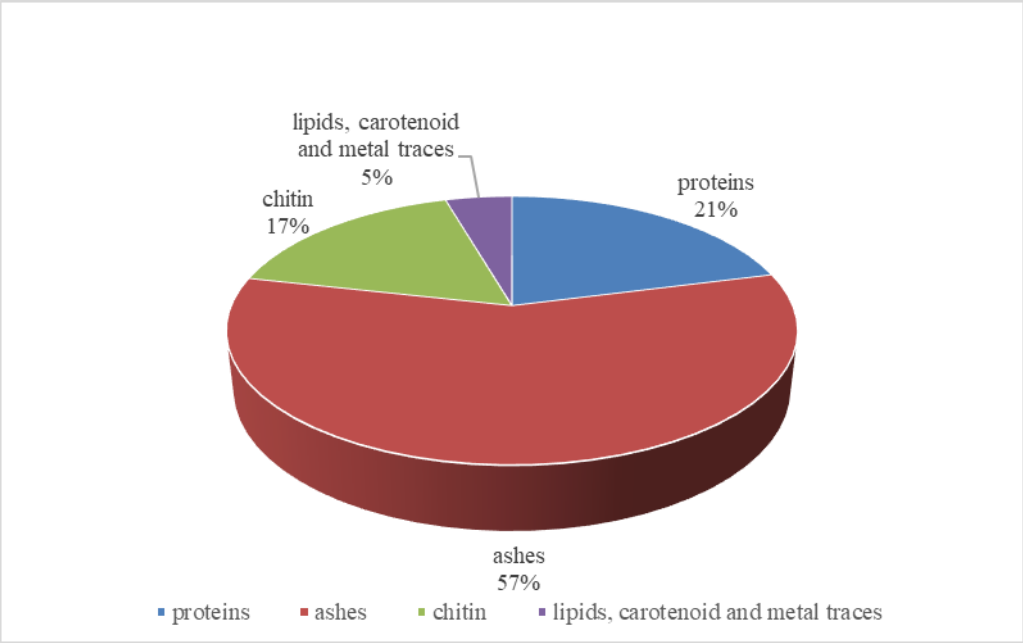

Figure 3.2: Pie chart representing all major components of spider crab (*Maja squinado*).

3.2 Chemical extraction

Chemical extraction was performed by adapting a procedure reported in literature[59]. Spider crab shells were treated as explained in detail in section 1.5.1. Briefly: the biomass was subjected to subsequent acidic and basic treatments and after every step the product was washed until neutral pH and dried in a vacuum oven.

Chitin extract was obtained as a white solid and its purity and DA were confirmed by ^{1}H-NMR and FTIR analysis. The results, compared to commercial chitin from shrimp shells, are reported below in figures 3.3 and figure 3.4 respectively.

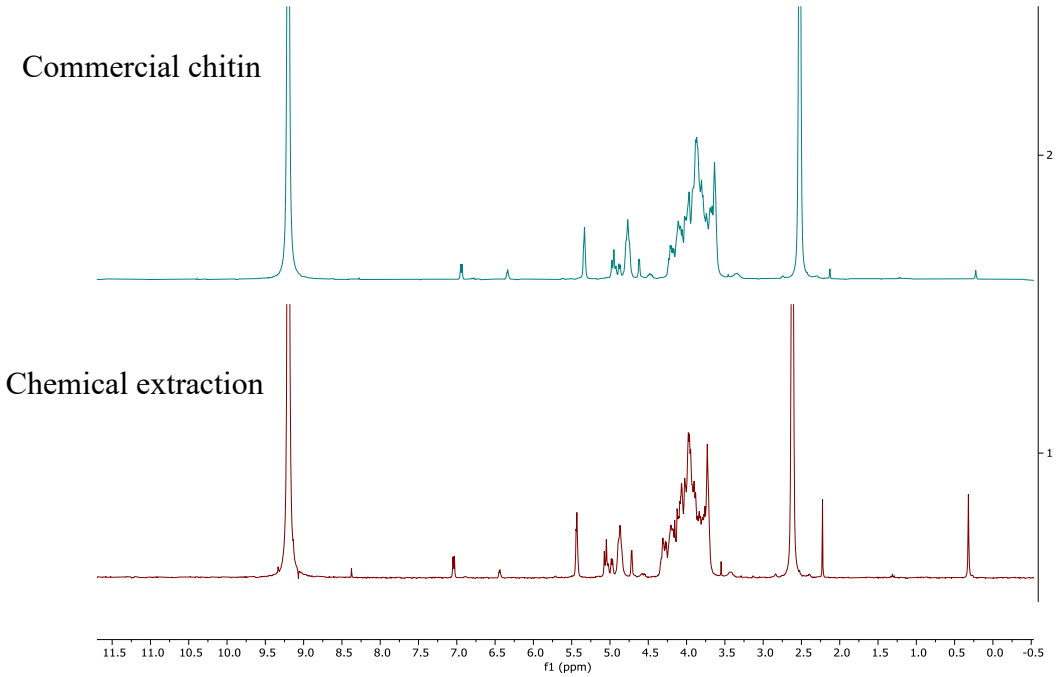

Figure 3.3: ^{1}H-NMR spectra (300 MHz) of commercial chitin (top) and chitin extracted with chemical method (bottom) in DCl at 25°C. Chemical shifts are given relative to TMS at 0.00 ppm.

The two NMR spectra present all the characteristic resonances associated with chitin. Comparative analysis showed that chitin extracted with the chemical method was more prone to deacetylation under acidic treatment (necessary for complete dissolution of the sample). In fact, in the second spectrum the signals associated with acetic acid at 2.16 ppm and H-2 proton of de-N-acetylated units resulted to be more intense.

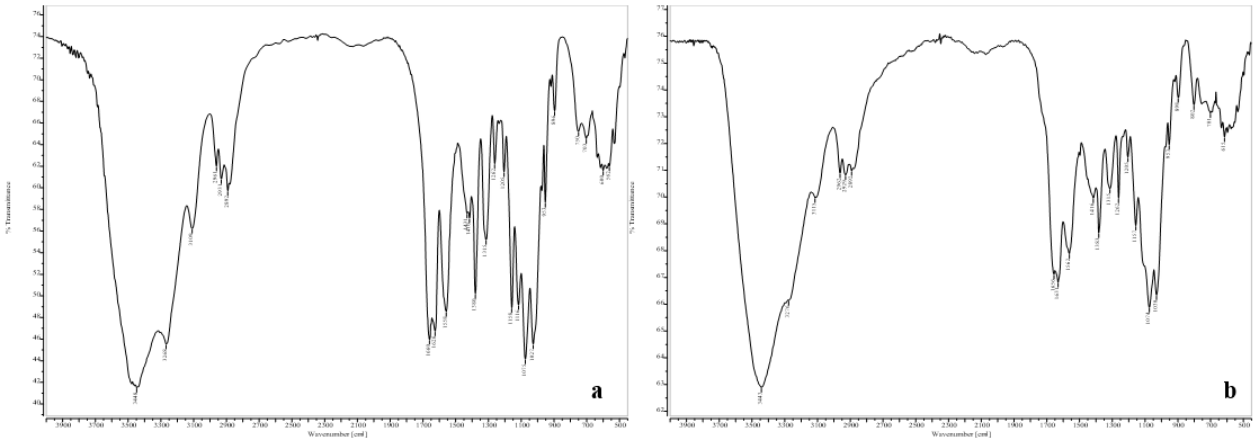

Figure 3.4: FT-IR spectrum of commercial chitin (a) and chitin extracted with chemical method (b).

The two IR spectra present all the characteristic peaks associated with chitin vibrational spectrum. In this case only one difference can be observed, associated with the signal of ν (C-O) at 1116 cm^{-1},

that in the chitin extracted with chemical method shows bad resolution and lower transmittance values.

3.3 Pulping with ammonium acetate

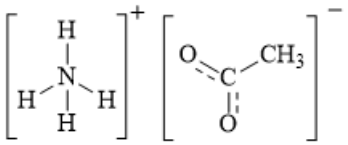

Figure 3.5: Chemical structure of ammonium acetate.

Each extraction was performed in two ways: using the neat IL as solid salt or synthesizing it *in-situ*, by sequential addition of acetic acid and ammonia aqueous solution 30-33 wt% or vice versa. All the experiments were performed in triplicate to ensure reproducibility.

In all cases, a 10 wt % of loading of biomass was used with respect to total mass of solution (IL and biomass), on basis of a previously reported work[68], 5 times higher than the chemical extraction method (< 2 wt %).

Concerning the solid salt, ground crab shells were mixed with solid $[NH_4][OAc]$ and the solution was heated at 145 °C for two hours. At the end of the reaction the mixture was diluted with DI water, a yellowish solid precipitated while impurities were confined in the aqueous phase. The solid was centrifuged and washed with water to neutral pH and dried in oven overnight under reduced pressure. The same procedure has been employed when ammonium acetate was formed *in situ* by sequential addition of the acid and base. At first, to perform the reaction in batch conditions and to avoid water evaporation, the reaction temperature was set to 100°C.

Table 3.4: Experimental condition tested with ammonium acetate.

	Entry	Temperature (°C)	Reaction time (min)	Yield (%)
Solid salt (m.p. 114°C)	1	145	120	16.4
A + B	2	100		30.0
	3	145		17.1
B+A	4	100		26.5
	5	145		22.9

It has to be noted that in the case of solid salt, the reaction temperature was increased to 145 °C (table 3.4, entry 1) due to higher melting point of the salt (m.p. 114°C), in comparison with the correspondent aqueous reagents. The chosen temperature is almost 30 °C higher with respect to the IL m.p. to avoid the recrystallization of the IL on the flask neck. For coherence. the tests with the *in situ* IL were then performed also at 145 °C in autoclave in order to have a better comparison of the results obtained with the solid ammonium acetate. At this temperature the yields of the pulping procedures (16.4 %, 22.9% and 17.1%; see Table 3.4 entries 1, 3 and 5), indicated that the reaction was more efficient operating at higher temperature of 145 °C for both solid salt or formed *in situ*.

To verify the purity of the pulped-material, TGA and ICP-OES were performed on the samples of chitin obtained with solid ammonium acetate and formed *in situ* by sequential addition of acid and base or vice versa at 100°C (see table 3.4, entries 1, 2, 4). FTIR and ^{1}H-NMR analysis were carried out for all condition tested. Characterization results will be described in the following paragraphs.

In figure 3.6 TGA curves for the three conditions tested are shown.

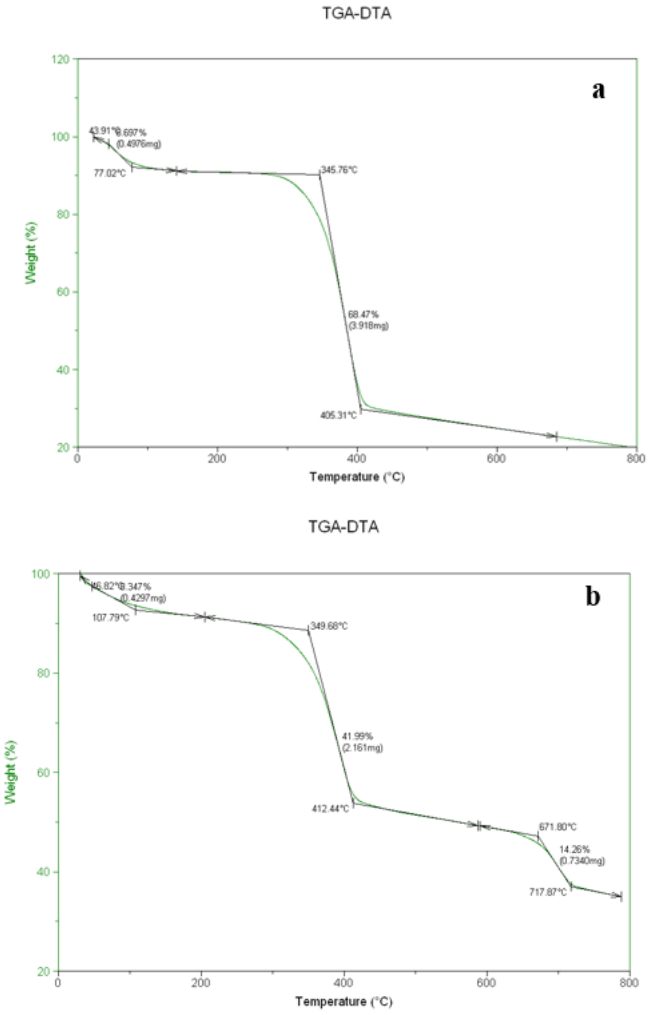

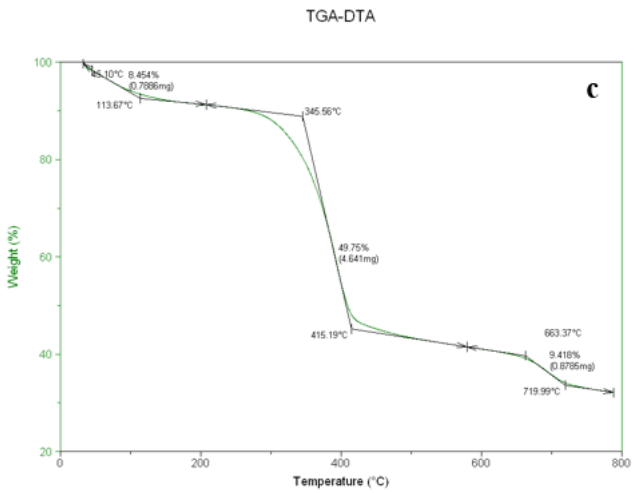

Figure 3.6: TGA-DTA curves of chitin extracted with ammonium acetate in the forms of solid salt at 145 °C (**a**), and prepared in situ by sequential addition of acid and base (**b**) or base and acid (**c**) at 100°C.

In all cases two main weight-losses can be observed: the first weight-loss in the range 40-115 °C accounting for 8-9 wt% was due to water bonded to chitin chains, and a second weight loss between 345- 415°C % accounting for 42-69 wt%, caused by depolymerisation/decomposition of polymer chains through deacetylation and cleavage of glycosidic linkages. At higher temperature, in the range 415-670 °C a progressive weight-loss can be observed. As previously described, it may be due to the thermal destruction of pyranose ring and the decomposition of the residual carbon. A third and clearly visible weight loss is present in Figure 3.6 **b** and 3.6 **c**, due to release of CO_2, which is indicative of the presence of residual calcium carbonate in the pulped chitin.

To quantify the total amount of calcium salts in the pulped-chitins, ICP-OES analysis were performed. The results are summarised in table 3.5.

Table 3.5: ICP-OES results for chitin pulped with solid ammonium acetate or formed in situ at 100°C in batch conditions. [a]: calculated with the hypothesis that all calcium is in form of carbonate salt; [b]: calcium carbonate content from TGA analysis [C]: obtained from subtraction of the two previous values (A-B).

IL form	Entry	Quantity (mg)	Ca (µg/L)	Ca (%)	$CaCO_3$ (%)[a]	$CaCO_3$ (%) from TGA [b]	Other Calcium salts (%) [c]
Solid salt	1	15.55	26360	1.69	4.20	0	4.2
(A+B)	2	25.56	334100	13.07	32.70	14.26	18.44
(B+A)	3	24.81	184800	7.44	18.60	9.42	9.18

The relative percentage of calcium in each sample was then obtained from the quantity of calcium, expressed in µg/L. Considering the molecular and atomic weight of calcium carbonate and elemental

calcium respectively, the value of calcium carbonate and other calcium salts can be extrapolated. In all cases calcium salts are present, and in the case of ILs formed *in situ* their content is significant. From these results it can be deduced that in this case reaction temperature is a key parameter for the effectiveness of demineralization of crab shells residues. In fact the solid salt seems to be more efficient in calcium salts removal, maybe due to the higher temperature of 145 °C tested with respect of *in situ* formed IL at 100°C.

^{1}H-NMR was employed to verify the presence of protein residues in the pulped material and to quantify the DA% of all samples. In figure 3.7 a comparison between the pulping procedures with ammonium acetate has been reported.

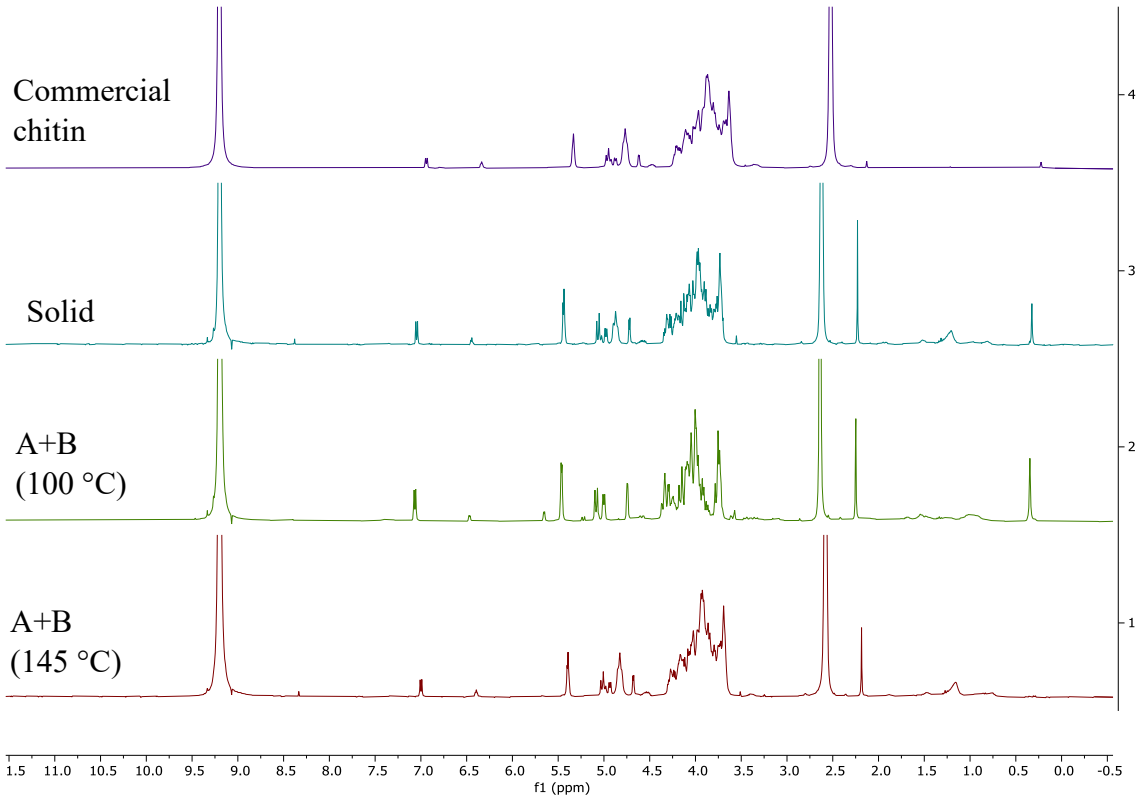

Figure 3.7: Comparison of ^{1}H-NMR spectra (300 MHz) of commercial chitin (purple), chitin pulped with ammonium acetate as solid salt (blue), chitin extracted adding acid + base (green) and base + acid (red). Dissolved in concentrated DCl at 25°C. Chemical shifts are given relative to TMS at 0.00 ppm. A: acid; B: base.

From all ^{1}H-NMR spectra, chitin structure and relative signals are clearly present. Furthermore, between 1.0 and 1.5 ppm the resonances of methyl-proton from protein in the sample are present, although in small quantity. The spectrum of the treatment with the *in situ* formed IL by sequential addition of base and then acid was very similar and was not reported for simplicity.

To verify that the resonances between 1.0 – 1.5 ppm were ascribable to proteins as indicated in the literature, chemical deproteinization was performed on a representative pulped chitin sample, in which signals between 1.0-1.5 ppm were clearly evident. NMR spectra of pulped chitin before and after DP were registered, and the results are reported in figure 3.8.

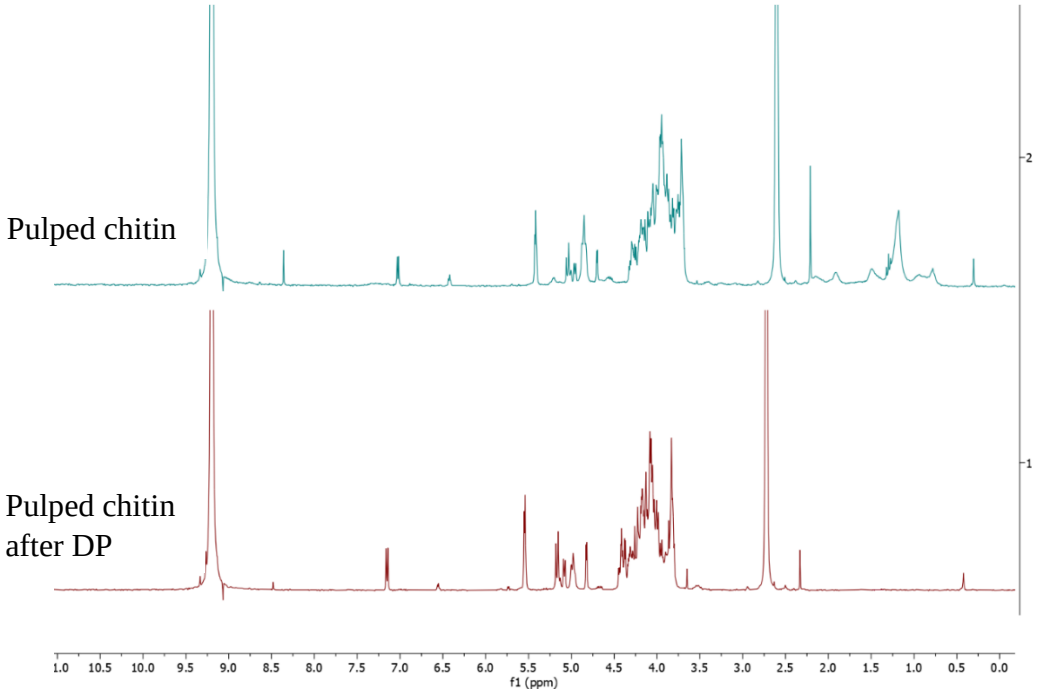

Figure 3.8: ^{1}H-NMR spectra (300 MHz) of a representative sample of pulped chitin before (top) and after (bottom) chemical deproteinization, dissolved in concentrated DCl at 25°C. Chemical shifts are given relative to TMS at 0.00 ppm.

NMR results confirm that the signals under discussion are unambiguously attributable to methyl protons of proteins, and that harsh DP conditions are efficient for their removal. We can conclude that the five procedures studied employing ammonium acetate were not able to remove all the protein residues, probably because of the limited acidity of the IL in respect to the traditional acids used in the chemical extraction.

From all spectra, both the equations described in section 2.7 were used to calculate the DA (results in table 3.6).

Table 3.6: DA of samples pulped with ammonium acetate.

IL form	Entry	Temperature (°C)	Method 1 DA%	Method 2 DA%
Solid salt	1	145	98.8	98.8
A+B	2	100	88.2	92.8
	3	145	95.7	92.0
B+A	4	100	96.6	97.4
	5	145	98.5	98.6

Partial deacetylation occurred during dissolution of all samples in the deuterated solvent causing an increase of the signals related to acetic acid and H-2 proton of de-N-acetylated chitin. This was taken into account in all calculation methods in order to avoid underestimation of DA. Results shows that the two methods are in good agreement, though in all cases DA calculated with method 1 are slightly inferior. Considering that partial de-N-acetylation occurred in the solvent used for NMR analysis and errors in the integration, these values are only indicative of DA. In any case, it was found that chitin pulped with ammonium formate has DA > 85%.

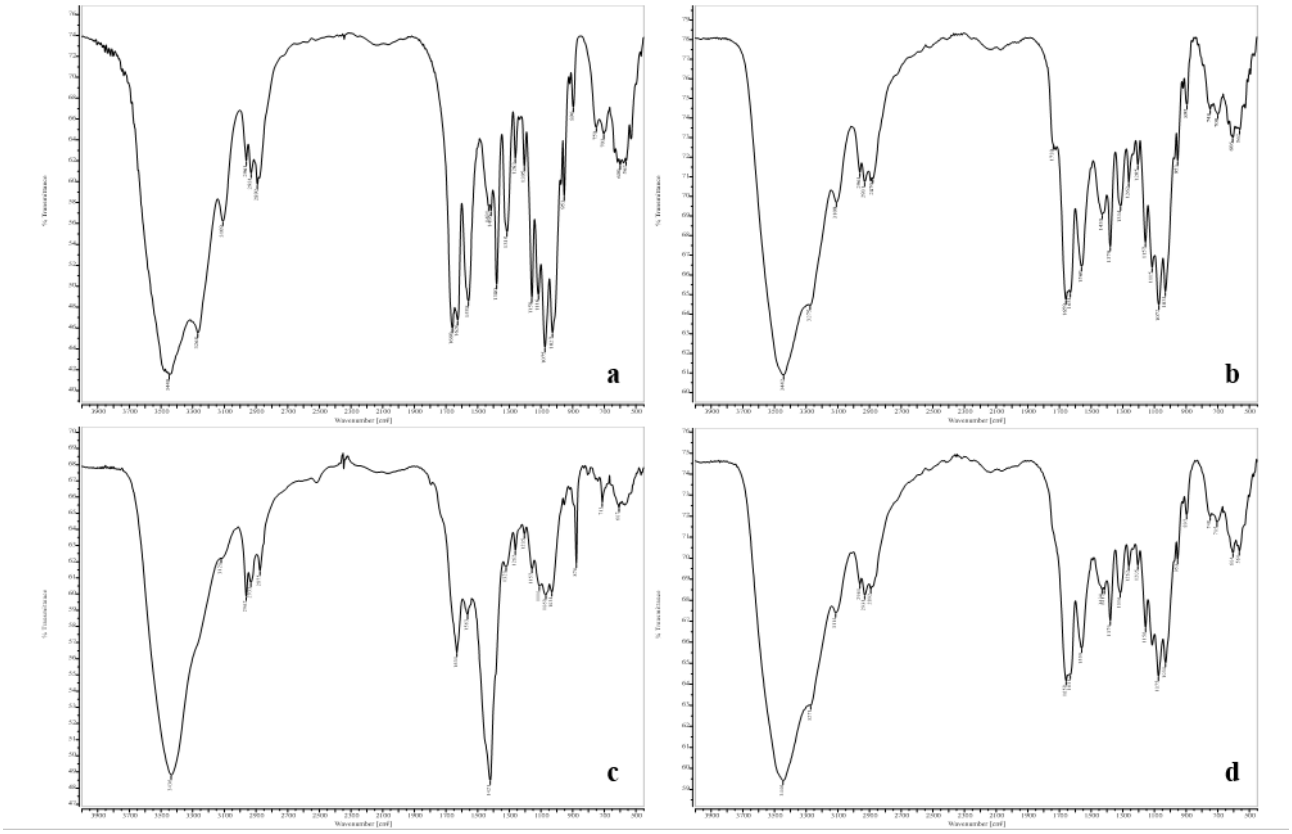

Figure 3.9: FT-IR spectrum of commercial chitin (**a**) and chitin pulped with ammonium acetate in the form of solid salt (**b**) or prepared in situ by sequential addition of acid and base at 100 °C (c) and 145 °C (**d**).

As can be clearly deduced from Figure 3.9, all FT-IR spectra show all characteristic signals associated with chitin and are comparable to commercial sample. Only in the sample treated at 100 °C signals associated with calcium carbonate are present (1420-30 cm^{-1} and 874 cm^{-1}), demonstrating that harsh reaction condition of 145 °C improved the demineralization process, allowing better purification of the pulped material.

All experimental results obtained with ammonium acetate suggest that basic and acidic functions of the IL promote pulping albeit with incomplete removal of inorganic components and protein. Better results are achieved only at higher temperature of 145 °C.

3.4 Pulping with ammonium formate

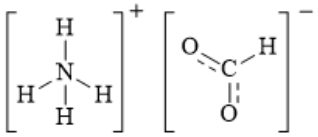

Figure 3.10: Chemical structure of ammonium formate.

Each extraction was performed in two ways: using the IL as solid salt or synthesizing it *in-situ*, by sequential addition of acetic acid and ammonia solution 30-33 wt% or vice versa. All the experiments were performed in triplicate to verify the reproducibility of the proposed method.

In all cases, a 10 wt % of loading of biomass was used with respect to total mass of solution (IL and biomass), on basis of a previously reported work[68], 5 times higher than the chemical extraction method (< 2 wt %).

Concerning the solid salt, ground crab shells were mixed with solid $[NH_4][HC(O)O]$ and the solution was heated at reflux (130 °C) for two hours. At the end of the reaction the mixture was diluted with DI water, a yellowish solid precipitated while impurities were confined in the aqueous phase. The solid was centrifuged and washed with water to neutral pH and dried in oven overnight under reduced pressure. The same procedure has been employed when ammonium formate was formed *in situ* by sequential addition of the acidic and basic functionalities. At first, to perform the reaction in batch conditions and to avoid water evaporation, the reaction temperature was 100°C.

Table 3.6: Experimental condition tested with ammonium formate.

IL form	Entry	Temperature (°C)	Reaction time (min)	Yield (%)
Solid salt (m.p. 119°C)	1	130	120	20.3
A + B	2	100		17.2
	3	130		17.2
B+A	4	100		17.6
	5	130		18.8

It has to be noted that in the case of solid salt, reaction temperature was increased to 130 °C (table 3.7, entry 1) due to higher melting point of the salt (m.p. 119°C), in comparison with the correspondent aqueous reagents. The tests with the *in situ* IL were then performed also at 130°C in autoclave in order to have a better comparison of the results obtained with the solid ammonium formate. In this case no substantial differences between the two tested temperatures were observed in terms of product yield.

To verify the purity of the pulped-material, TGA and ICP-OES were performed on chitin pulped with solid ammonium acetate and formed *in situ* by sequential addition of acid and base (or vice versa) at 100°C (see table 3.7, entries 1, 2, 4). FTIR and ^{1}H-NMR analysis were carried out for all condition tested. Characterization results will be described in the following paragraphs.

In figure 3.11 TGA curves for the three conditions tested are shown.

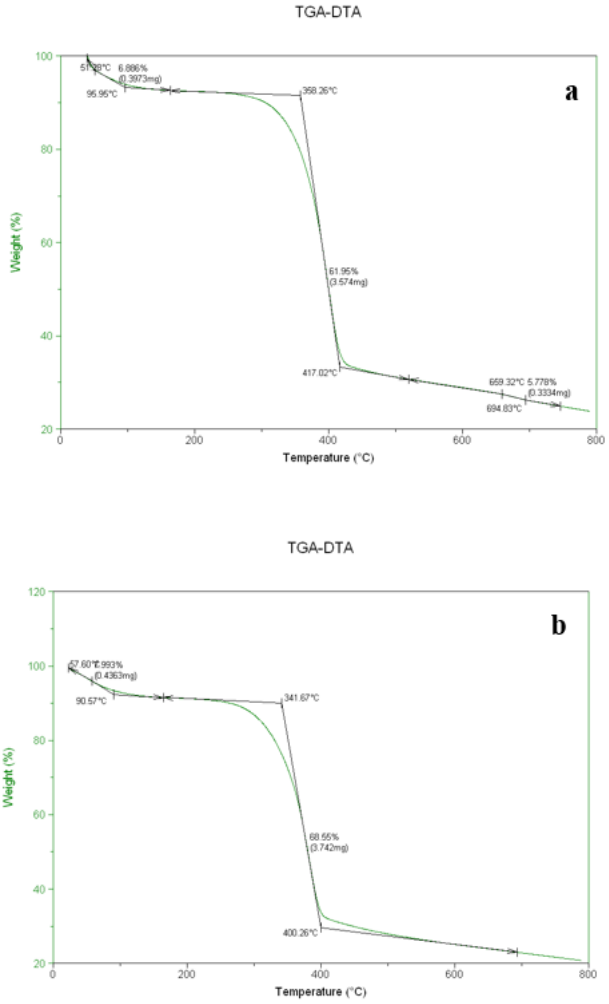

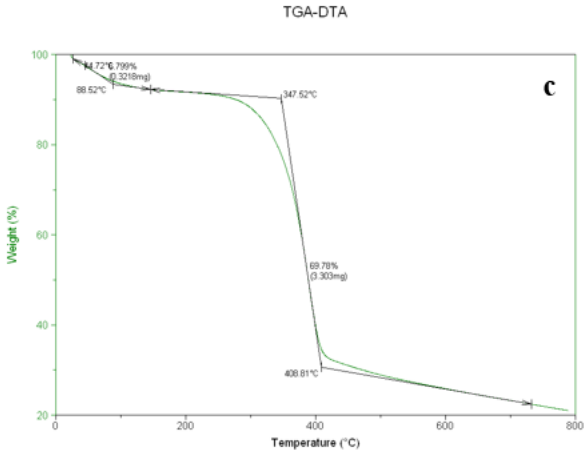

Figure 3.11: TGA-DTA curves of chitin extracted with ammonium formate in the form of solid salt (**a**), and prepare in situ by sequential addition of acid and base (**b**) or base and acid (**c**) at 100°C.

In all cases two main weight-losses can be observed: the first weight-loss in the range 44-96 °C accounting for 6-8 wt% due to water loss, and a second weight loss between 341- 417°C % accounting for 61-70 wt%, caused by depolymerisation/decomposition of polymer chains through deacetylation and cleavage of glycosidic linkages. At higher temperature, in the range 417-660 °C a progressive weight-loss can be observed, that may be due to the thermal destruction of pyranose ring and the decomposition of the residual carbon. A third and clearly visible weight loss is present only in chitin pulped with solid ammonium formate (Figure 3.11 **a**), due to release of CO_2 accounting for ca. 5.78 wt% loss, which is indicative of the presence of residual calcium carbonate, while whit ammonium formate prepared *in situ* the curve is absent. This indicate that the sequential addition of acid and base is effective in calcium salts removal. This fact may be due to the use of aqueous reagents and their minor viscosity, which allow better penetration of chemicals in chitin chains domain thus removing all $CaCO_3$ residue.

This fact was also confirmed by ICP-OES analysis, and the results are reported in table 3.8.

Table 3.8: ICP-OES results for chitin pulped with solid ammonium formate or formed in situ at 100°C in batch conditions. [a]: calculated with the hypothesis that all calcium is in form of carbonate salt; [b]: calcium carbonate content from TGA analysis [C]: obtained from subtraction of the two previous values (A-B).

IL form	Entry	Quantity (mg)	Ca (µg/L)	Ca (%)	$CaCO_3$ (%)[a]	$CaCO_3$ (%) from TGA [b]	Other Calcium salts (%) [c]
Solid salt	6	20.09	87280	4.34	10.85	5.78	5.07
A+B	7	20.24	8428	0.42	1.05	0	1.05
B+A	9	17.92	8568	0.48	1.20	0	1.20

ICP-OES results shows that, using the IL prepared in-situ, only a maximum of 1.2 % of calcium salts are present in the pulped material. When performing the reaction with the solid salt, this quantity was almost ten times greater.

^{1}H-NMR was employed to verify the presence of protein residues in the pulped material and to quantify the DA% of all samples. In figure 3.12 a comparison between the pulping procedures tested with ammonium formate has been reported.

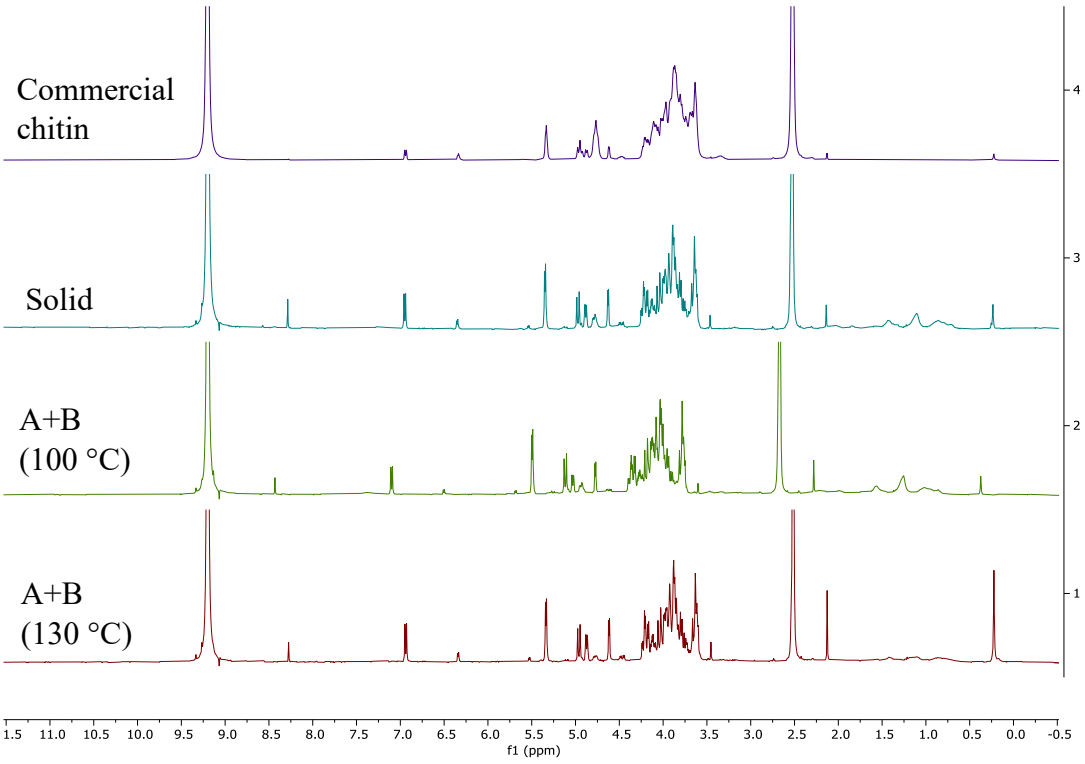

Figure 3.12. Comparison of ^{1}H-NMR spectra (300 MHz) of commercial chitin (purple), chitin pulped with ammonium formate as solid salt (blue), chitin extracted adding acid + base at 100°C (green) and at 130°C (red). Dissolved in concentrated DCl at 25°C. Chemical shifts are given relative to TMS at 0.00 ppm. A: acid; B: base.

From all ^{1}H-NMR spectra, all signals associate with chitin are clearly present. Furthermore between 1.0 and 1.5 ppm the resonances of methyl-proton from proteins in the sample are present, although in small quantity. The spectrum concerning the treatment with the *in situ* formed IL by sequential addition of base and then acid was very similar and were not reported for simplicity.

Both the equations described in section 2.7 were used to calculate the DA (results in table 3.9) from all spectra.

Table 3.9: DA values of chitin pulped with ammonium formate.

IL form	Entry	Temperature (°C)	Method 1 DA%	Method 2 DA%
Solid salt	1	130	94.2	95.0
A+B	2	100	96.7	96.5
	3	130	94.9	95.9
B+A	4	100	94.0	95.1
	5	130	86.1	90.5

Partial deacetylation occurred during dissolution of all samples in the deuterated solvent causing an increase of the signals related to acetic acid and H-2 proton of de-N-acetylated. This was taken into account in all calculation methods in order to avoid underestimation of DA. The two methods used are in good agreement, though DA value of samples treated with the in situ formed IL at 130 °C by addition of basic prior than acid (table 3.9, entry 5) differs ca. 4.5%. In all cases DA calculated with method 1 are slightly inferior. Considering that partial de-N-acetylation occurred in the solvent choose for the analysis and that possible error in the integration and/or interpretation of the spectra could have been made, these values are not precise and only indicative of DA. In conclusion it was found that chitin pulped with ammonium formate has DA > 86%.

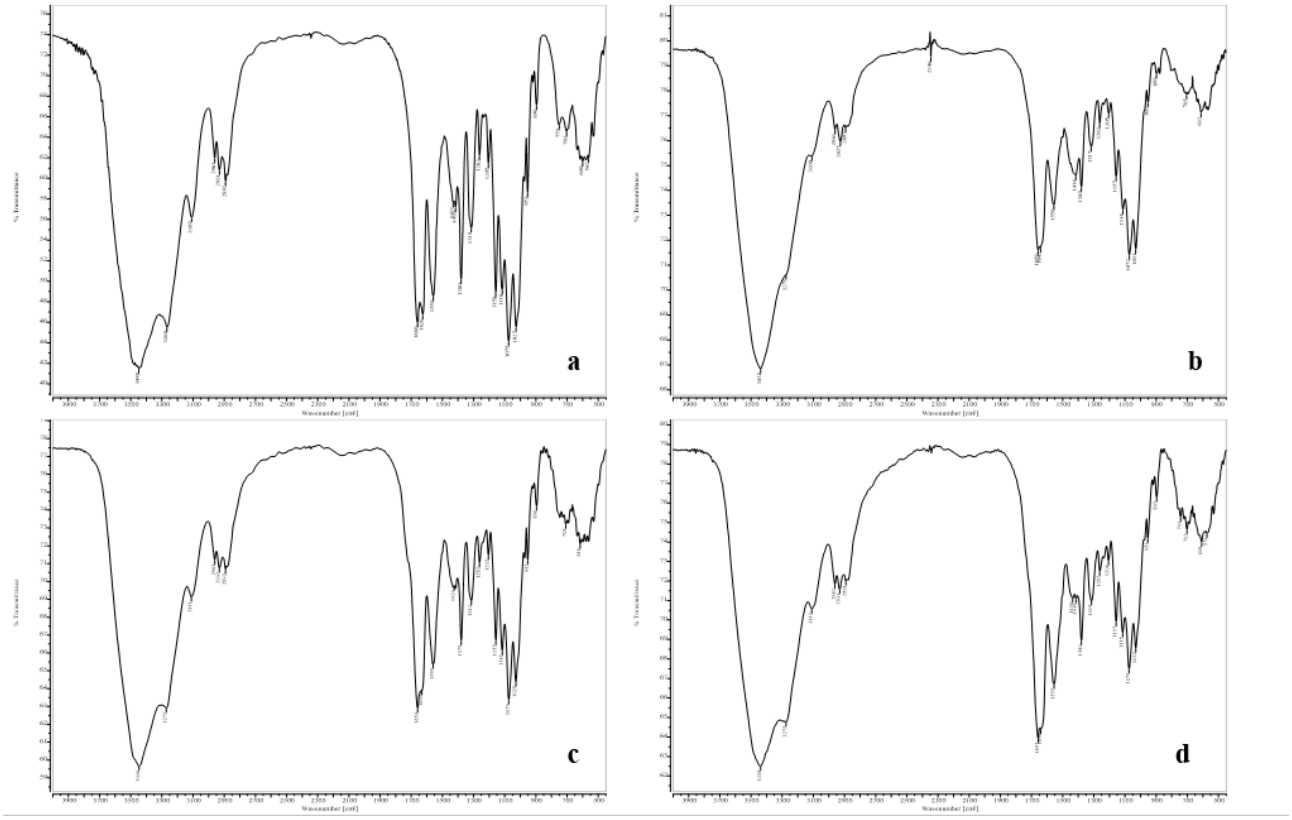

Figure 3.13: FT-IR spectrum of commercial chitin (**a**) and chitin pulped with ammonium formate in the form of solid salt (**b**) or prepared in situ by sequential addition of acid and base at 100 °C (c) and 145 °C (**d**).

As can be clearly deduced from Figure 3.13, the FT-IR spectra showed all characteristic signals associated with chitin and they are comparable to commercial sample. From pure FT-IR analysis no signals associated with carbonate salts could be detected, confirming that ammonium formate is effective in minerals removal.

3.5 Pulping with hydroxylammonium acetate

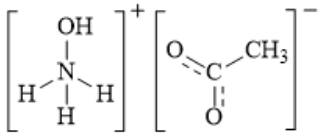

Figure 3.14: Chemical structure of hydroxylammonium acetate.

Each extraction was performed in two ways: using the IL as solid salt or synthesizing it *in-situ*, by sequential addition of acetic acid and hydroxylamine aqueous solution 50 wt% or vice versa. All the experiments were performed in triplicate to verify the reproducibility of the method proposed.

In all cases, a 10 wt % of loading of biomass was used with respect to total mass of solution (IL and biomass), on basis of a previously reported work[68], 5 times higher than the chemical extraction method (< 2 wt %).

In this case solid hydroxylammonium acetate was prepared in our laboratory according to a reported procedure[68]. Hydroxylamine solution 50 wt% was kept under magnetic stirring at 0 °C. Acetic acid was added dropwise to the stirring solution and then was allowed to heat to room temperature and stirred overnight. The mixture was then gently purged with air and heated to concentrate the solution. The precipitate was washed with methanol and diethyl ether to remove residual acetic acid in the product and dried in oven under reduced pressure (15 mbar) overnight. The final product was obtained as a white solid and was fully characterised by NMR spectroscopy (^{1}H and ^{13}C) using DMSO-d_6 and D_2O as solvents. TGA analysis was also performed to confirm the purity of the product (see appendix section).

After solid salt IL synthesis, the general procedure of pulping previously described has been applied. Concerning the solid salt, ground crab shells were mixed with solid $[NH_3OH][CH_3COOH]$ and the solution was heated at 100 °C for two hours. At the end of the reaction the mixture was diluted with DI water, a yellowish solid precipitated while impurities were confined in the aqueous phase. The solid was centrifuged and washed with water to neutral pH and dried in oven overnight under reduced pressure. The same procedure has been employed when hydroxylammonium acetate was formed *in situ* by sequential addition of the acidic and basic functionalities.

All condition tested are summarized in table 3.10.

Table 3.10: Experimental condition tested with hydroxylammonium acetate.

IL form	Entry	Temperature (°C)	Reaction time (min)	Yield (%)
Solid salt (m.p. 87°C)	1	100	120	29.3
A + B	2			19.9
B+A	3			20.7

In this case pulping experiments could be performed at 100 °C in batch for all conditions, due to the low melting point of hydroxylammonium acetate (m.p. 87 °C). Yields deviate from theoretical chitin content in crab shells (17%), especially for pulping with hydroxylammonium acetate in the form of solid salt.

To verify the purity of the pulped-material, TGA, ICP-OES, FTIR and ^{1}H-NMR were performed on pulped chitin for all condition tested. Characterization results will be described in the following paragraphs.

In figure 3.15 TGA curves for the three conditions tested are shown.

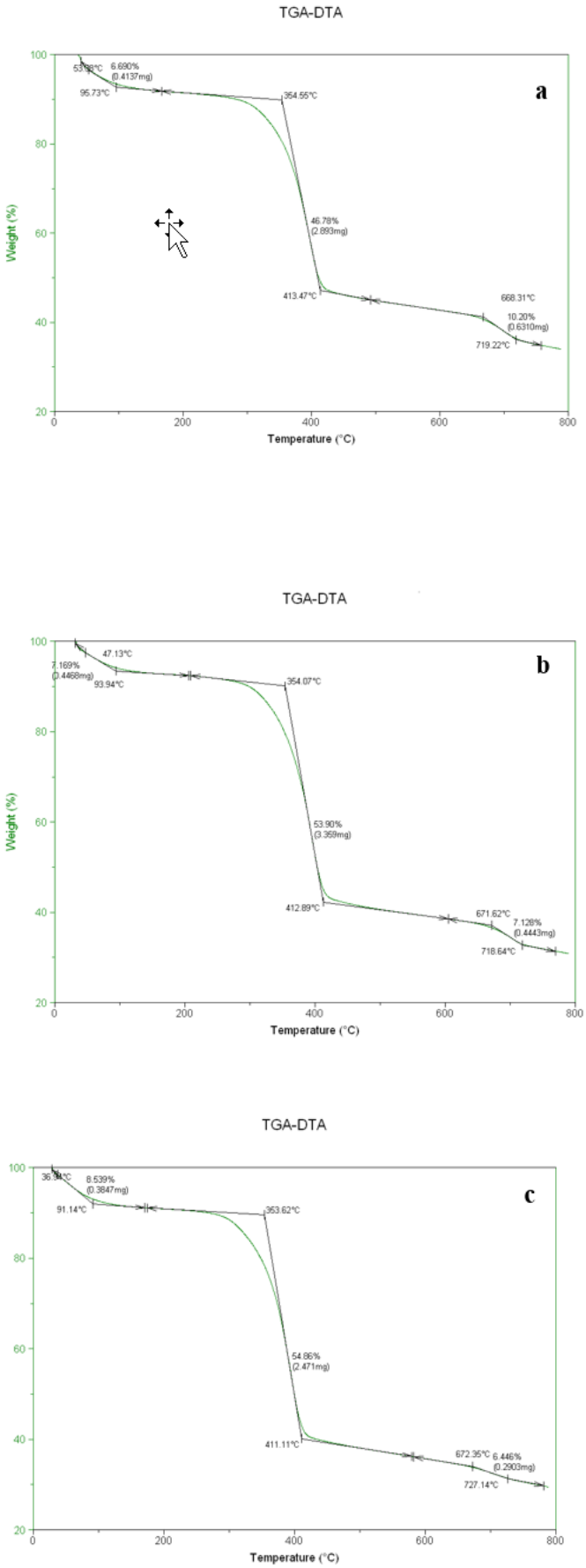

Figure 3.15: TGA-DTA curves of chitin extracted with hydroxylammonium acetate in the form of solid salt (**a**), and prepared in situ by sequential addition of acid and base (**b**) or base and acid (**c**) at 100°C.

In all cases three main weight-losses can be observed: the first weight-loss in the range 37-97 °C accounting for 6-9 wt% due to water loss a second one between 354-414°C % accounting for 46-55 wt%, caused by depolymerisation/decomposition of polymer chains through deacetylation and cleavage of glycosidic linkages and a third weight loss due to release of CO_2 accounting for ca. 6-10 wt% loss, which is indicative of the presence of residual calcium carbonate. At higher temperature, in the range 414-670 °C a progressive weight-loss can be observed, that may be due to the thermal destruction of pyranose ring and the decomposition of the residual carbon. TGA results confirm that acetic acid as acidic function, which is responsible of the demineralization of crab shells matrix, is too weak and non-completely efficient in the removal of calcium salts. These assumptions are confirmed by ICP-OES results, summarized in table 3.11.

Table 3.11: ICP-OES results for chitin pulped with solid hydroxylammonium acetate or formed in situ at 100°C in batch conditions. [a]: calculated with the hypothesis that all calcium is in form of carbonate salt; [b]: calcium carbonate content from TGA analysis [C]: obtained from subtraction of the two previous values (A-B).

IL form	Entry	Quantity (mg)	Ca (µg/L)	Ca (%)	$CaCO_3$ (%)[a]	$CaCO_3$ (%) from TGA [b]	Other Calcium salts (%) [c]
Solid salt	11	37.75	560100	14.84	37.10	10.20	26.90
A+B	12	23.29	165700	7.11	17.80	7.13	10.67
B+A	13	25.00	244500	9.78	24.45	6.45	18.00

In this case, significant variations in calcium salts content can be observed. ILs prepared *in situ* seem more efficient in minerals removal, like in the previous experiments described, but in this case also the order of addition acid and base seems to play a crucial role. This can be due probably to the fact that previous treatment with acetic acid accomplishes partial demineralization, removing minerals which constitute the major component of crab shells, facilitating the deproteinization step performed by aqueous hydroxylamine. However, if it was the case, it is not clear why this phenomenon was observed only with this IL.

^{1}H-NMR was employed to verify the presence of protein residues in the pulped material and to quantify the DA% of all samples. In figure 3.16 a comparison between the pulping procedures tested with ammonium formate has been reported.

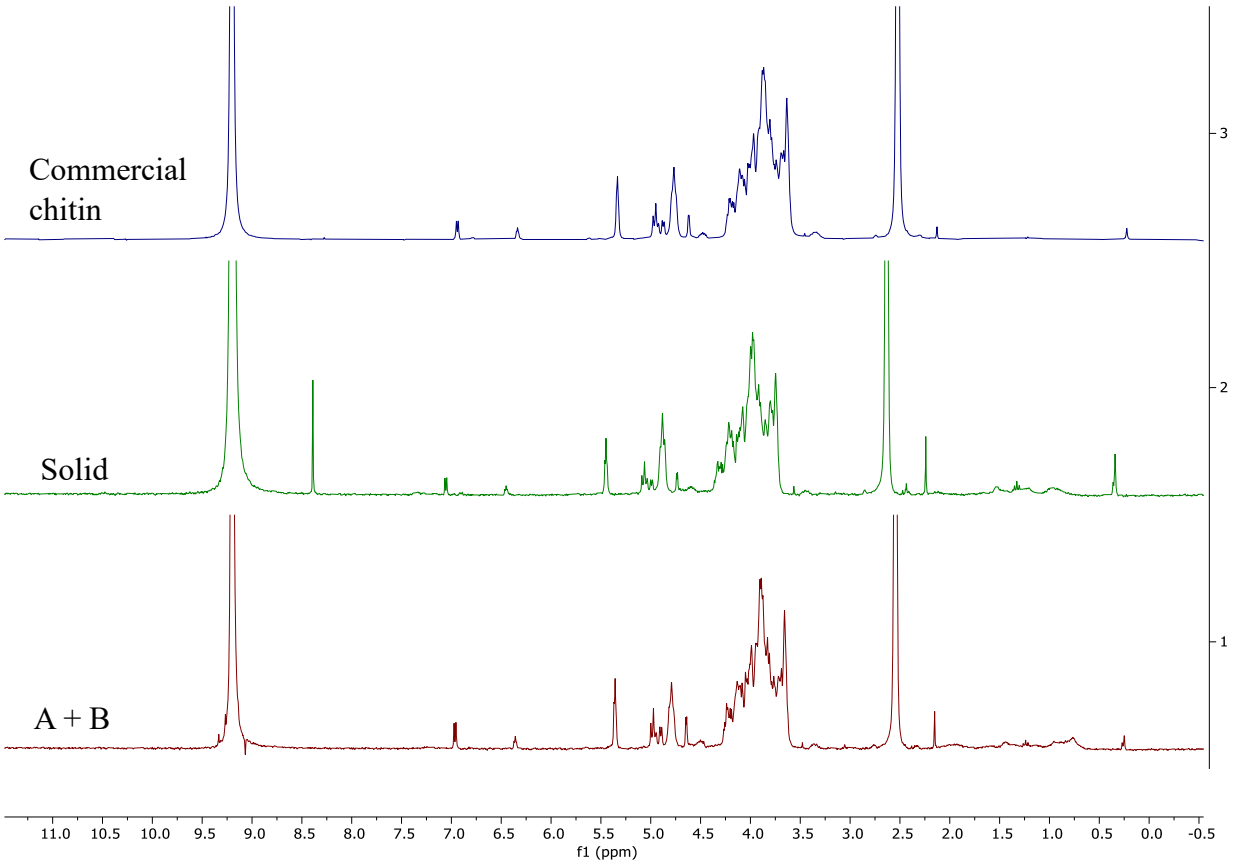

Figure 3.16: Comparison of ^{1}H-NMR spectra (300 MHz) of commercial chitin (blue), chitin pulped with solid hydroxylammonium acetate (green) and extracted adding acid + base (red) dissolved in concentrated DCl at 25°C. Chemical shifts are given relative to TMS at 0.00 ppm. A: acid; B: base.

NMR spectra show all characteristics signals associated with chitin. Signals associated with protein residues between 1.0 and 1.5 ppm are present as well, although their intensity seems inferior with respect to prior pulping methods proposed in this work.

From all spectra, both the equations described in section 2.7 were used to calculate the DA (results in table 3.12).

Table 3.12: DA values of chitin pulped with hydroxylammonium acetate.

IL form	Entry	Temperature (°C)	Method 1 DA%	Method 2 DA%
Solid salt	1	100	-	-
A+B	2	100	96.2	97.3
B+A	3	100	92.7	94.5

Partial deacetylation occurred during dissolution of all samples in the deuterated solvent causing an increase of the signals related to acetic acid and H-2 proton of de-N-acetylated. This was taken into

account in all calculation methods in order to avoid underestimation of DA. Results shows that the two method are in good agreement, though in all cases DA calculated with method 1 are slightly inferior. Considering that partial de-N-acetylation occurred in the solvent chosen for the analysis and possible errors in the integration of the spectra, these values should be considered indicative. DA for solid hydroxylammonium acetate salt was not calculated, because the signals associated with H-2 of internal de-N-acetylated units was strongly affected by background noise or possible impurities still present in the specific sample.

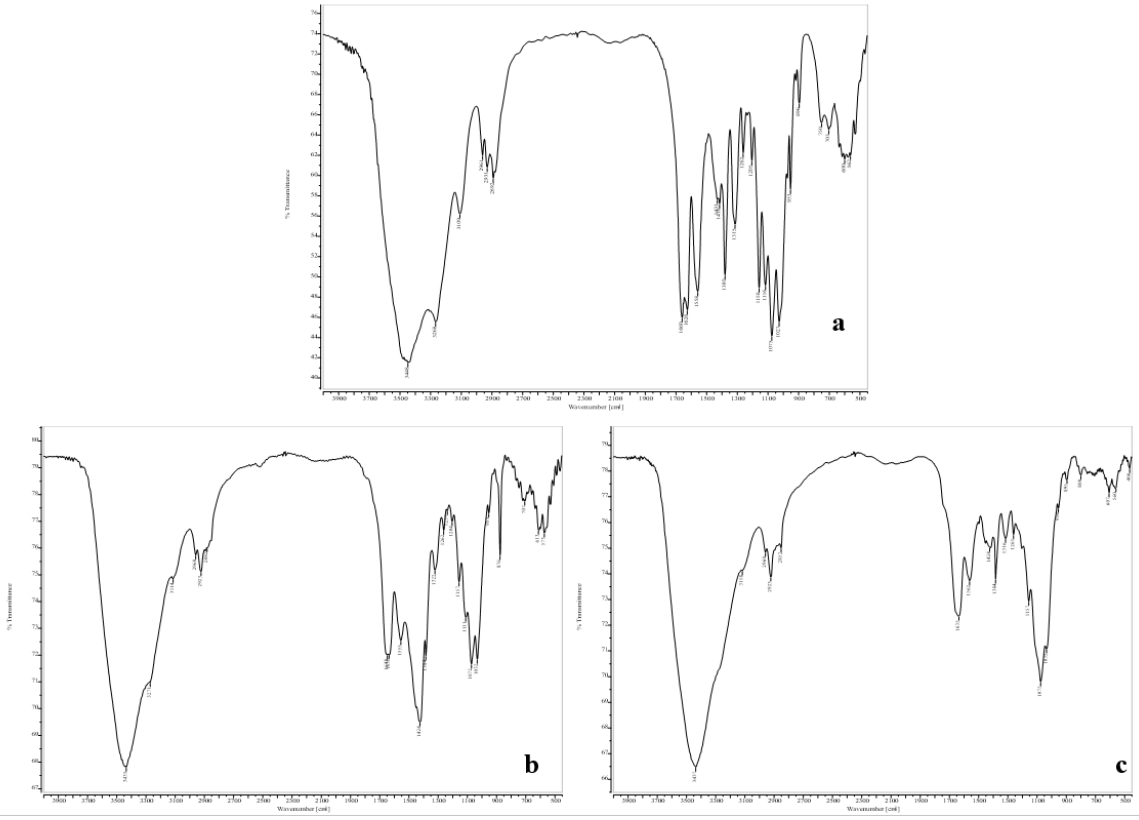

Figure 3.17: FT-IR spectrum of commercial chitin (**a**) and chitin pulped with hydroxylammonium acetate in the form of solid salt (**b**) or prepared in situ by sequential addition of acid and base at 100 °C (**c**).

As can be clearly deduced from Figure 3.17, all FT-IR spectra show all characteristic signals associated with chitin and are comparable to the commercial sample, but signals associated with calcium carbonate are present (1420-30 cm^{-1} and 876 cm^{-1}) with variable intensities, demonstrating that hydroxylammonium acetate is less effective in calcium salt removal.

3.6 Pulping with hydroxylammonium formate

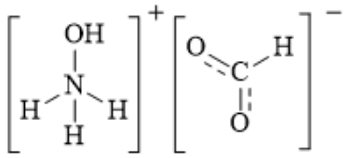

Figure 3.18: Chemical structure of hydroxylammonium formate.

Each extraction was performed in two ways: using the IL as solid salt or synthesizing it *in-situ*, by sequential addition of formic acid and hydroxylamine aqueous solution 50 wt% or vice versa. All the experiments were performed in triplicate to verify the reproducibility of the method proposed.

In all cases, a 10 wt % of loading of biomass was used with respect to total mass of solution (IL and biomass), on basis of a previously reported work[68], 5 times higher than the chemical extraction method (< 2 wt %).

Hydroxylammonium acetate in the form of solid salt was prepared in our laboratory according to a reported procedure[68]. Hydroxylamine solution 50 wt% was kept under magnetic stirring at 0 °C. Formic acid was added dropwise to the stirring solution and then was allowed to room temperature and stirred overnight. The mixture was then gently purged with air and heated to concentrate the solution. The precipitate was washed with methanol and diethyl ether to remove residual acetic acid in the product and dried in oven under reduced pressure (15 mbar) overnight. The final product was obtained as a white solid and was fully characterised by NMR spectroscopy (^{1}H and ^{13}C) using DMSO-d_6 and D_2O as solvents. TGA analysis was also performed to confirm the purity of the product (see appendix section).

After solid salt IL synthesis, the general procedure of pulping previously described has been applied. Ground crab shells were mixed with solid $[NH_3OH][HC(O)O]$ and the solution was heated at 100 °C for two hours. At the end of the reaction the mixture was diluted with DI water, a yellowish solid precipitated while impurities were confined in the aqueous phase. The solid was centrifuged and washed with water to neutral pH and dried in oven overnight under reduced pressure. The same procedure was used for hydroxylammonium acetate formed *in situ* by sequential addition of the acid and base.

All condition tested are summarized in table 3.13.

Table 3.13: Experimental condition tested with hydroxylammonium formate.

IL form	Entry	Temperature (°C)	Reaction time (min)	Yield (%)
Solid salt (m.p. 76°C)	1	100	120	22.2
A + B	2			16.8
B+A	3			16.6

Considering the pulping yields, it seems that complete chitin isolation was achieved with hydroxylammonium formate prepared *in situ*, while in the case of solid salt the yield was slightly higher with respect to the chitin expected in our substrate (17%), which could be indicative of some residual calcium carbonate or proteins in the product. Pulping reactions could be performed at 100 °C in batch for all conditions tested, due to the low melting point of hydroxylammonium formate (m.p. 76 °C). In this specific case, TGA and ICP-OES analysis were not performed. Only ^{1}H-NMR and FT-IR spectra were recorded, and the results are reported below.

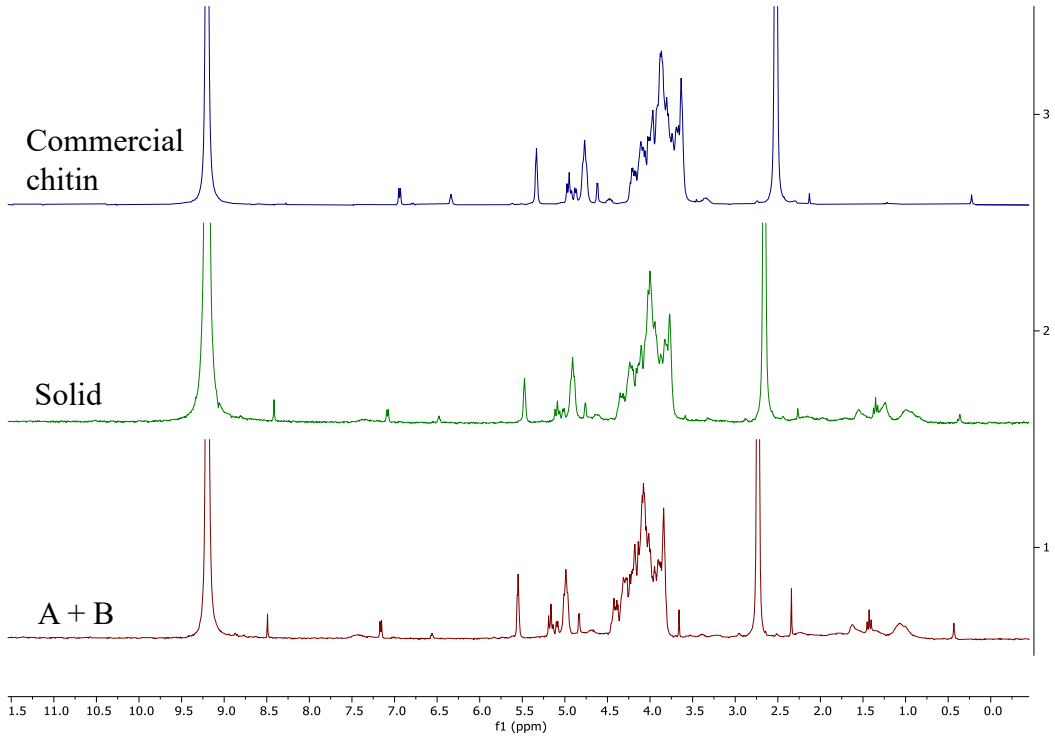

Figure 3.19: Comparison of ^{1}H-NMR spectra (300 MHz) of commercial chitin (blue), chitin pulped with solid hydroxylammonium formate (green) and extracted adding acid + base (red) dissolved in concentrated DCl at 25°C. Chemical shifts are given relative to TMS at 0.00 ppm. A: acid; B: base.

All NMR spectra (see figure 3.19) resemble to commercial chitin and all signals are clearly present. Also in this case protein residues can be detected, demonstrating that also these conditions did not afford complete deproteinization of our substrate.

For these samples of chitin pulped with hydroxylammonium formate spectroscopic signals are poorly resolved. From all spectra, both the equations described in section 2.7 were used to calculate the DA % (results in table 3.7).

Table 3.7: DA values for chitin pulped with hydroxylammonium formate.

Treatment	Entry	Temperature (°C)	Method 1 DA%	Method 2 DA%
Solid salt	1	100	97.6	97.9
A+B	2	100	94.3	96.4
B+A	3	100	98.8	98.4

Partial deacetylation occurred during dissolution of all samples in the deuterated solvent causing an increase of the signals related to acetic acid and H-2 proton of de-N-acetylated. This was taken into account in all calculation methods in order to avoid underestimation of DA.

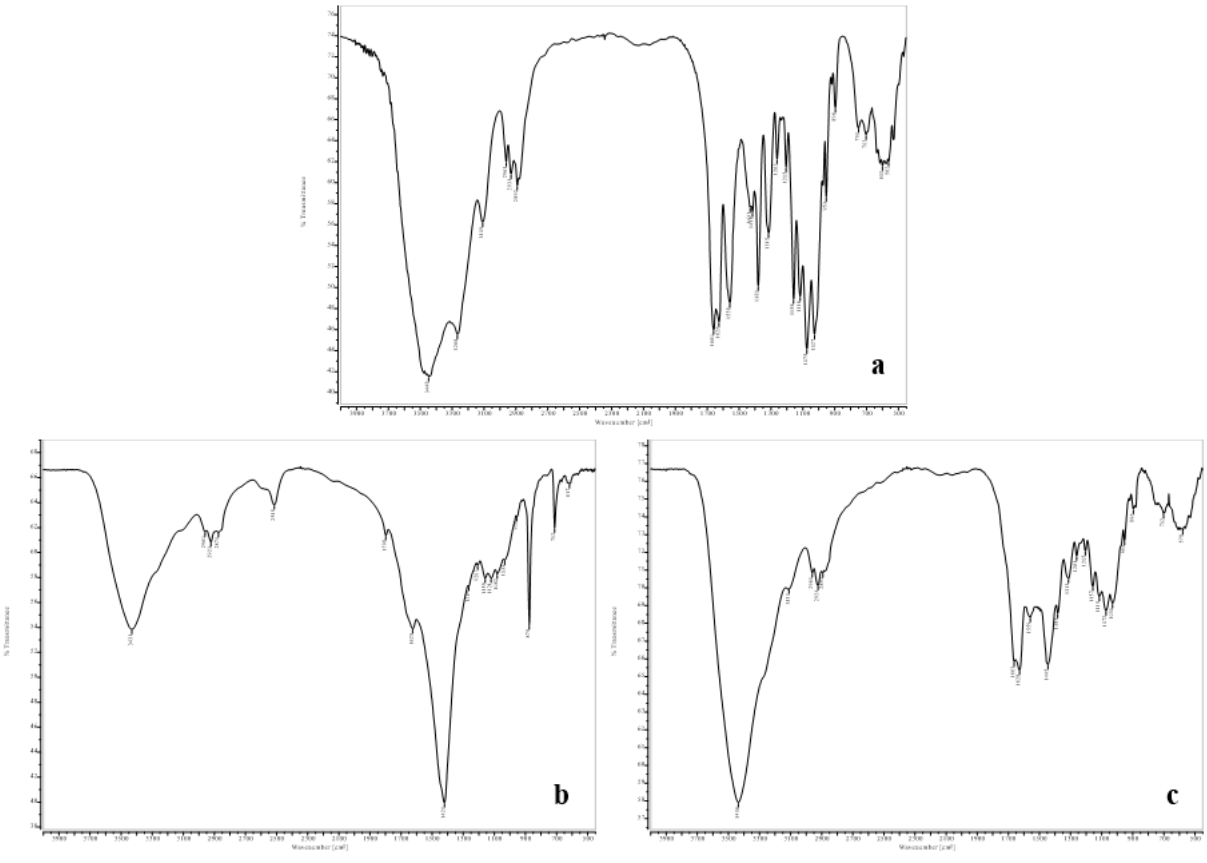

Figure 3.20: FT-IR spectrum of commercial chitin (**a**) and chitin pulped with hydroxylammonium formate in the form of solid salt (**b**) or prepared in situ by sequential addition of acid and base at 100 °C (**c**).

The FT-IR spectrum shows significant presence of calcium carbonate (1420-1450 cm^{-1} and 874-876 cm^{-1}) for all condition tested. In addition, all the signals suffer from impurities present in the pulped material and only few characteristic peaks associated with chitin could be identified.

3.7 Comparison between ILs

Results of the preliminary screening on the four ILs tested are summarized in Table 3.8.

Table 3.8: Experimental results obtained with all pulping methods tested in this work.

IL	Method	Temperature (°C)	Yield (%)	$CaCO_3$	Protein Presence	DA (%)
$[NH_4][CH_3COO]$	Solid salt	145	16.4	0	yes	98.8
	A + B	100	30.0	14.26	yes	90.5
		145	17.1	-	yes	93.4
	B + A	100	26.5	9.42	yes	97
		145	22.9	-	yes	98.6
$[NH_4][HC(O)O]$	Solid salt	130	20.3	5.78	yes	94.6
	A + B	100	17.2	0	yes	96.6
		130	17.2	-	yes	95.4
	B + A	100	17.6	0	yes	94.6
		130	18.8	-	yes	88.3
$[NH_3OH][CH_3COO]$	Solid salt	100	29.3	10.20	yes	-
	A + B		19.9	7.13	yes	96.8
	B + A		20.7	6.45	yes	93.7
$[NH_3OH]$ $[HC(O)O]$	Solid salt	100	22.2	-	yes	97.8
	A + B		16.8	-	yes	94.4
	B + A		16.6	-	yes	98.6

It can be deduced that all pulped chitins contain a small amount of protein residues, indicating that further optimization is possible to obtain pure chitin. Concerning the DM step, $CaCO_3$ residues were eliminated using ammonium acetate both as a solid salt and ammonium formate prepared *in situ* by sequential addition of acid and base or vice versa. Although ammonium acetate was used in the solid form, easy to handle and ready to use, higher reaction temperature of 145 °C was used, which could cause more extensive depolymerization of the final product (resulting in lower MW). To minimize costs of pulping process and reduce energy demand, ammonium formate formed in situ seems to be a promising choice. Concerning DA values extrapolated from 1H-NMR analysis, all methods proposed produced chitin with high DA in the range 88-99%.

3.8 Further study on chitin pulped with ammonium formate

Mesh influence

In view of the above-mentioned considerations, further experiments were performed only with ammonium formate in batch condition, prepared by sequential addition of formic acid and ammonia. Other than reaction temperature, the influence of the mesh of the ground shells was also evaluated. For this purpose, crab shells residues were ground at different mesh sizes of 20, 60 and ≥ 150, to verify if this parameter affected the purity of pulped chitin, with particular attention to protein residues.

Pulping protocol previously described was then applied, and ^{1}H-NMR analysis performed to verify the purity of products. The results are shown in figure 3.21.

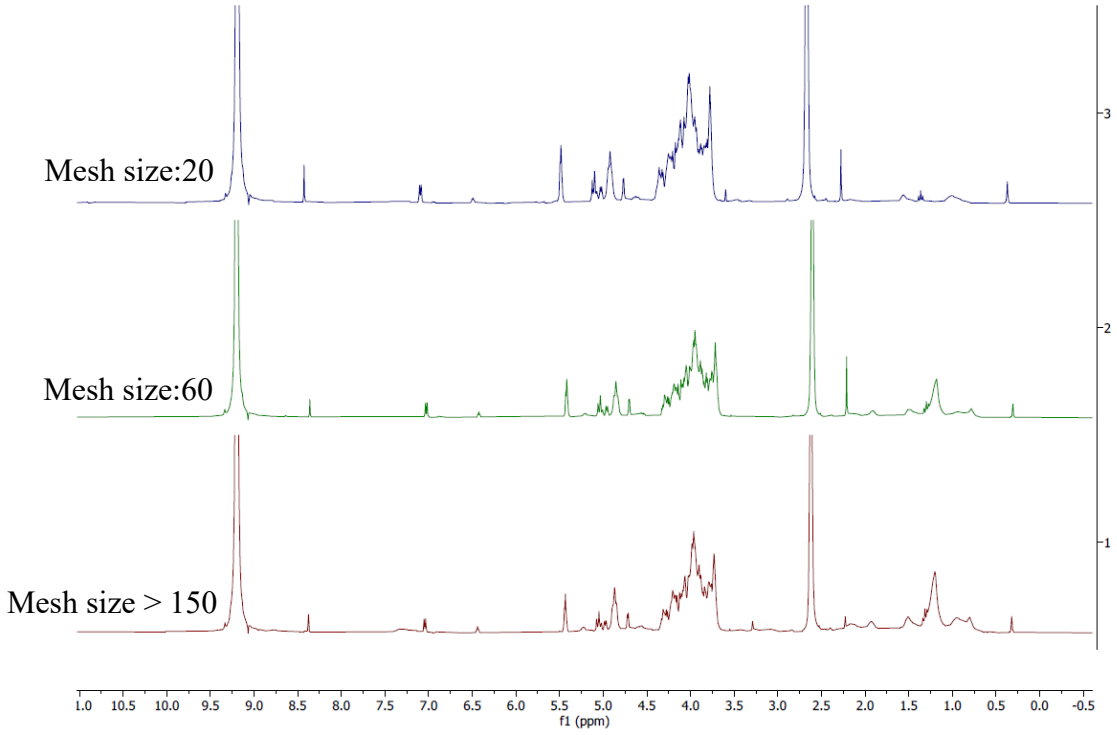

Figure 3.21: ^{1}H-NMR spectra (300 MHz) of chitin with different mesh sizes pulped with ammonium formate, dissolved in concentrated DCl at 25°C. Chemical shifts are given relative to TMS at 0.00 ppm.

All NMR spectra resemble to commercial chitin and all signals are clearly present. Also in this case protein residues can be detected for all three dimensions of the substrate under discussion, demonstrating that mesh sizes did is not a significant parameters for the obtainment of chitin. Although the obtained yields were comparable using the three meshes, the powder sample (mesh > 150) is recommended. For the majority of the further characterizations, in fact, a powdered sample is

needed. However, using a fine powder can lead to more difficult manipulation during the washing steps.

XRD

To determine the CI of the pulped material, XRD analyses were performed. A comparison between al XRD diffractograms is shown in figure 3.22.

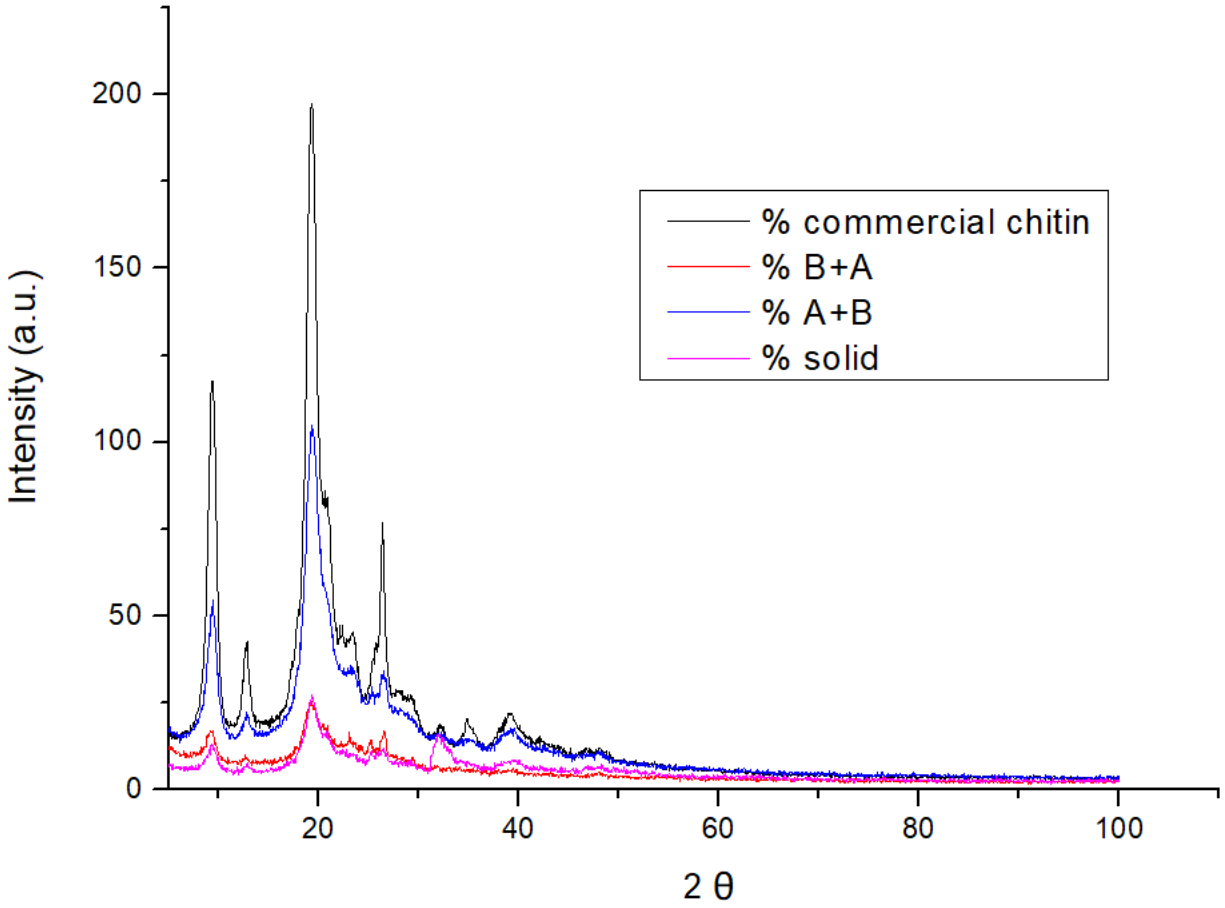

Figure 3.22: XRD diffractograms of commercial chitin and chitin pulped with ammonium formate in the three conditions tested.

To determine the actual degree of crystallinity, a quantitative X-ray phase analysis was performed. The background signal was subtracted and the diffractogram corrected. Crystalline and amorphous domain areas were properly deconvoluted and separated to provide CI with good accuracies. CI of all samples are reported in Table 3.9.

Table 3.9: CI % extrapolated from XRD analysis.

Sample	CI %
Commercial chitin	56.5
Solid salt	39.3
A + B	38.9
B + A	46.0

Results show that commercial chitin sample possess the higher CI of 56.5%. While chitin pulped with the solid salt and formed *in situ* by sequential addition of formic acid prior to ammonia aqueous solution show comparable CI of 39.3 and 38.9 respectively, it seems that pre-treatment with the base and then the acid function yield chitin with higher crystallinity.

3.9 Deacetylation to chitosan and GPC measurements

Measurement of the MW distribution of chitin is difficult due to its limited solubility in common solvents and to the need to use hazardous and toxic solvents such as LiCl/NMP and LiCl/DMAc mixtures and strong carboxylic acids, such as dichloroacetic acid and trichloroacetic acid[37], other than polar fluorinated solvents such as hexafluoroisopropyl alcohol, hexafluoroacetone sesquihydrate[38].

To evaluate the MW distribution of chitin avoiding the use of hazardous and toxic solvent systems, we decided to carry out an indirect measurement on the more soluble chitin derivative, chitosan. Thus, chitin samples pulped with ammonium formate were further deacetylated to chitosan under heterogeneous conditions. As a base NaOH (70% w/v and ratio solid:alkali 1:10) was used and two different temperatures, namely 80 and 110 °C, were tested. The reactions were conducted in a two-neck round bottom flask in inert atmosphere (to avoid peeling degradation by β-oxidation) and the mixture was stirred for three hours. To determine the variation of MW and polydispersity for the two temperature conditions tested, samples were taken at different reaction times. The precipitates were washed several times with milliQ water until neutral pH and then filtered. The washing was a critical step because of partial solubilization of almost all chitosan samples in water. This phenomenon could be explained by the slightly acidity of water, that in normal condition has a pH 6 due to CO_2 dissolved in it. Considering pKa value of amine groups of the polymer, in these conditions it was partially soluble, resulting in operational problems. For each sample GPC measurements were performed, and experimental results concerning MW distribution and polydispersity are summarized in figure 15 and table 3.10.

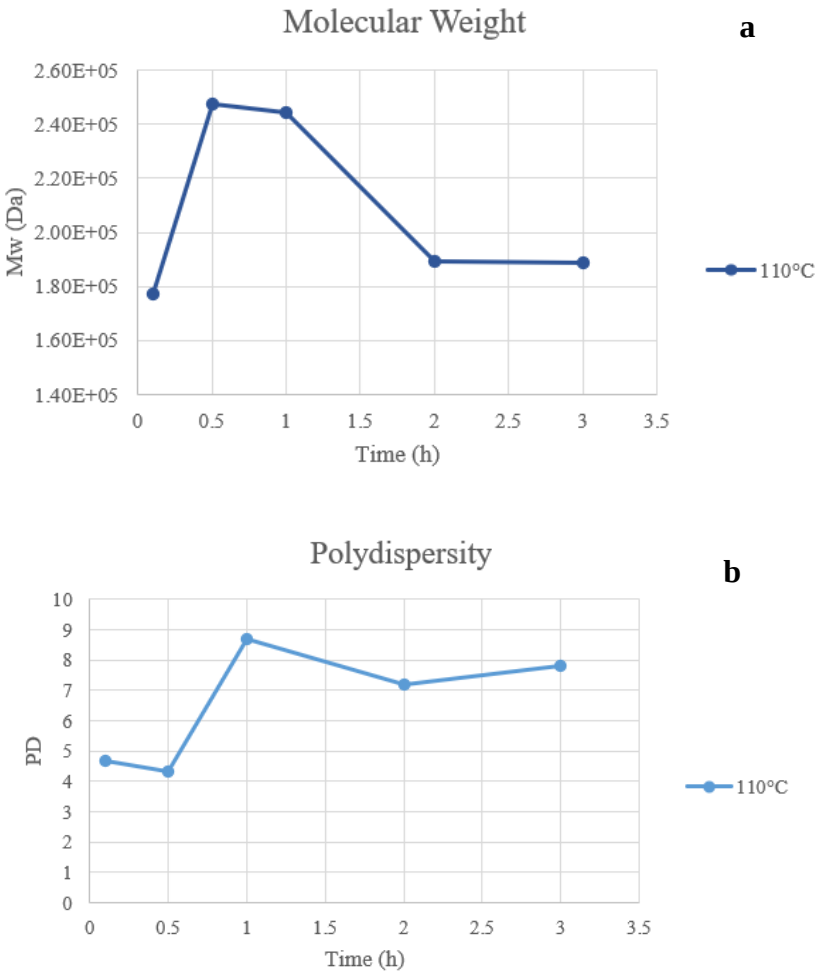

Figure 15: Trend of the molecular weight (**a**) and polydispersity (**b**) of chitin during time.

Table 3.10: Values of Mp, Mn, Mw and PD obtained from GPC analysis for chitosan samples.

Chitosan obtained at 110 °C				
Time (hours)	**Mp**	**Mn**	**Mw**	**PD**
0.1	1.24 E+05	3.78 E+04	1.77 E+05	4.69
0.5	1.05 E+05	5.73 E+04	2.47 E+05	4.32
1	8.16 E+04	2.81 E+04	2.45 E+05	8.7
2	8.88 E+04	2.61 E+04	1.89 E+05	7.2
3	8.16 E+04	2.40 E+04	1.89 E+05	7.8

Results shows that all chitosan samples obtained by partial deacetylation at 80°C were not soluble in the solvent system chosen for the analysis, indicating that in these conditions DA values were too high and not sufficient to obtain soluble chitosan samples. Concerning MW distribution and

polydispersity for chitosan obtained at 110 °C, it can be hypothesized that during the first half hour of the reaction, smaller chitosan chains are solubilized in the eluent phase, bringing to small PD values and a progressive increase in MW distribution. It is clear that during the first hour of the reaction, deacetylation occurred at high-speed rates, and bring to soluble chitosan samples. After the first hour, depolymerization occurred competing with deacetylation mechanism. This fact could be deduced by the progressive decrease in MW distribution of samples and higher PD. After two hours treatment, MW distribution levels off, and MW values between 2-3 hours are very similar.

4 CONCLUSIONS AND FUTURE PERSPECTIVES

In this study, we evaluated the efficiency of four different ILs for chitin pulping, as an alternative and green method to conventional chemical extraction procedures. Ammonium acetate, ammonium formate, hydroxylammonium acetate and hydroxylammonium formate were proposed and tested. There are numerous advantages in using ILs for chitin pulping: they are easy to handle, readily available and versatile. Other than that, single ILs include both basic and acidic functions, necessary for the removal of proteins and inorganic minerals (e.g. $CaCO_3$), which constitute the major components of crustacean shells and cuticles. In this way a single IL could potentially replace both the acid and the base (usually HCl and NaOH) from the industrial process, allowing the design of one-pot pulping procedures. As starting chitin source spider crab *Maja Squinado* shells were chosen. The choice of this complex, unusual and poorly studied substrate was made in order to design a system able to overcome the pulping issues associated with matrix complexity and presence of impurities.

Prior to pulping tests, the chemical composition of spider crab shells was determined to better understand the exact amount of protein, inorganic minerals and other minor components in the biomass substrate. Results showed that ashes, which represent the total amount of mineral salts and other inorganic matter, constitute the major component, accounting for ca. 57 wt % on dry weight basis. The other major components were in order proteins (21%) and chitin (17%) while lipids, pigments and other metals represented only the 5%. Results were in good agreement with previously reported data, although minimal variations in all components could be noted. This fact is not surprising, considering the variability of natural substrates. Chemical composition, in fact, is subjected to continuous variation due to catching period, sex, dimensions, larval stage, climate changes, diet of the specific individual, and vary significantly in different species.

After this preliminary evaluation, conventional chemical procedure was performed and validated, to verify its effectiveness and applicability. ^{1}H-NMR and FT-IR analysis both confirm product purity, and all characteristics signals associated with chitin molecule could be clearly identified.

Pulping procedures were then performed in two ways: by using the neat IL as solid salt or by synthesizing it *in-situ* as an aqueous solution in batch conditions. In the specific cases of solid salts, to choose the appropriate reaction temperature, the melting points of the different ILs were taken into account.

In all cases, 10 wt % of loading of biomass was used with respect to total mass of solution (IL and biomass), on basis of a previously reported work[68], five times higher than the chemical extraction

method (< 2 wt %), presuming the favourable economics of the process from a chemicals perspective, but this does not address possible environmental regulations, energy usage, etc. which could factor into a commercial process. All characterization data confirm that in the conditions tested, ammonium formate prepared *in-situ* seems to be the most promising IL for chitin one-pot pulping process, allowing the quantitative isolation of chitin with high purity and a high degree of acetylation (DA > 90%). Mesh size of the initial substrate apparently does not influence pulping efficiency, although it is advisable the use of powdered crab shells samples due to its heterogeneous matrix and because all characterization technique require the use of very finely powdered samples. TGA and ICP-OES analysis confirm that all calcium minerals were efficiently removed. However, all ^{1}H-NMR spectra show signals associated with methyl protons of proteins between 1.0 and 1.5 ppm, demonstrating that in these conditions proteins were still present, in both reaction condition tested (100 °C and 130°C). This may be indicative that deproteinization in this case is not strongly influenced by temperature, but further experiments are needed to confirm this hypothesis. In alternative, to assess pulping efficiency of all ILs, other parameter such reaction time and biomass/total mass of solution ratio should be tested. Furthermore, we have to highlight the fact that in all procedure great amount of wastewater were generated during washing step of the pulped material. Further studies could be aimed at eliminating residual proteins and to minimize water consumption in order to improve process intensification and ensure eco-sustainability.

Due to lack of solubility of chitin in almost all common organic solvents and water, the characterization of the product was very challenging. To evaluate purity and DA of chitin samples, ^{1}H-NMR has been extensively used in literature and was chosen in this work. However, the strong acidic conditions required for sample dissolution caused in all cases competitive deacetylation and depolymerization, making interpretation and signal identification elaborate. It was also noted that the same treatment used for dissolution, caused different polymer degradations depending on the sample treated. FT-IR spectroscopy was used in order to verify the possible presence of impurities and assess chitin obtainment. Although infrared spectroscopy enables also quantitative evaluation of the DA, in this case it was not employed because it requires prior knowledge of an approximate DA range. In addition, the presence of protein residues could affect absorbance intensities of specific bands implied in the calculation of the DA.

In the second part of the study, further characterizations were performed on chitin pulped with ammonium formate, including XRD and GPC measurements. In this case it seems that the addition order of reactants played a crucial role and strongly influenced the polymer crystallinity: higher CI were obtained for samples treated with the *in-situ* formed IL by sequential addition of base and then acid.

To overcome the intractability and solubility problems of chitin samples, deacetylation to chitosan under heterogeneous alkali condition yielded a sample suitable for GPC: analysis of the so obtain derivate at different reaction times and temperature were performed. Results showed that deacetylation temperature of 80 °C did not provide sufficient DA of pulped chitin and all sample collected were insoluble in the buffer solution used as eluent. Only reaction temperature of 110°C was effective and produced soluble chitosan with different MW distribution and PD. Taking into account that these pulping procedures has not been previously tested on *Maja squinado* species, comparison with previously reported data is not possible.

In conclusion we proposed a preliminary study on the use of innovative and simple ILs for one-pot chitin pulping. The IL can be used neat or made *in- situ* by the sequential addition of acid and base. Though pulping with ammonium formate is the more promising procedure, the varying production costs, applicability on different fishing waste-derived substrates and safety issues are still unknown. This work presents a step toward narrowing the choices for chitin isolation technologies that can lead to an economically and environmentally sustainable process replacing the current hazardous, energy consuming, and environmentally unsafe process.

5 EXPERIMENTAL SECTION

5.1 MATERIALS AND METHODS

Chemicals

All reagents and solvents employed were used without further purification. Chitin from shrimp shells, NaOH, HCl, NH_2OH aqueous solution 50 wt%, acetic acid, NH_3 solution 30-33 wt%, formic acid, ammonium formate salt, ammonium acetate salt and KBr were ACS grade and were all purchased from Sigma-Aldrich.

Chitinous biomass

Spider crab shells were obtained from a local restaurant in Venice, already washed with a detergent solution. Shells were chopped into smaller pieces with a hammer, grounded and then sieved into three different meshes (20, 60 and ≥150).
Powders of spider crab shells were weighed and stored in glass bottles at ambient temperature before usage.

5.2 Determination of the chemical composition of spider crab shells

Ash content

Ash content was determined using the Standard Test Method for Ash in Biomass E1755-01. For this purpose, 1.0 g of dried crab shells were placed in a porcelain crucible and put in a muffle furnace at 600°C for 3 h. The crucible was then removed, set in a desiccator, and allowed to cool to room temperature. The system was weighted to the nearest 0.1 mg. After weighing, the crucible was inserted again into the furnace for 1 h at 600°C, cooled in the desiccator, and reweighed. This last step was repeated until the mass of the crucible varied by less than 0.3 mg from the previous weighing. The procedure was performed in duplicate, and a mean-value calculation determined ash content.

Protein content

Protein content was determined by chemical deproteinization of crab shells. 0.5 g of spider crab shells powder was suspended in aqueous NaOH (1 M; 20 mL/g of solid), at 70 °C for 3 hours under

continuous stirring. The solid product was centrifuged (6000 rpm for 10 minutes), washed with water until neutral pH, and dried in oven under reduced pressure (15 mbar) overnight.
Protein percentage with respect to dry crude shell weight was then calculated.

5.3 SYNTHESIS - GENERAL PROCEDURES

5.3.1 Synthesis of Hydroxylammonium acetate

Hydroxylammonium acetate and was prepared according to a reported procedure[68]. Hydroxylamine solution 50 wt% (26.42 g, 0.4 mol) was stirred at 0 °C in a 250 mL round-bottomed flask while acetic acid (26.4 g, 0.44 mol) was added dropwise over three hours. The solution was then allowed to reach room temperature overnight under continuous stirring. The mixture was then gently purged with air and heated at 40 °C to concentrate the solution. The precipitate was washed with methanol (100 mL) and diethyl ether (100 mL) to remove residual acetic acid and dried in oven under reduced pressure (15 mbar) overnight. The final product was obtained as a white solid (11.9 g, yield 32 %) and was characterised by NMR spectroscopy (^{1}H and ^{13}C in$DMSO\text{-}d_6$ or D_2O). Melting point was also determined. Characterisation data are reported in the Appendix section 6.1.

5.3.2 Synthesis of Hydroxylammonium formate

Hydroxylammonium formate was prepared adapting a reported procedure[68]. Hydroxylamine solution 50 wt% (26.42 g, 0.4 mol was stirred at 0 °C in a 250 mL round-bottomed flask while formic acid (20.25 g, 0.44 mol) was added dropwise over three hours. The solution was then allowed to reach room temperature overnight under continuous stirring. The mixture was then gently purged with air and heated at 40 °C to concentrate the solution. The precipitate was washed with methanol (100 mL) and diethyl ether (100 mL) to remove residual acetic acid and dried in oven under reduced pressure (15 mbar) overnight. The final product was obtained as a white solid (11.9 g, yield 32 %) and was fully characterised by NMR spectroscopy (^{1}H and ^{13}C in$DMSO\text{-}d_6$ or D_2O). Characterisation data are reported in the Appendix section 6.1.

5.4 Chemical extraction protocol

In a typical procedure, a powdered sample (1 g) of spider crab shells was suspended in aqueous HCl (0.5 M; 40 mL/g of waste) and stirred at room temperature for 15 min. The residual solid was centrifuged (6000 rpm for 10 minutes), water was added to neutral pH, and the resulting solid was dried in oven under reduced pressure (15 mbar) overnight. The demineralised powder was then

suspended in aqueous NaOH (1 M; 20 mL/g of solid), at 70 °C for 3 hours under continuous stirring. The solid product was centrifuged (6000 rpm for 10 minutes), washed with water until neutral pH, and dried in oven under reduced pressure (15 mbar) overnight. The final product was obtained as a white solid (0.337 g, yield 17.0 %).

5.5 Pulping protocols

5.5.1 General Procedure for Chemical Pulping of Crab shells using IL solid salt

This protocol is suitable for pulping of spider crab in ratio 10 wt% of biomass with respect to the total mass of solution (See table 5.1). Ground crab shells (0.5 g) were mixed with solid IL (4.587g) in a 100 mL round-bottom flask. The solution was kept under magnetic stirring for 2 hours in an oil bath heated at 100 °C. After complete melting of the IL, a vigorous bubbling/foaming could be observed. A yellowish solid precipitated after the desired reaction time of two hours, while impurities were confined in the aqueous phase. The mixture was diluted with 50 mL of DI water and separated in a spin-dryer. The solid was washed with water (5 × 50 mL) until neutral pH was reached and dried in oven under reduced pressure (15 mbar) overnight. The final product was obtained as a yellow-white solid.

For all ILs in the form of solid salts 10% of biomass with respect to total mass of solution was maintained. This implies that the mole of each specific IL will vary in dependence to their MW (see table 5.1).

5.5.2 General Procedure for Chemical Pulping of Crab shells using IL prepared *in situ* in batch conditions by addition of acid and base aqueous solutions

This protocol is suitable for pulping of spider crab in ratio 10 wt% of biomass with respect to the total mass of solution (see table 5.1). 0.500 g of ground crab shells were put in a 100 mL two-necked round-bottom flask and acidic function was added, followed by dropwise addition of aqueous basic solution over several minutes, using a syringe. The solution was kept under stirring for 2 hours in an oil bath heated at 100 °C. A yellowish solid precipitated after the desired reaction time, while impurities were confined in the aqueous phase. The mixture was diluted with 50 mL of DI water and separated in a spin-dryer. The solid was washed with water (5 × 50 mL) until neutral pH was reached and dried in oven under reduced pressure (15 mbar) overnight. The final product was obtained as a yellow-white solid. The same procedure was repeated by changing the addition order of reactants (first the base, then the acid) to verify if some differences were observed in the pulped material's purity and quality.

For all ILs 10% of biomass with respect to total mass of solution was maintained. This implies that the mole of each specific IL will vary in dependence to their MW (see table 5.1). In these cases, the acidic function was added in minimum excess (1.05 eq.) with respect to base (1 eq).

5.5.3 General Procedure for Chemical Pulping of Crab shells using IL prepared *in situ* by addition of acid and base aqueous solutions in autoclave

To 0.500 g of ground crab shells weighted directly in a 100 mL two-necked round-bottom flask was added the acidic function, followed by aqueous basic solution over several minutes, with the aid of a syringe (quantities reported in table 5.1). The solution was kept under magnetic stirring for ca. 0.5 hours until foaming and bubbling occurred. The mixture was then placed in a stainless-steel autoclave equipped with a Teflon reactor. It was kept under magnetic stirring for 2 hours and was allowed to cool to room temperature.

The mixture was then diluted with 50 mL of DI water and separated in a spin-dryer. The solid was washed with water (5 × 50 mL) until neutral pH was reached and dried in oven under reduced pressure (15 mbar) overnight. The final product was obtained as a yellow-white solid. The same procedure was repeated by changing the addition order of reactants (first the base, then the acid) to verify if some differences were observed in the pulped material's purity and quality.

For all ILs 10% of biomass with respect to total mass of solution was maintained. This implies that the mole of each specific IL will vary in dependence to their MW (see table 5.1). In these cases, the acidic function was added in minimum excess (1.05 eq.) with respect to base (1 eq).

Table 5.1: Quantity of ILs, acid and base used for chitin pulping and relative yields.

	Solid salt		Acid		Base		Yield (%)		
	g	**mol**	**g**	**mol**	**g**	**mol**	**Solid salt**	**Acid + Base**	**Base + Acid**
Ammonium acetate	4.587	0.0595	3.603	0.0599	3.977 (1.193 of pure base)	0.070	16.4 (145°C)	30 (100°C) 17.1 (145°C)	26.5 (100°C) 22.9 (145°C)
Ammonium formate	4.587	0.00727	3.383	0.0735	3.977 (1.193 of pure base)	0.070	20.3 (130°C)	17.2 (100°C) 17.2 (130°C)	17.6 (100°C) 18.8 (130°C)
Hydroxylammonium acetate	4.587	0.0493	2.982	0.0496	3.211 (1.605 of pure base)	0.0486	29.3 (100°C)	19.9 (100°C)	20.7 (100°C)
Hydroxylammonium formate	4.587	0.0580	2.670	0.0580	1.820 of pure base	0.055	22.2 (100°C)	16.8 (100°C)	16.6 (100°C)

5.6 Deacetylation of pulped chitin

Chemical deacetylation under heterogeneous conditions was performed according to a reported procedure[87]. Prior to analysis all sample were pulverized with an agar mortar. The parameters tested were 80ºC and 110ºC for the reaction temperature and 70% (w/v) for the NaOH concentration in a ratio solid:alkali (1:10). The reactions were conducted in a two-neck bottom flask in inert atmosphere (to avoid peeling degradation by β-oxidation) and the mixture was stirred over the course of three hours. Samples were taken at different reaction times of 10, 30, 60, 120, 180 minutes and the precipitates were washed several times with milliQ water (4 x 50 ml) until neutral pH and filtered.

5.7 Characterization of ILs prepared in our laboratory

^{1}H-NMR and ^{13}C-NMR

^{1}H-NMR and ^{13}C-NMR spectra were obtained using a Bruker NMR spectrometer Ascend 400 (AV400), operating at 400 MHz for ^{1}H nuclei and 100 MHz for ^{13}C at ambient temperature (298 K).

5.8 Characterization of extracted chitin

Fourier-transform infrared spectroscopy (FT-IR)

The samples for FTIR analysis were prepared by grinding the dry blended powders with powdered KBr, (ratio of 1:100 Sample: KBr) and then compressed to form pellets of 5 mm-diameter using a hydraulic press at a pressure of 10 tons for one minute.

FT-IR spectra were recorded on a Perkin-Elmer Spectrum One FT-IR spectrometer. All spectra were recorded in the middle infrared (4000 cm^{-1} to 450 cm^{-1}) with a resolution of 4 cm^{-1} in the absorbance mode for 16 scans at room temperature.

^{1}H-NMR

Chitin samples were dissolved in a deuterium chloride solution (DCl 35 wt % in D_2O) with vigorous stirring for 30 minutes at 50 °C. ^{1}H-NMR spectra were obtained using a Bruker UltraShield 300 operating at 300 MHz at ambient temperature (298 k) for 64 scans with a spectral window of 20 ppm.

Chitin signals- ^{1}H NMR (300 MHz, DCl 35% in D_20, 298 K) δ (ppm): 6.94 (d, H-1*), 5.33 (br, α-H1A), 4.95-4.98 (br, β-H1A + H1D), 4.87-4.88 (d, H-2*), 4.77 (br, H1A), 4.61 (d, H-3*), 3.5-4.3 (m, H2/H6), 2.53 (s, H-Acetyl), 2.13 (s, H-acetic acid). Signals denoted with an asterisk refers to glucofuranosyl oxazolidinium ion existing in equilibrium with GlcNAc in concentrated DCl.

TGA

The thermogravimetric analyses were carried out in a TA instruments SDT 2960. About 5 mg of all samples were placed in aluminium crucible and heated from ambient temperature to 800 °C with a heating rate of 10 °C/min. under a nitrogen atmosphere (flow rate 1 mL/min).

ICP-OES

ICP-OES measurements were performed on a Perkin Elmer ICP -OES 5300 DV. All chitin samples were digested in nitric acid (3 mL) and hydrochloric acid (2 mL), dilute to 10 mL of final volume, and heated at 150 °C for 20 minutes to ensure complete dissolution.

XRD

XRD measurements were performed employing a Philips diffractometer with a PW 1319 goniometer with Bragg-Brentano geometry, equipped with a focusing graphite monochromator and a proportional counter with a pulse-height discriminator. Nickel-filtered CuKα radiation and a step-by-step technique were employed (steps of 0.05° in 2θ), with a collection time of 30 s per step.

GPC

Gel permeation chromatography was performed using an Agilent Infinity 1260 GPC instrument equipped with a viscosimetric and a refractometric detectors using an injection volume of 100 μL and a flow rate of 0.5 mL/min. A Polysep-GFC-P linear column (1 kDa-10 MDa) was used maintaining a constant temperature of 5°C during the analysis. An aqueous solution of acetic acid (0.3M) and sodium acetate (0.2M) was used as eluent and PEO/PEG standards with sample weights of 601–1020000 g/mol were used for the calibration. Prior to analysis 2 mg of chitosan samples were dilute in 1 mL of eluent phase, and the solution was filtered.

6 APPENDIX

6.1 Characterization of IL synthesized in our laboratory

^{1}H-NMR and ^{13}C-NMR

Hydroxylammonium acetate

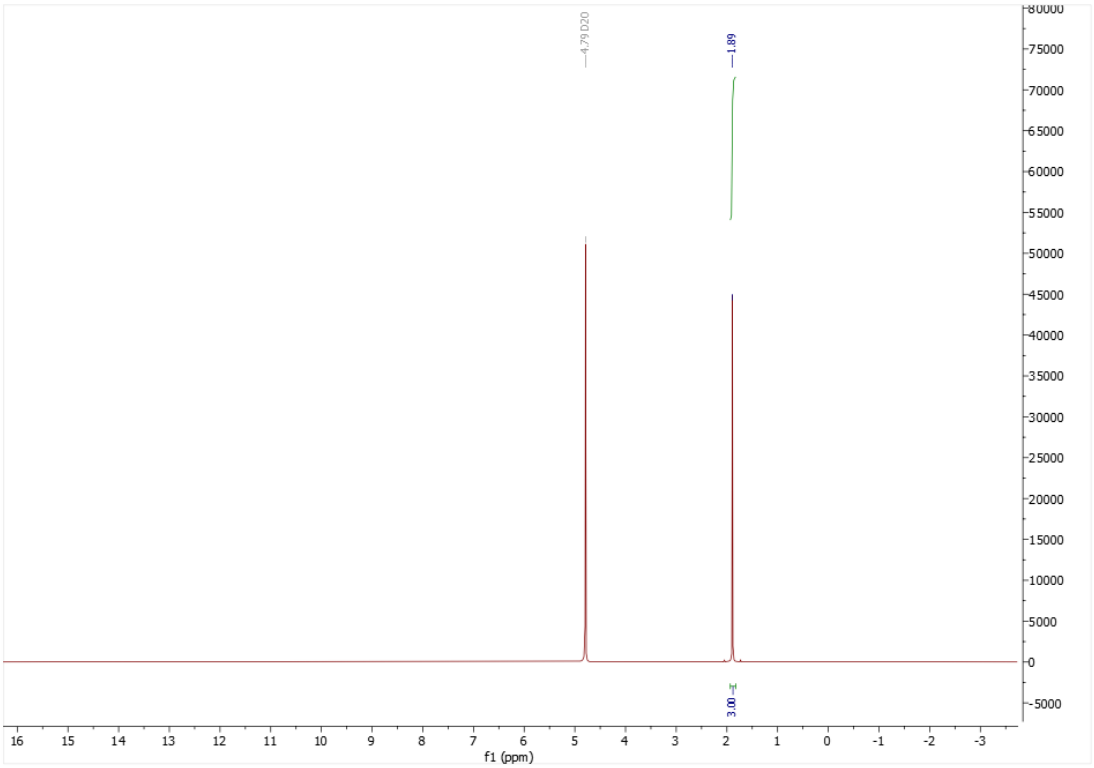

Figure 6.1.1: ^{1}H-NMR spectrum of hydroxylammonium acetate in D_2O.

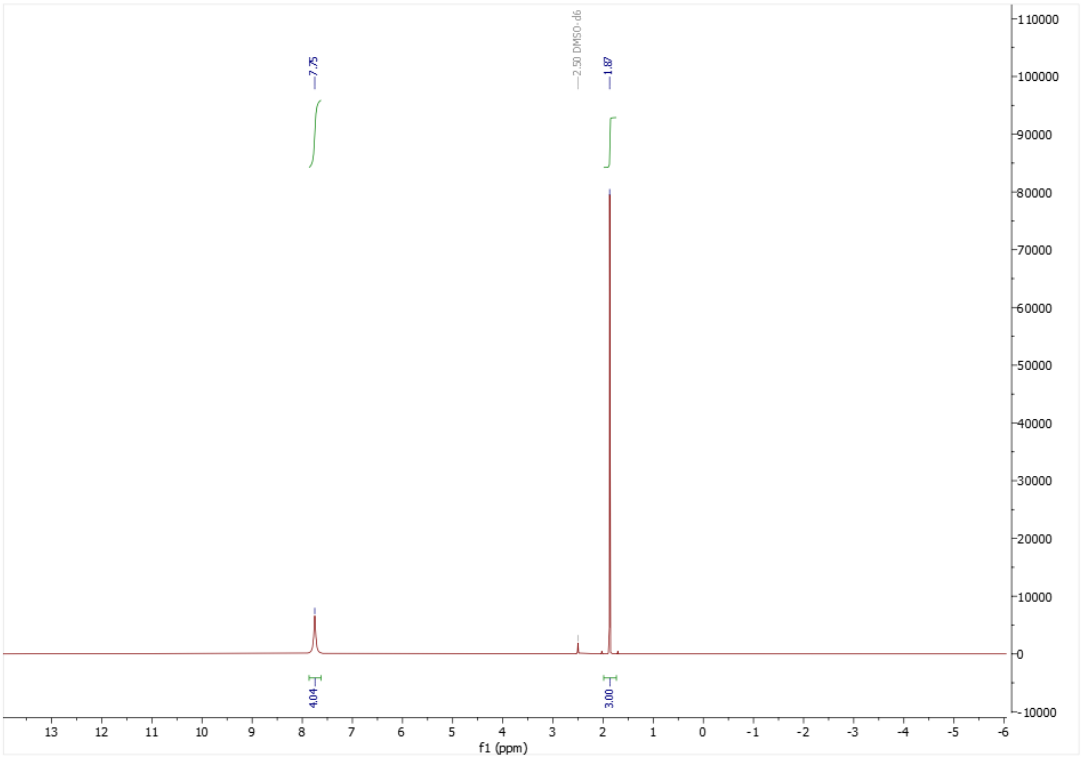

Figure 6.16.2: ^{1}H-NMR spectrum of hydroxylammonium acetate in DMSO-d_6.

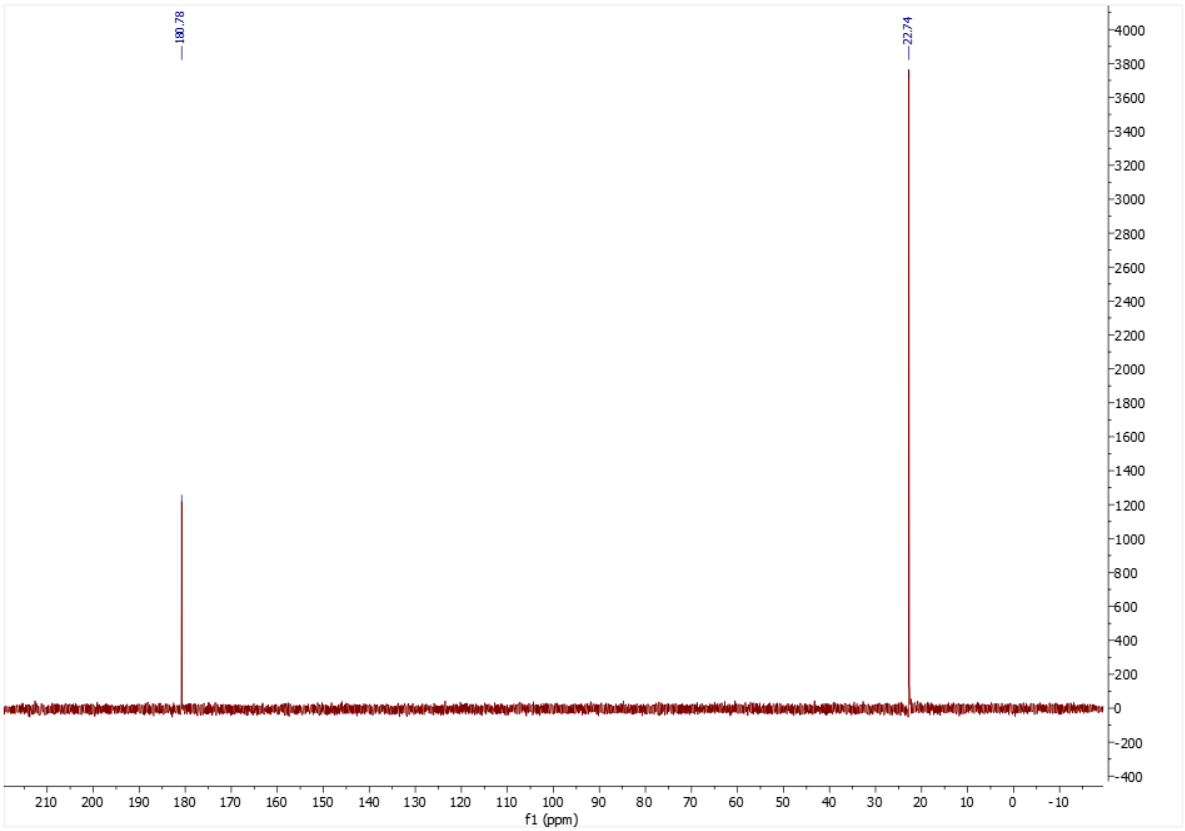

Figure 6.17.3: ^{13}C-NMR spectrum of hydroxylammonium acetate in D_2O.

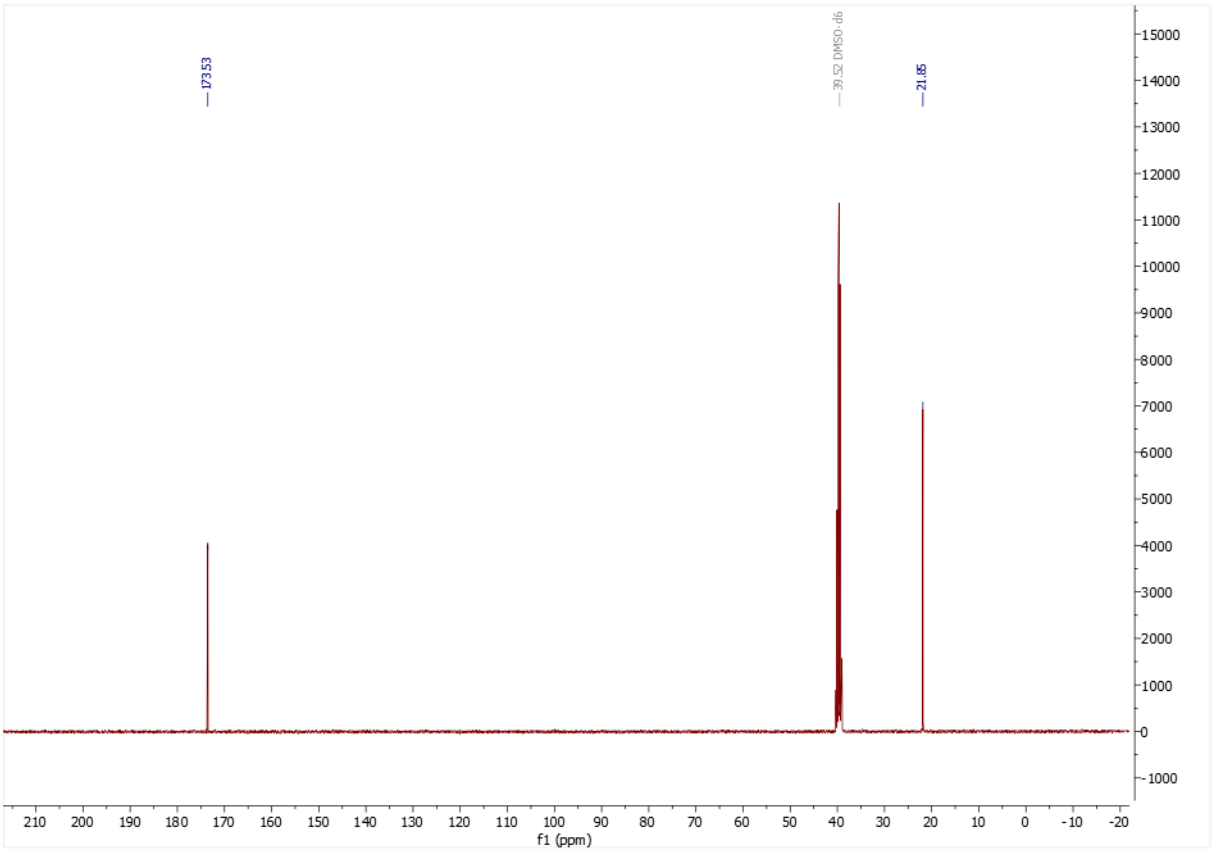

Figure 6.18.4: ^{13}C-NMR spectrum of hydroxylammonium acetate in DMSO-d_6.

Hydroxylammonium formate

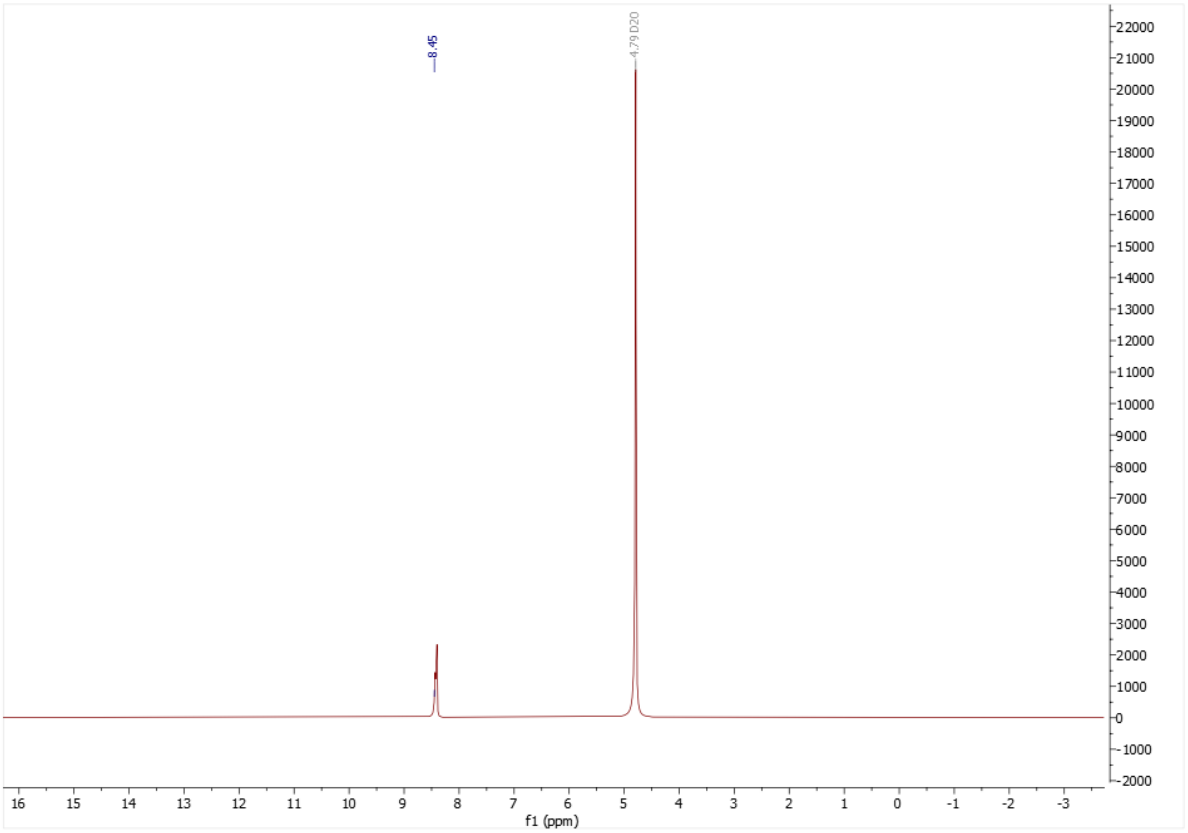

Figure 6.1.5: ^{1}H-NMR spectrum of hydroxylammonium formate in D_2O.

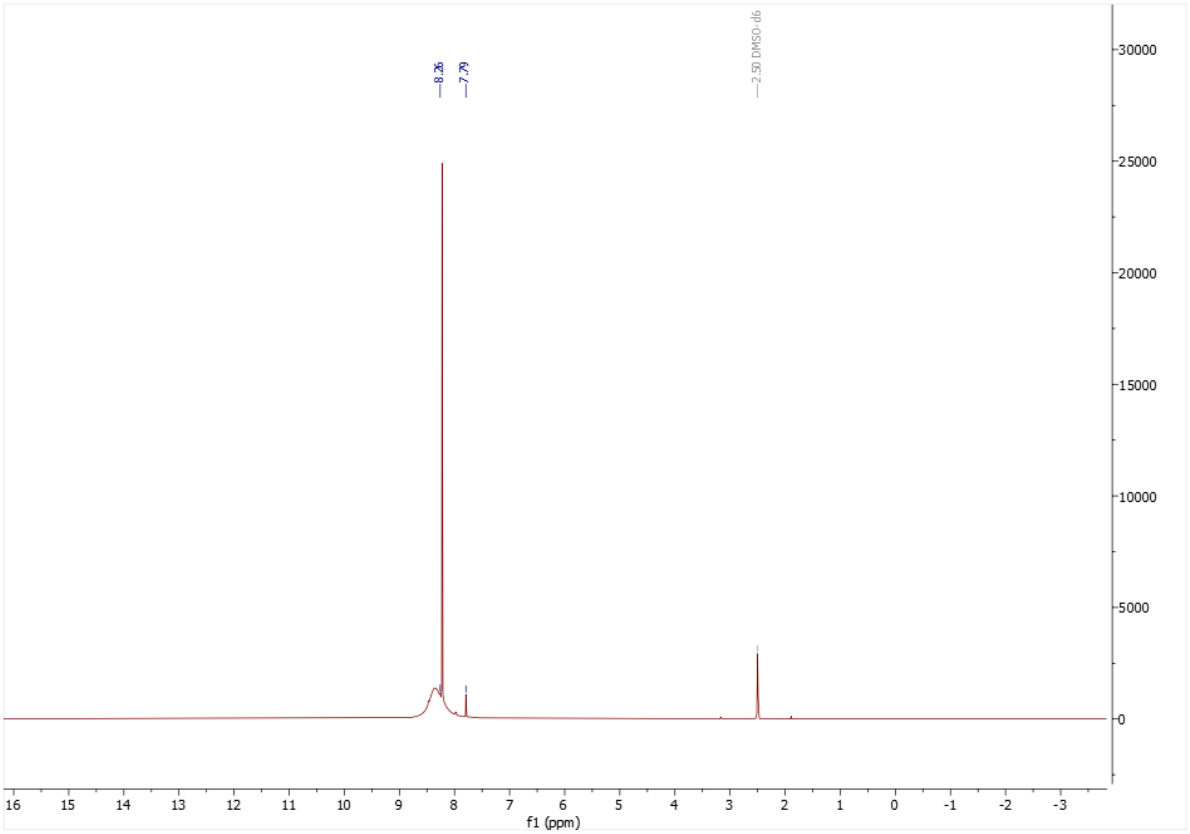

Figure 6.19.6: ^{1}H-NMR spectrum of hydroxylammonium formate in DMSO-d_6.

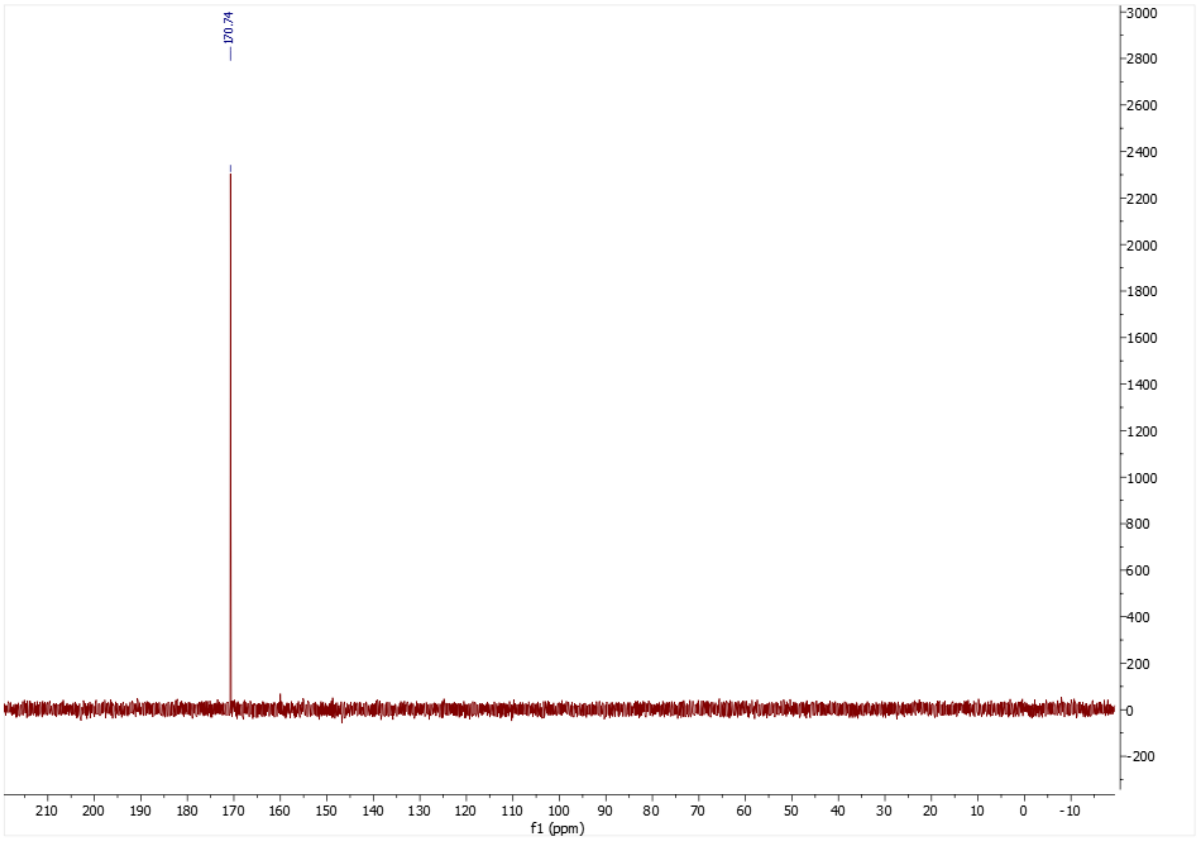

Figure 6.20.7: ^{13}C-NMR spectrum of hydroxylammonium formate in D_2O.

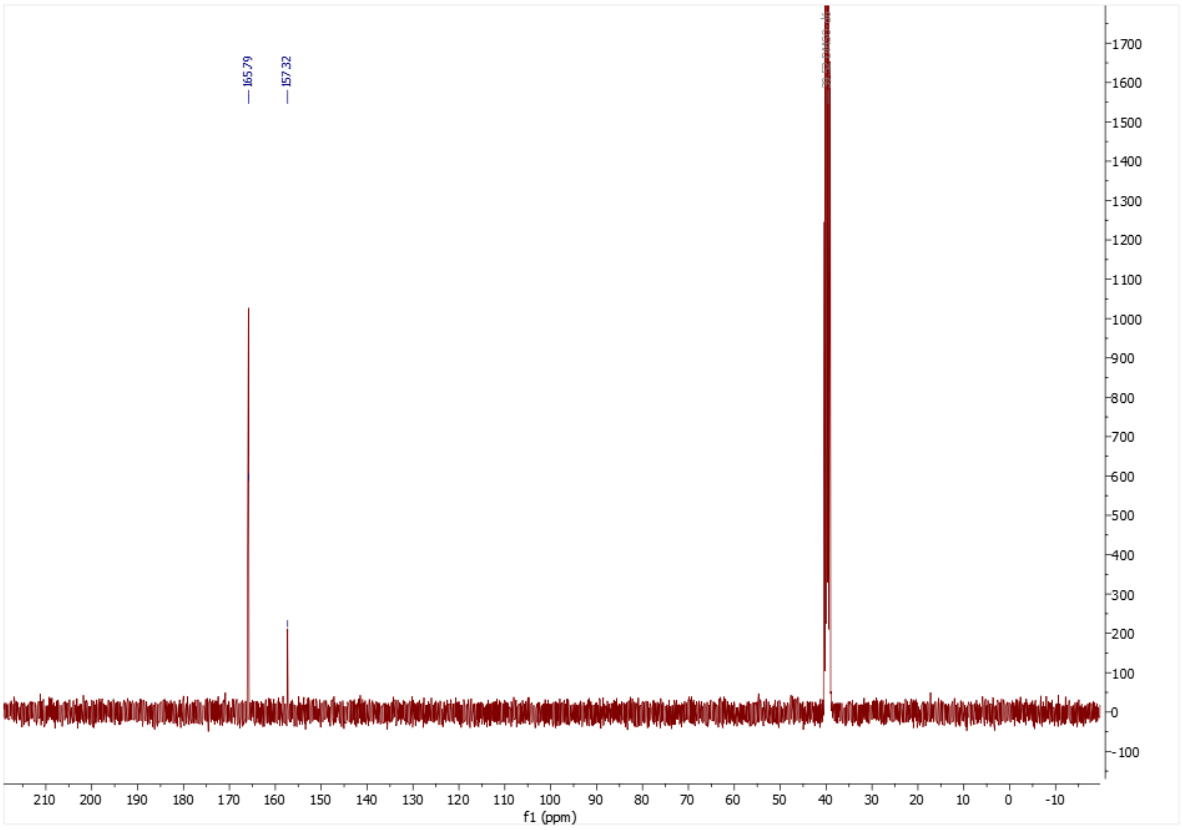

Figure 6.21.8: ^{13}C-NMR spectrum of hydroxylammonium formate in DMSO-d_6.

6.2 Characterization of pulped chitin

6.2.1 TGA

Pulping with ammonium acetate

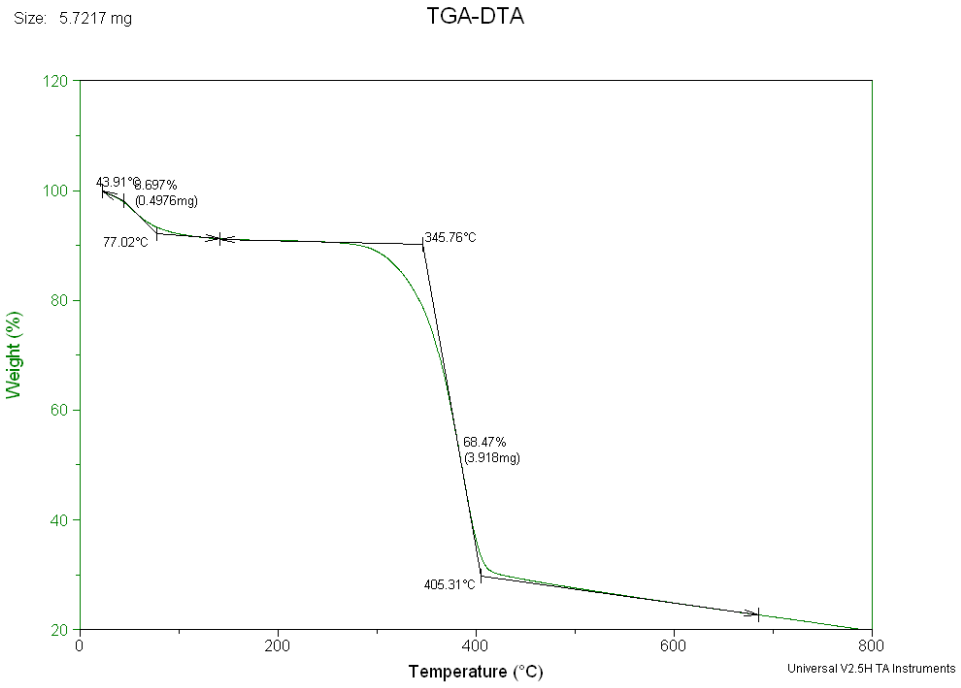

Figure 6.2.1.1: TGA curve of chitin extracted with ammonium acetate solid salt (at 145 °C) in the range 25°C-800°C in nitrogen atmosphere.

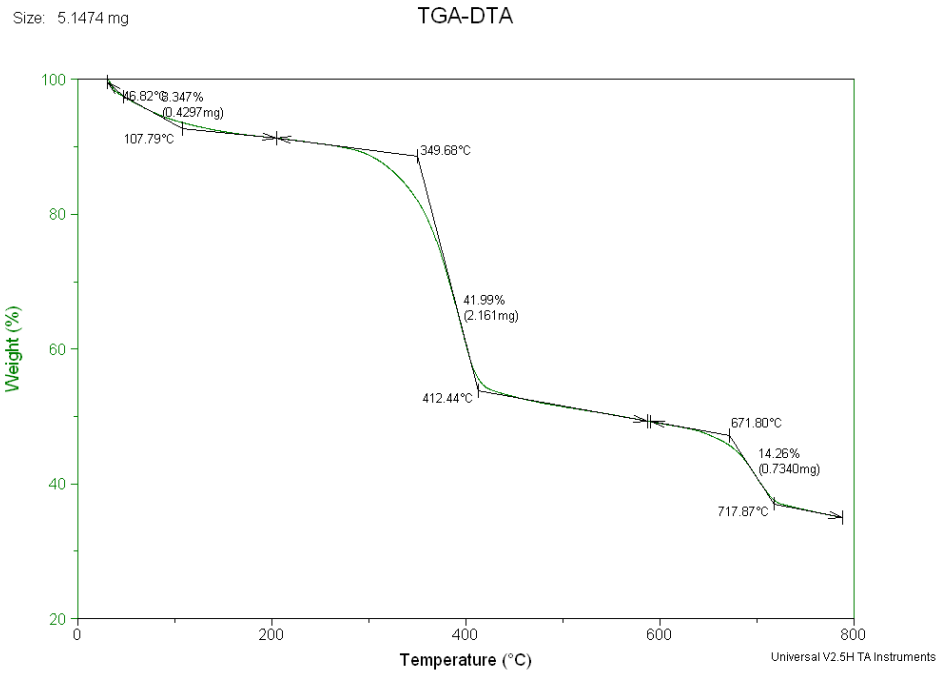

Figure 6.2.1.2: TGA curve of chitin extracted with ammonium acetate prepared in situ in batch condition (at 100 °C) by sequential addition of acid prior to base in the range 25°C-800°C in nitrogen atmosphere.

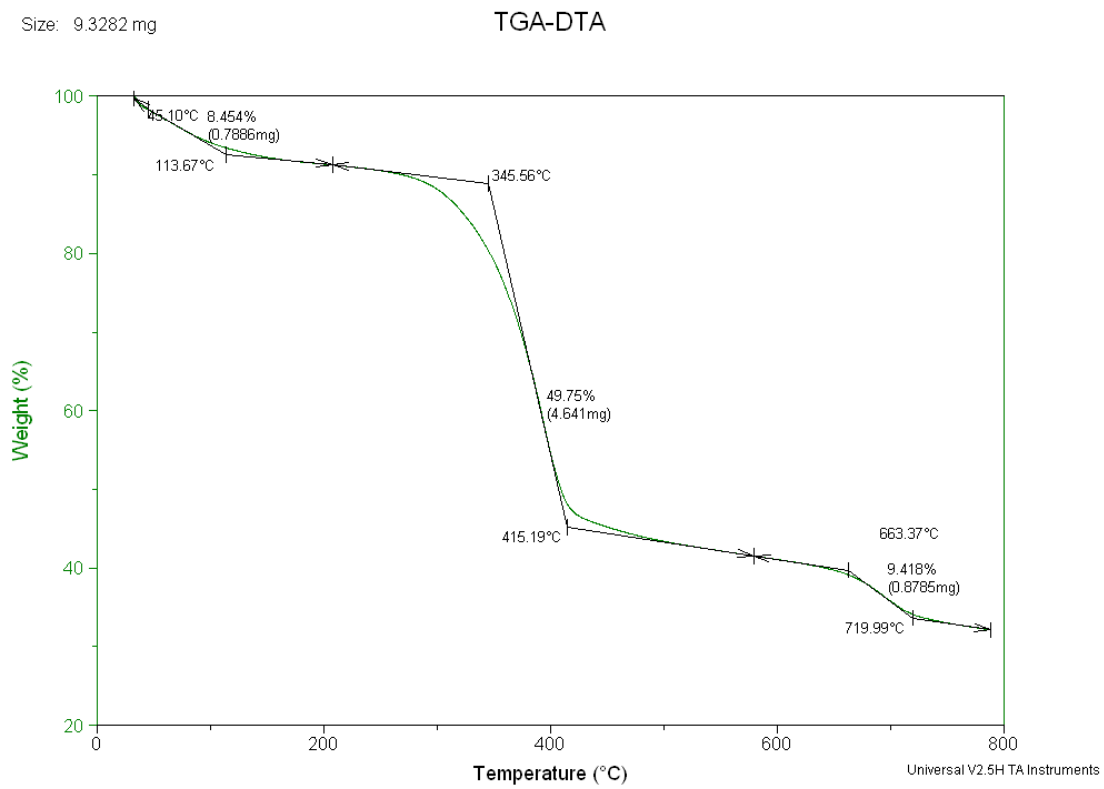

Figure 6.2.1.3: TGA curve of chitin extracted with ammonium acetate prepared in situ in batch condition (at 100 °C) by sequential addition of base prior to acid in the range 25°C-800°C in nitrogen atmosphere.

Pulping with ammonium formate

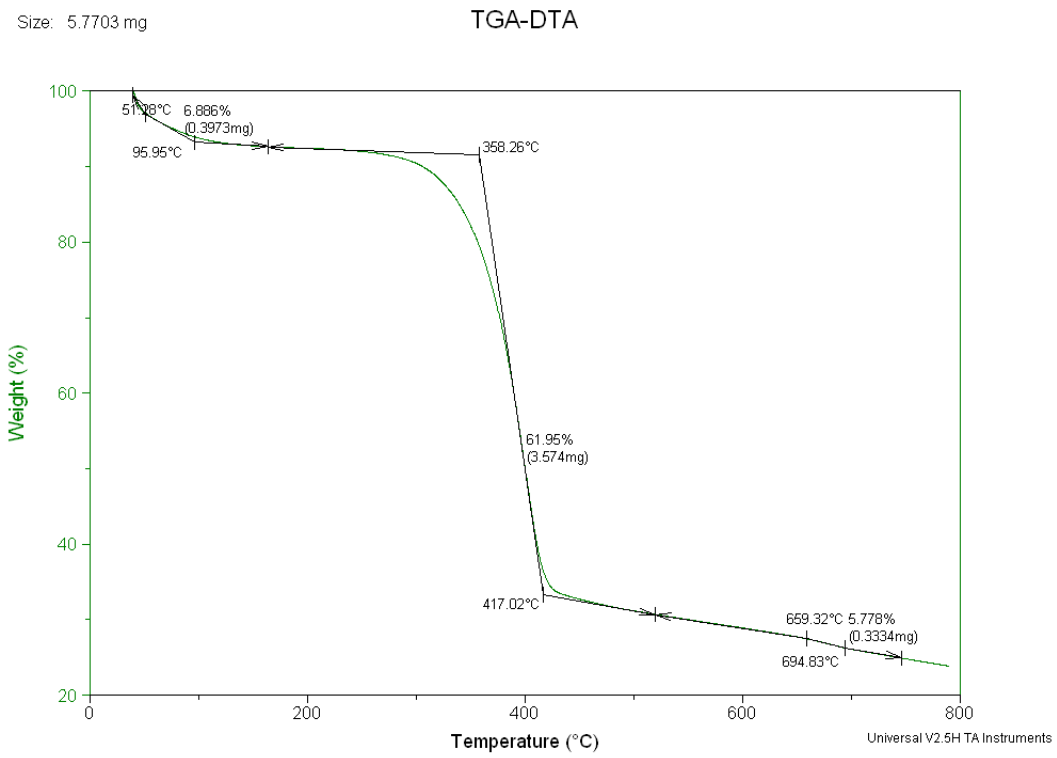

Figure 6.2.1.4: TGA curve of chitin extracted with ammonium formate solid salt (at 130 °C) in the range 25°C-800°C in nitrogen atmosphere.

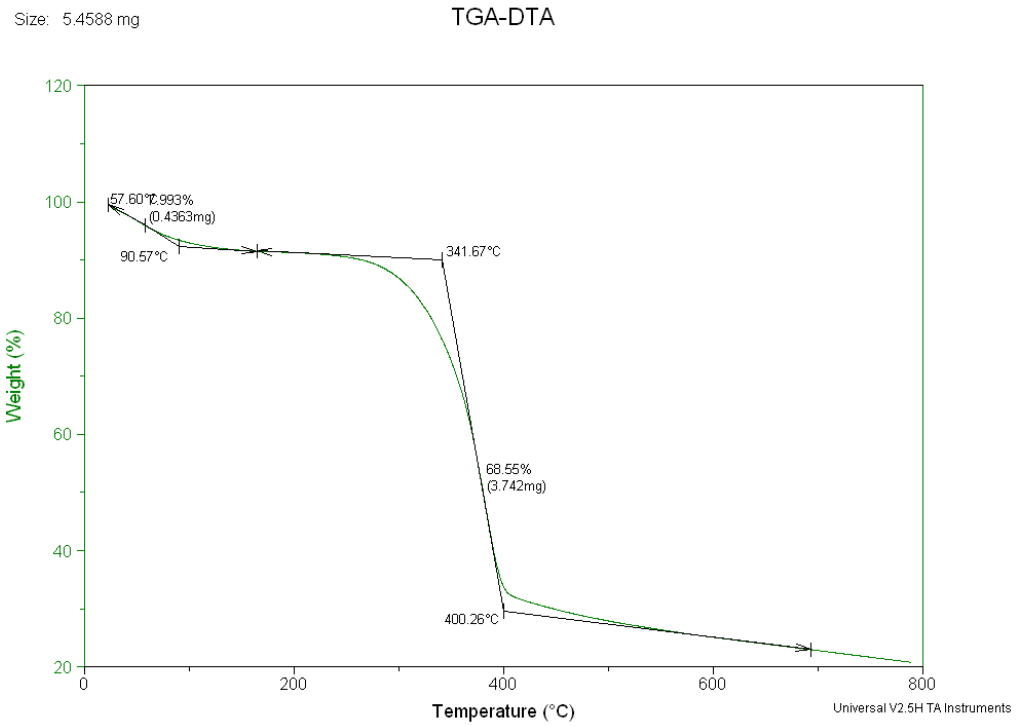

Figure 6.2.1.5: TGA curve of chitin extracted with ammonium acetate prepared in situ in batch condition (at 100 °C) by sequential addition of acid prior to base in the range 25°C-800°C in nitrogen atmosphere.

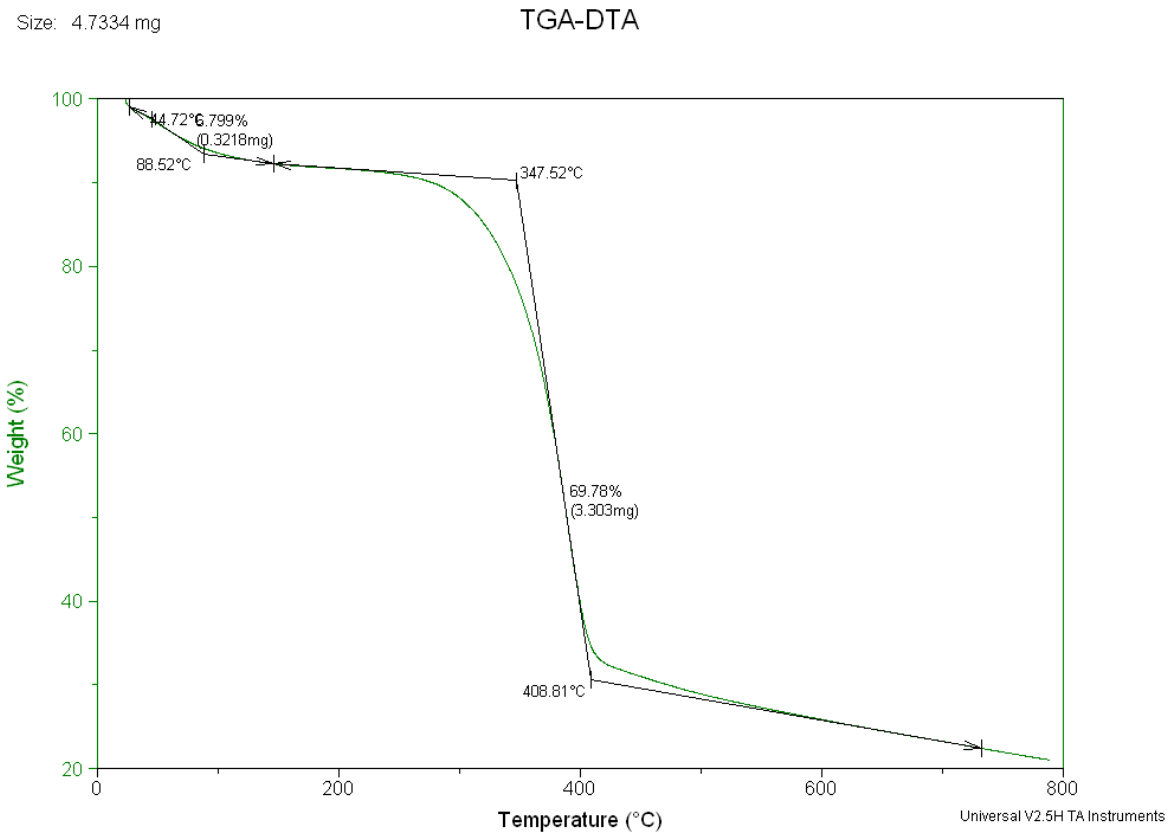

Figure 6.2.1.6: TGA curve of chitin extracted with ammonium acetate prepared in situ in batch condition (at 100 °C) by sequential addition of base prior to acid in the range 25°C-800°C in nitrogen atmosphere.

Pulping with hydroxylammonium acetate

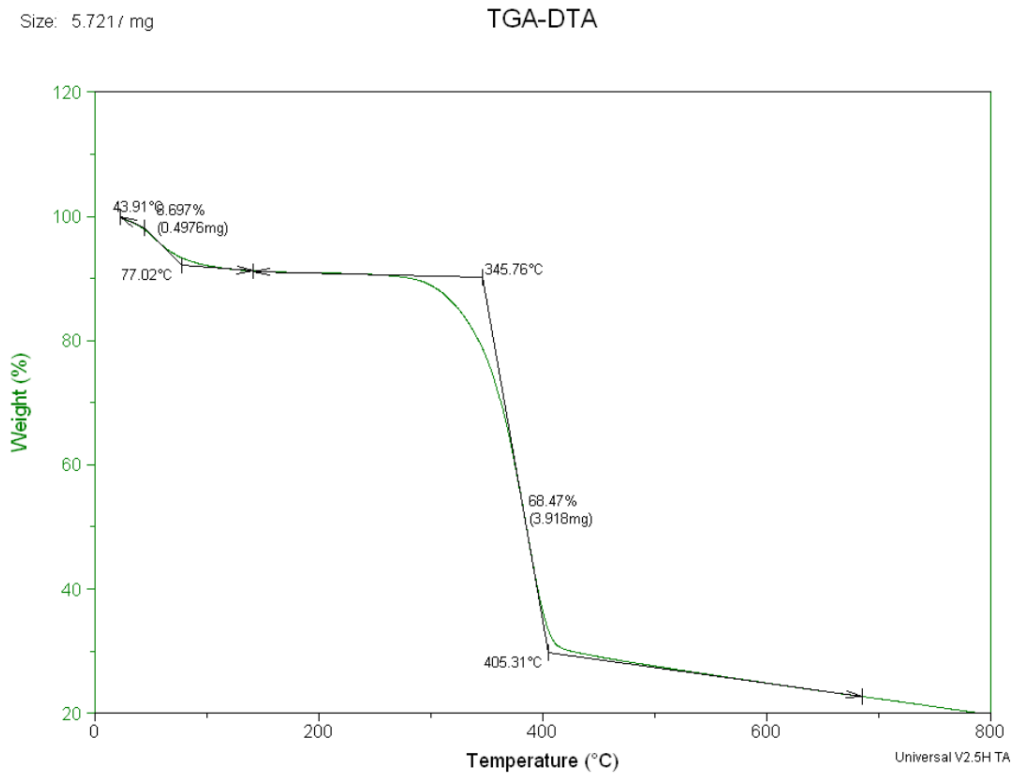

Figure 6.2.1.7: TGA curve of chitin extracted with hydroxylammonium acetate solid salt (at 100 °C) in the range 25°C-800°C in nitrogen atmosphere.

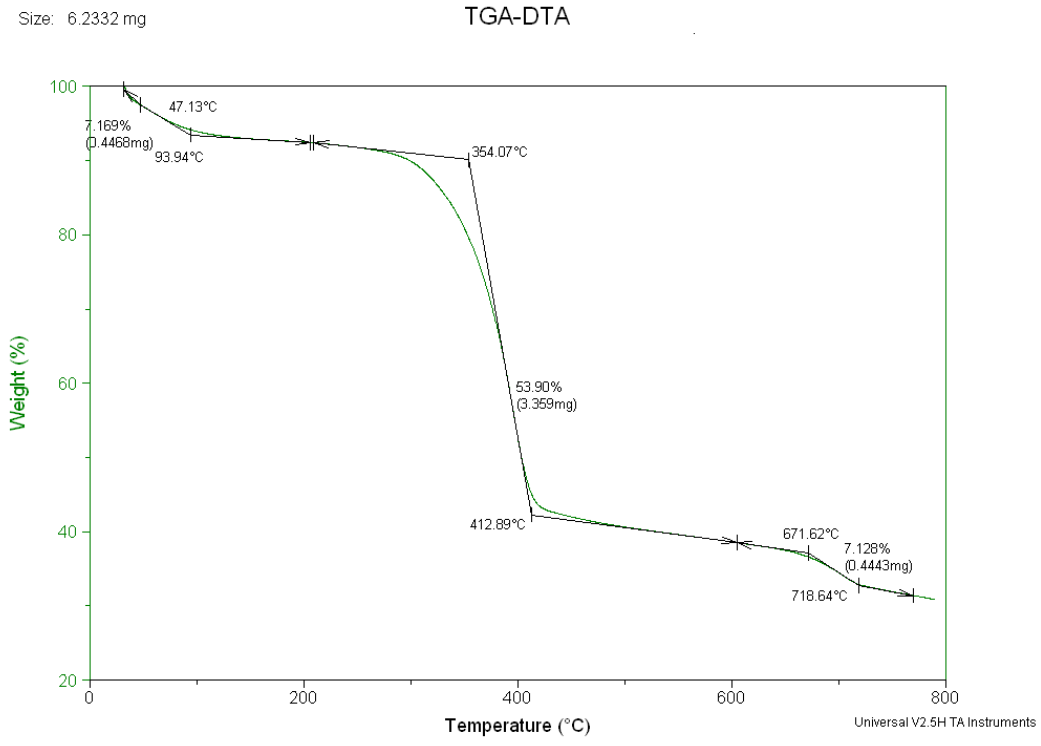

Figure 6.2.1.8: TGA curve of chitin extracted with hydroxylammonium acetate prepared in situ (at 100 °C) by sequential addition of acid prior to base in the range 25°C-800°C in nitrogen atmosphere.

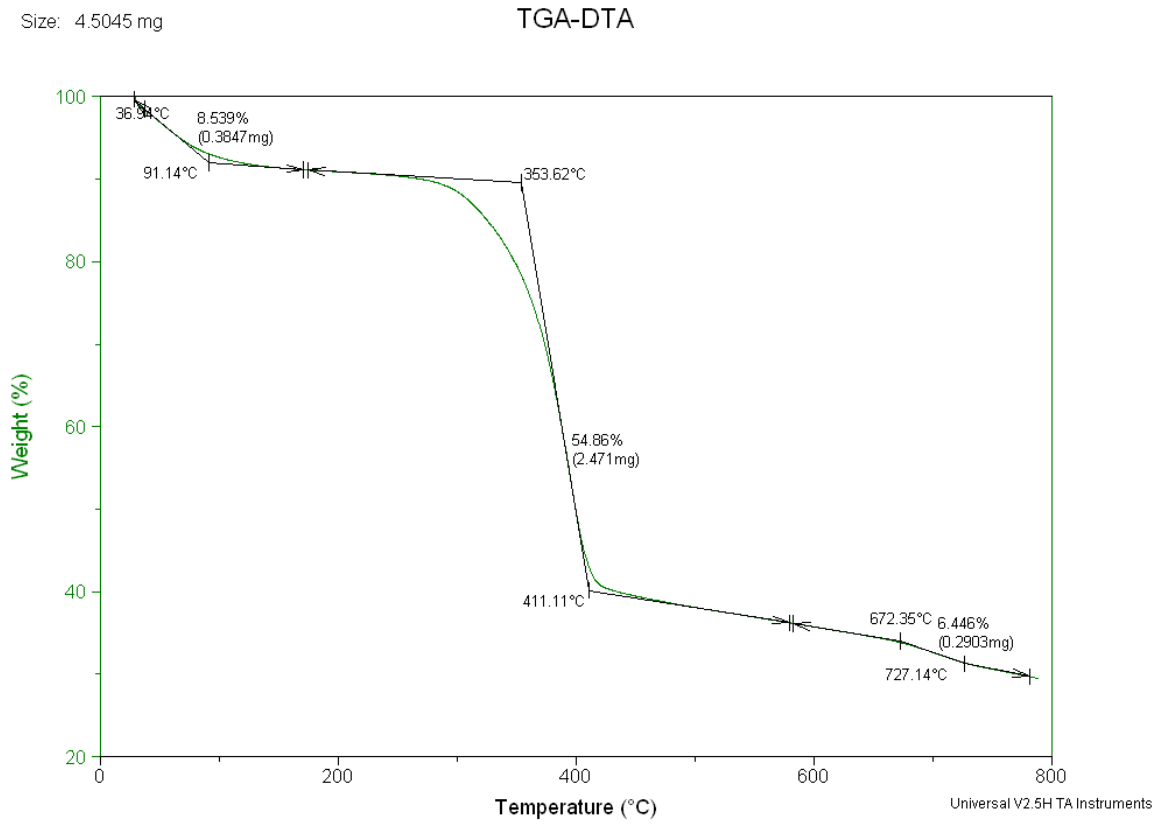

Figure 6.2.1.9: TGA curve of chitin extracted with hydroxylammonium acetate prepared in situ (at 100 °C) by sequential addition of base prior to acid in the range 25°C-800°C in nitrogen atmosphere.

6.2.2 ^{1}H-NMR

Pulping with ammonium acetate

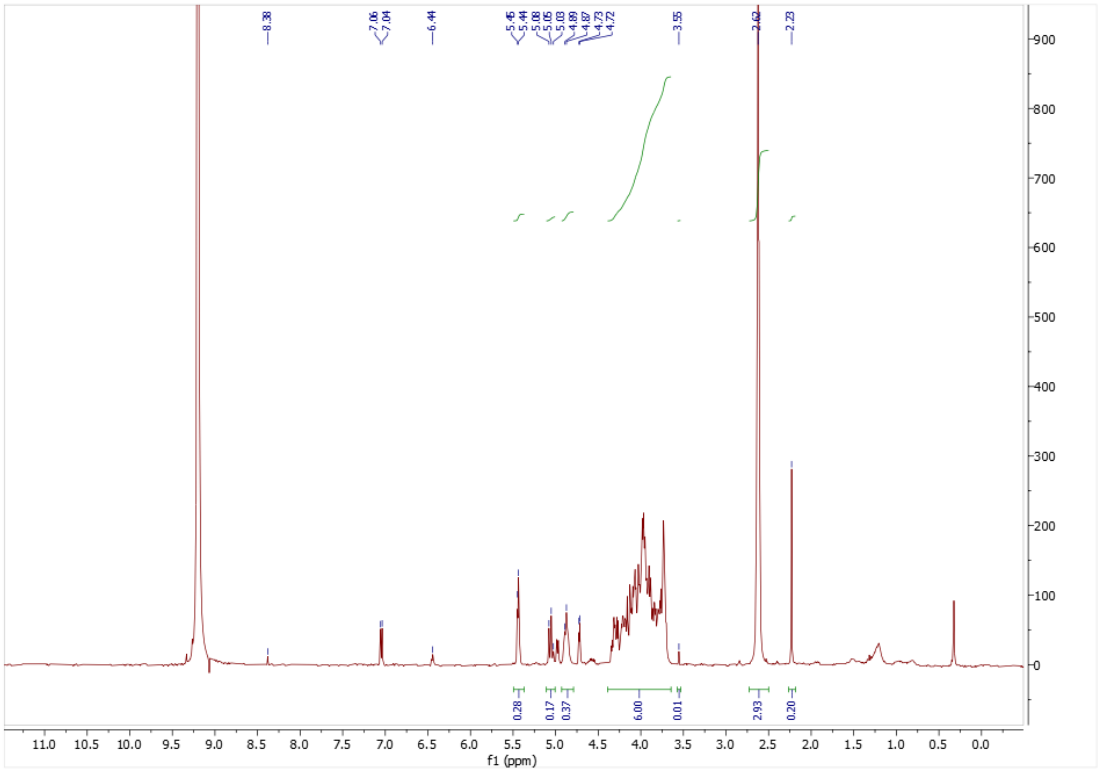

Figure 6.2.2.1: ^{1}H-NMR spectrum of chitin pulped with ammonium acetate solid salt in DCl 35% in D_2O.

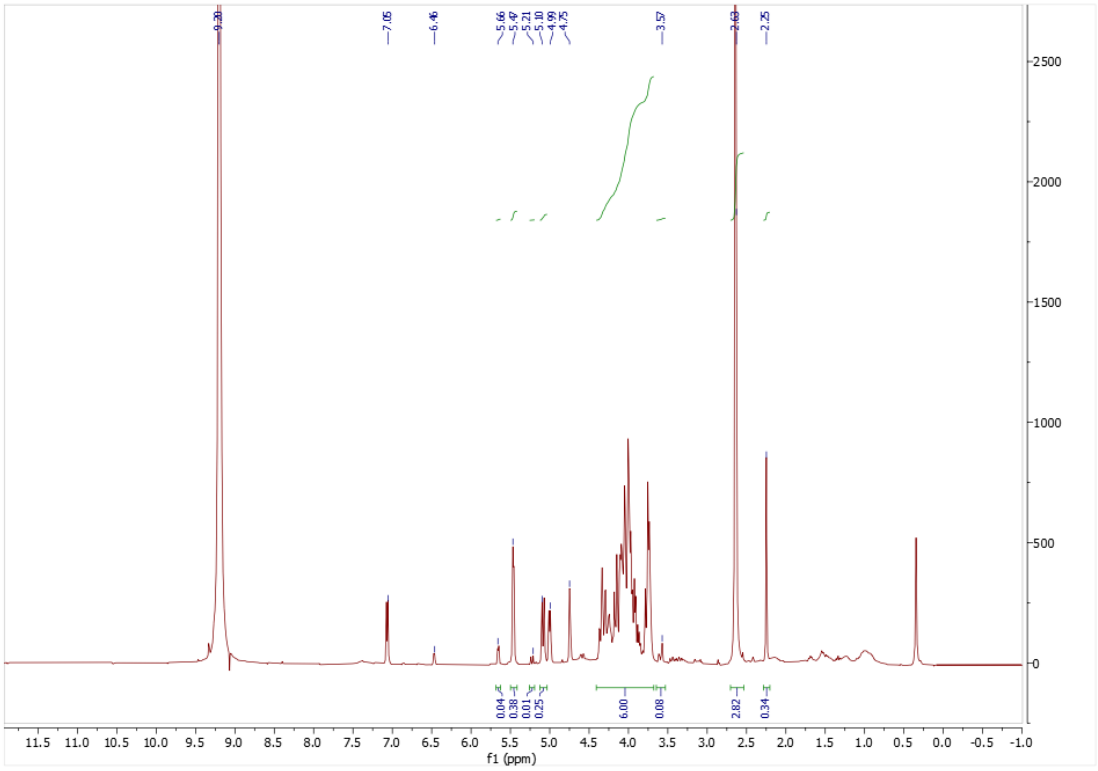

Figure 6.2.2.2: ^{1}H-NMR spectrum of chitin pulped with ammonium acetate prepared in situ in batch conditions (100 °C) by sequential addition of acid prior to base in DCl 35% in D_2O.

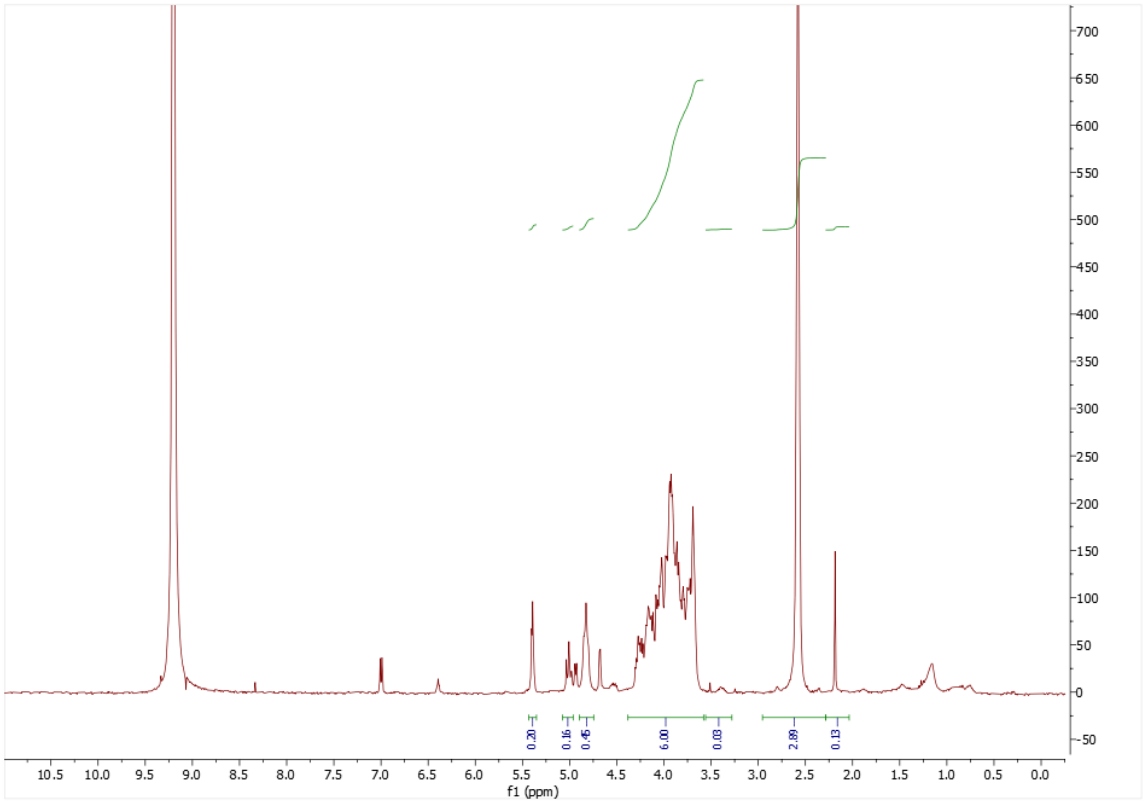

Figure 6.2.2.3: ^{1}H-NMR spectrum of chitin pulped with ammonium acetate prepared in situ in autoclave (145 °C) by sequential addition of acid prior to base in DCl 35% in D_2O.

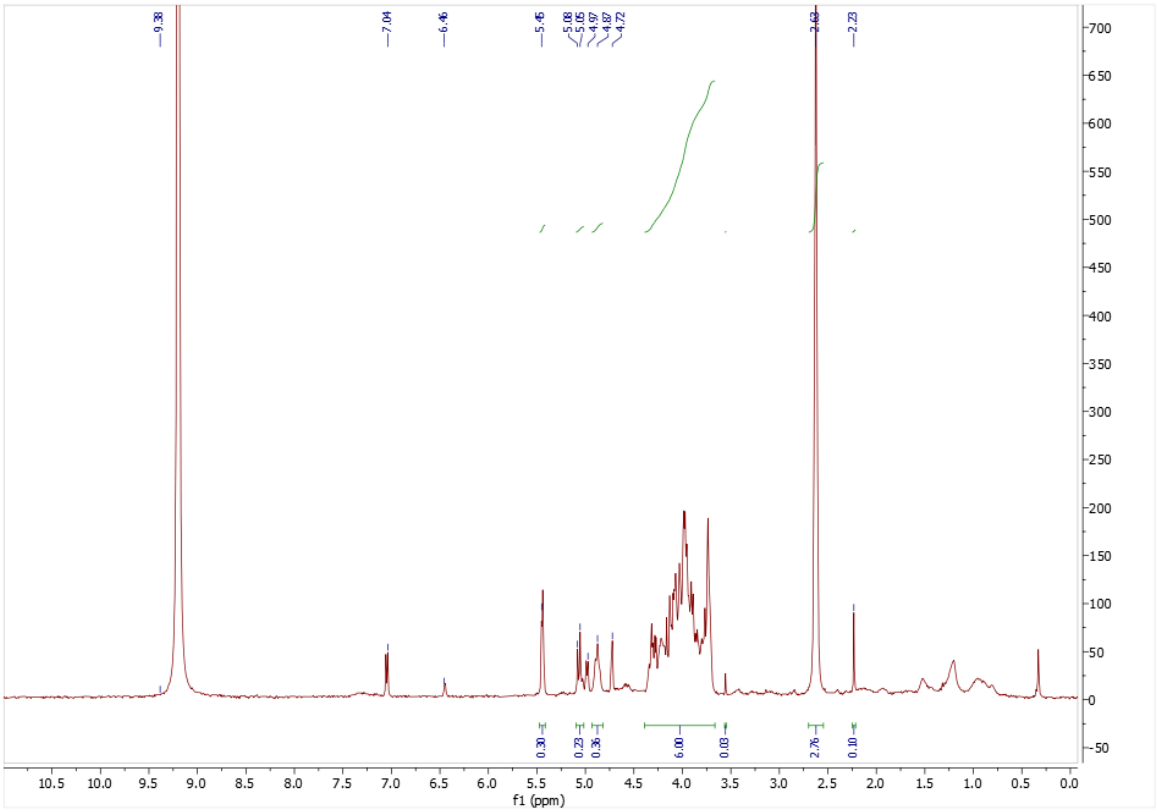

Figure 6.2.2.4: ^{1}H-NMR spectrum of chitin pulped with ammonium acetate prepared in situ in batch conditions (100 °C) by sequential addition of base prior to acid in DCl 35% in D_2O.

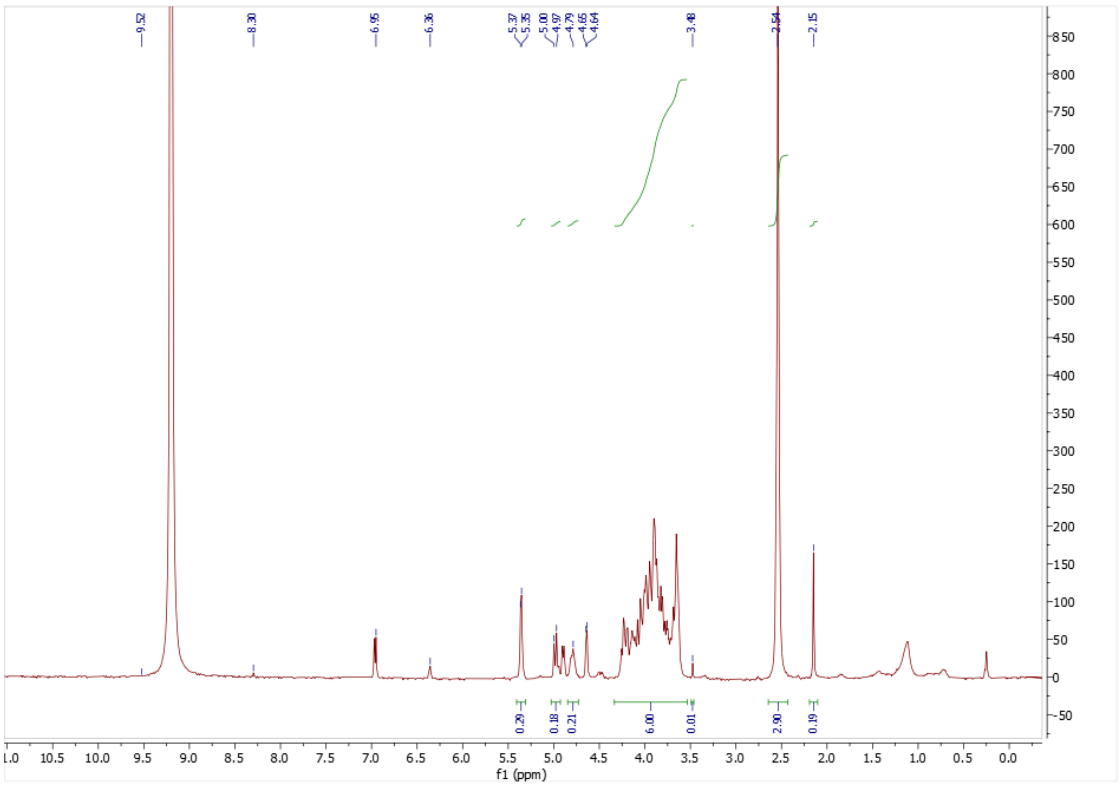

Figure 6.2.2.5: ^{1}H-NMR spectrum of chitin pulped with ammonium acetate prepared in situ in autoclave (145 °C) by sequential addition of base prior to acid in DCl 35% in D_2O.

Pulping with ammonium formate

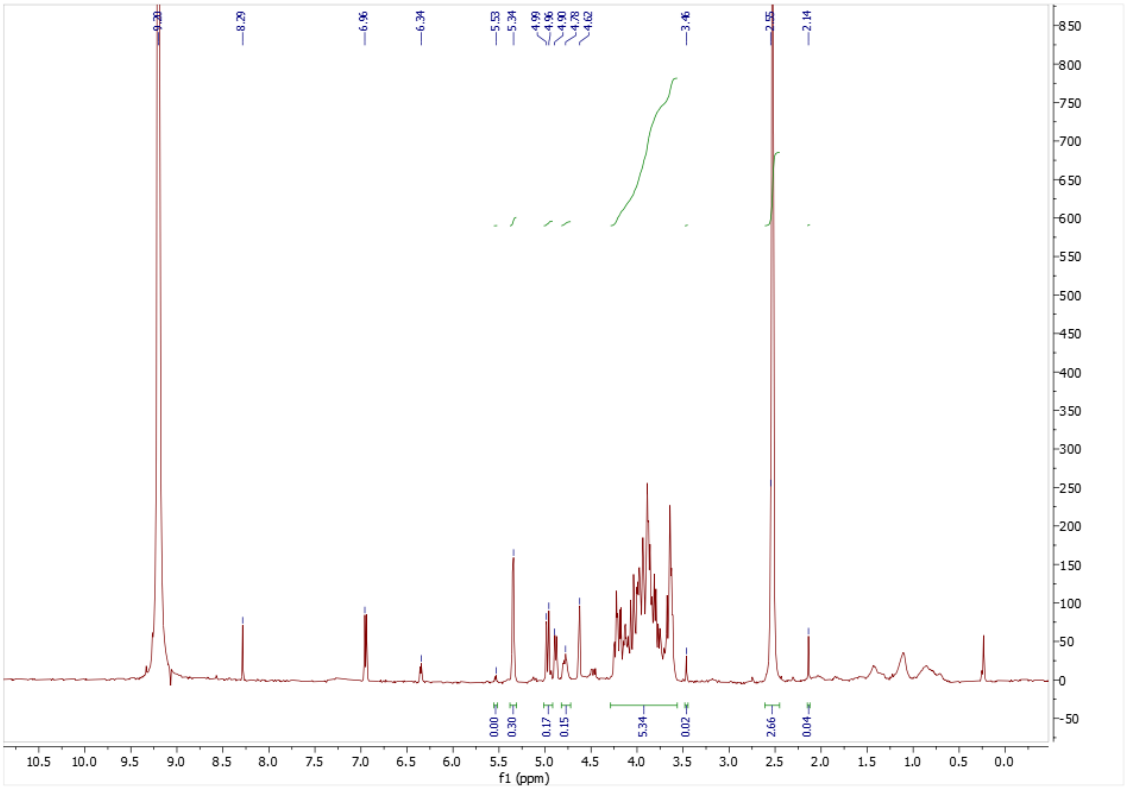

Figure 6.2.2.6: ^{1}H-NMR spectrum of chitin pulped with ammonium formate solid salt in DCl 35% in D_2O.

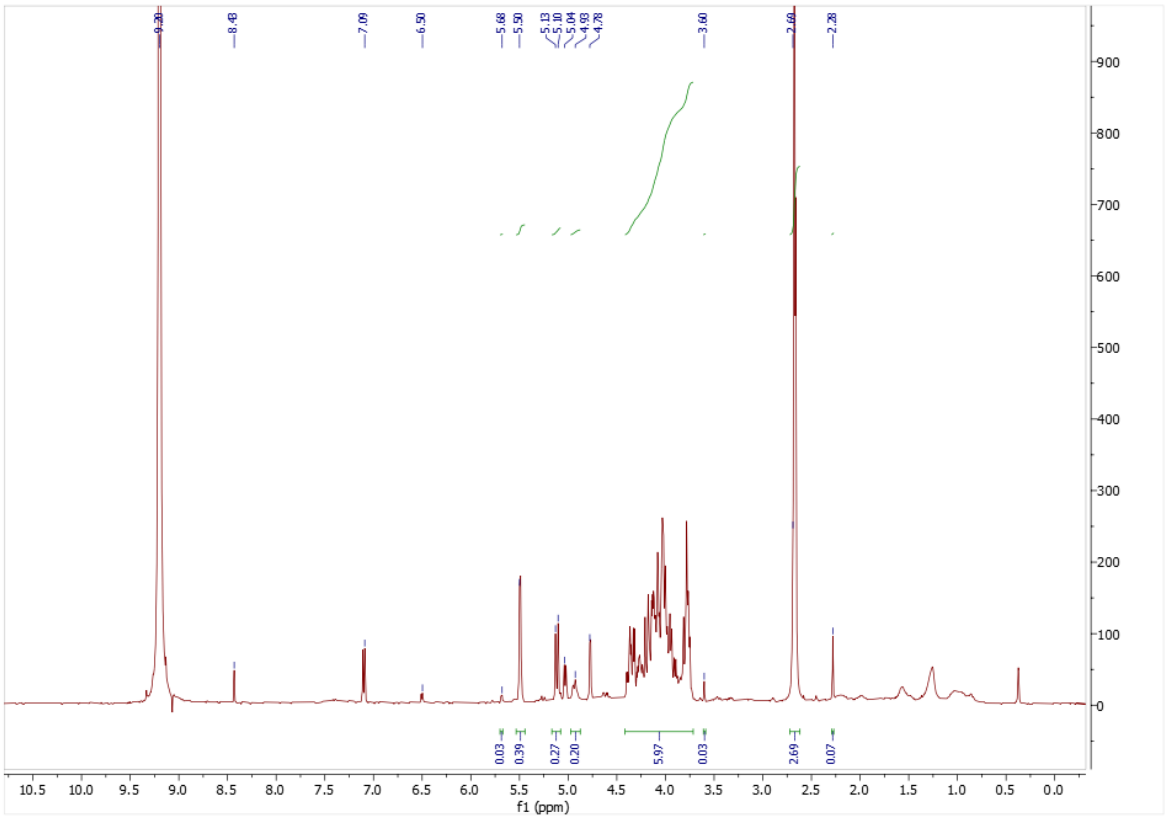

Figure 6.2.2.7: ^{1}H-NMR spectrum of chitin pulped with ammonium formate prepared in situ in batch conditions (100 °C) by sequential addition of acid prior to base in DCl 35% in D_2O.

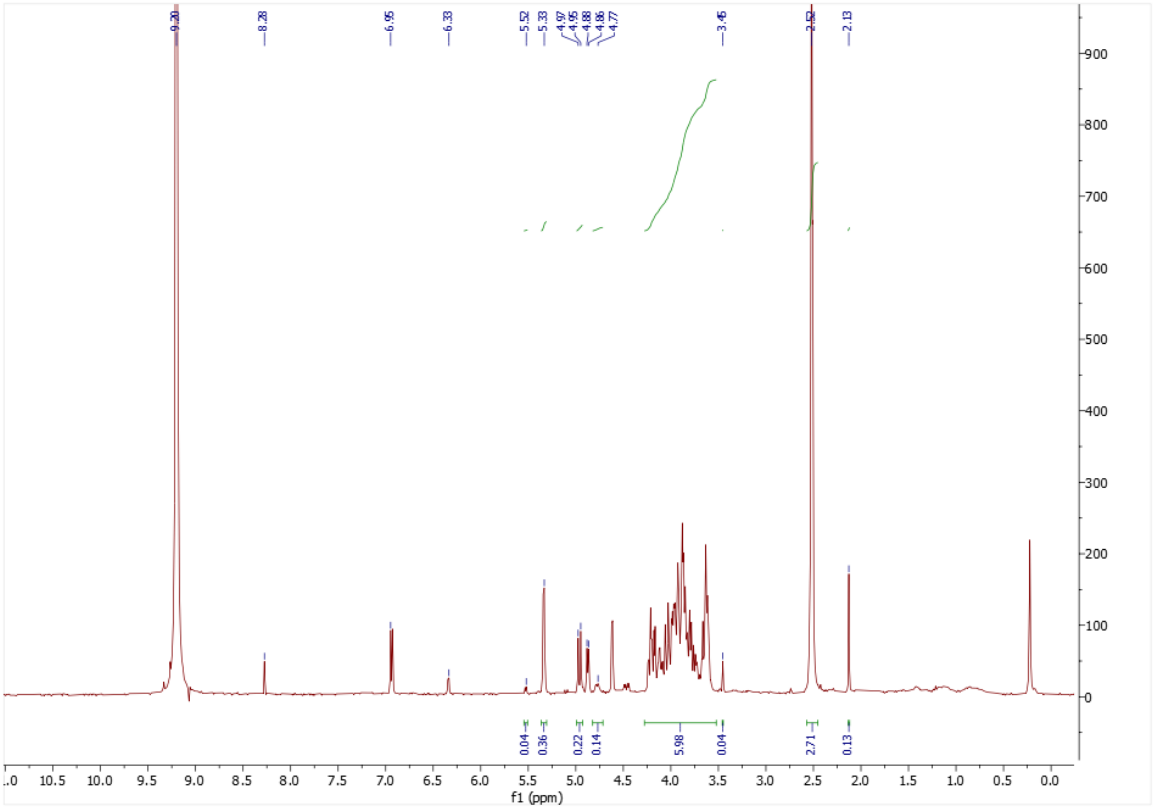

Figure 6.2.2.8: ^{1}H-NMR spectrum of chitin pulped with ammonium formate prepared in situ in autoclave (130 °C) by sequential addition of acid prior to base in DCl 35% in D_2O.

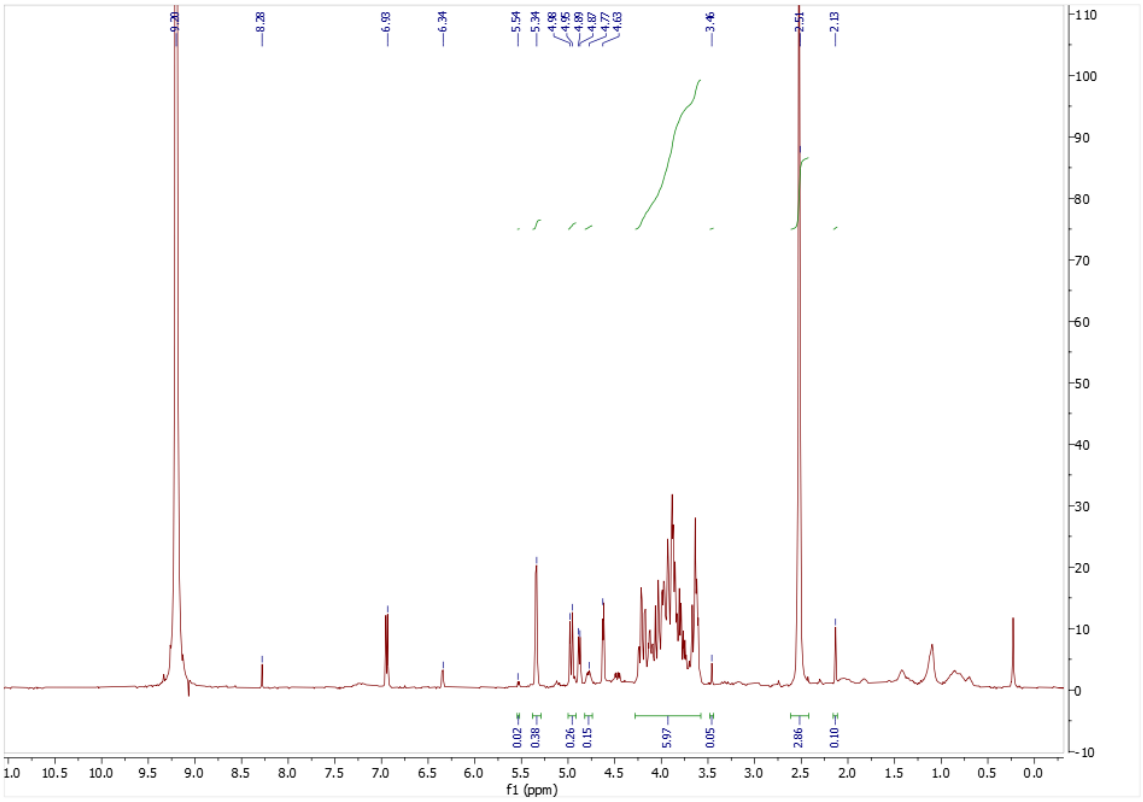

Figure 6.2.2.9: ^{1}H-NMR spectrum of chitin pulped with ammonium formate prepared in situ in batch conditions (100 °C) by sequential addition of base prior to acid in DCl 35% in D_2O.

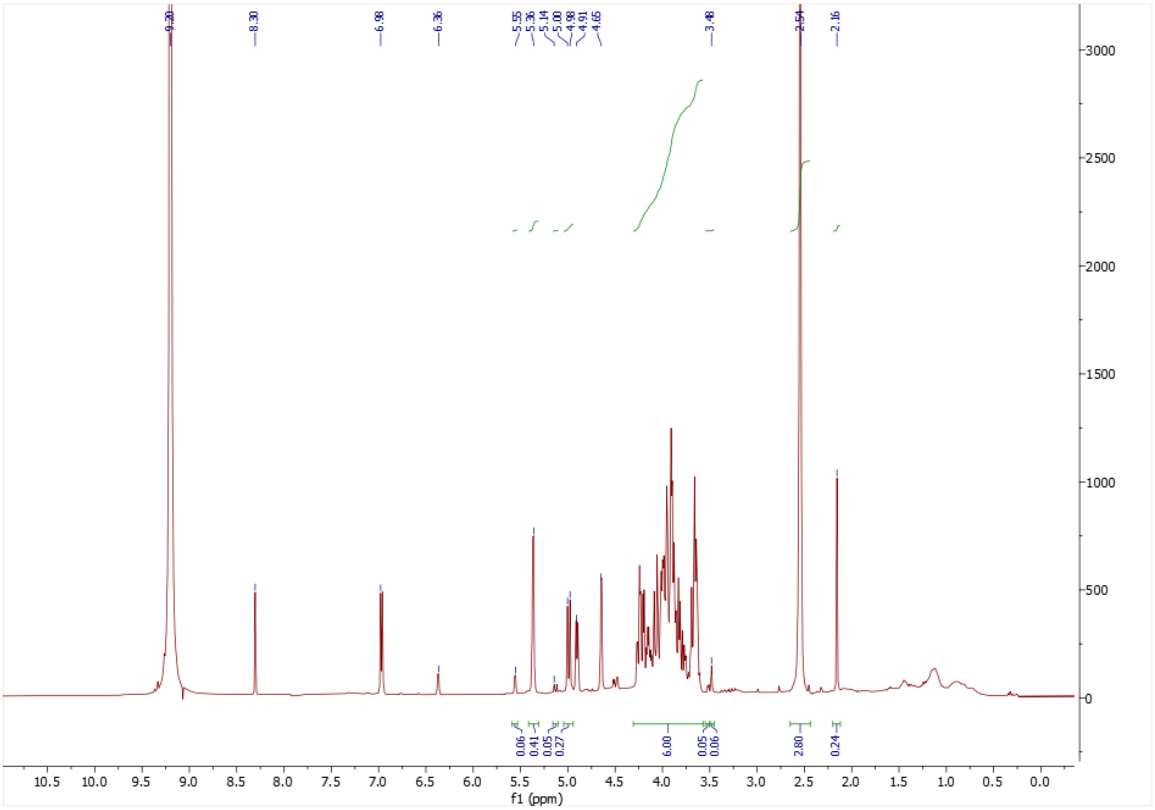

Figure 6.2.2.10: ^{1}H-NMR spectrum of chitin pulped with ammonium formate prepared in situ in autoclave (130 °C) by sequential addition of base prior to acid in DCl 35% in D_2O.

Pulping with hydroxylammonium acetate

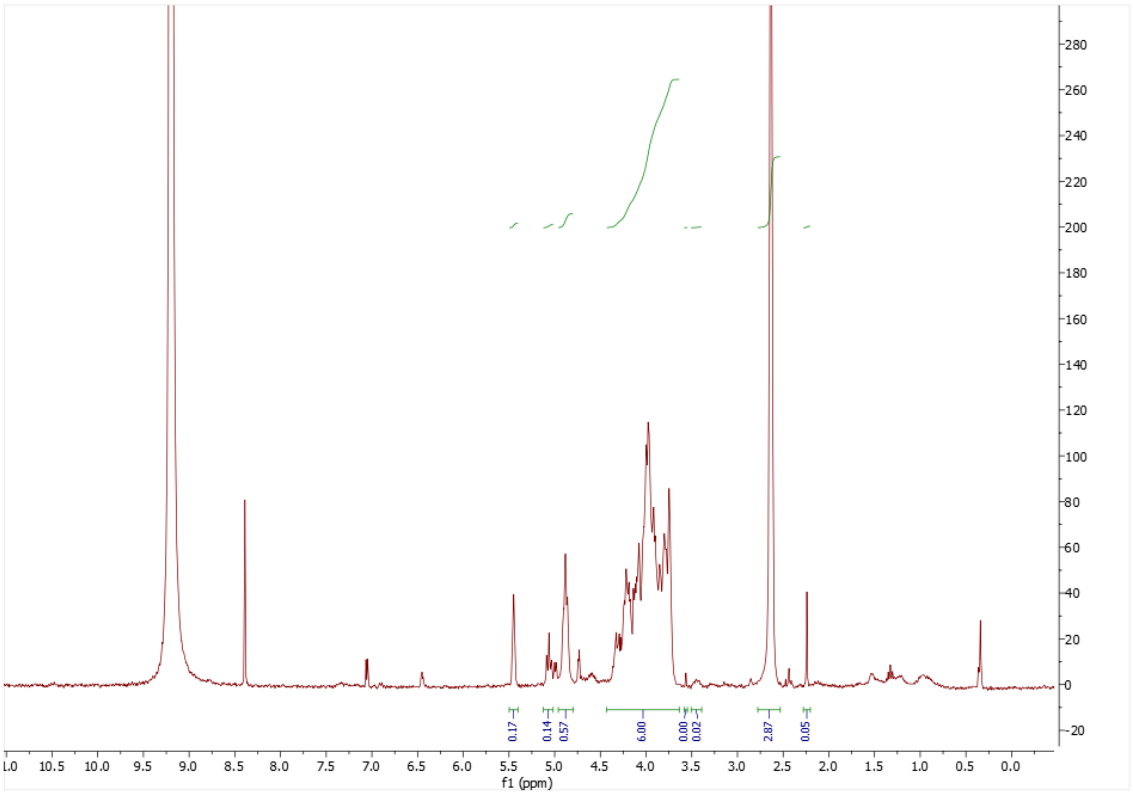

Figure 6.2.2.11: ^{1}H-NMR spectrum of chitin pulped with solid hydroxylammonium acetate in DCl 35% in D_2O.

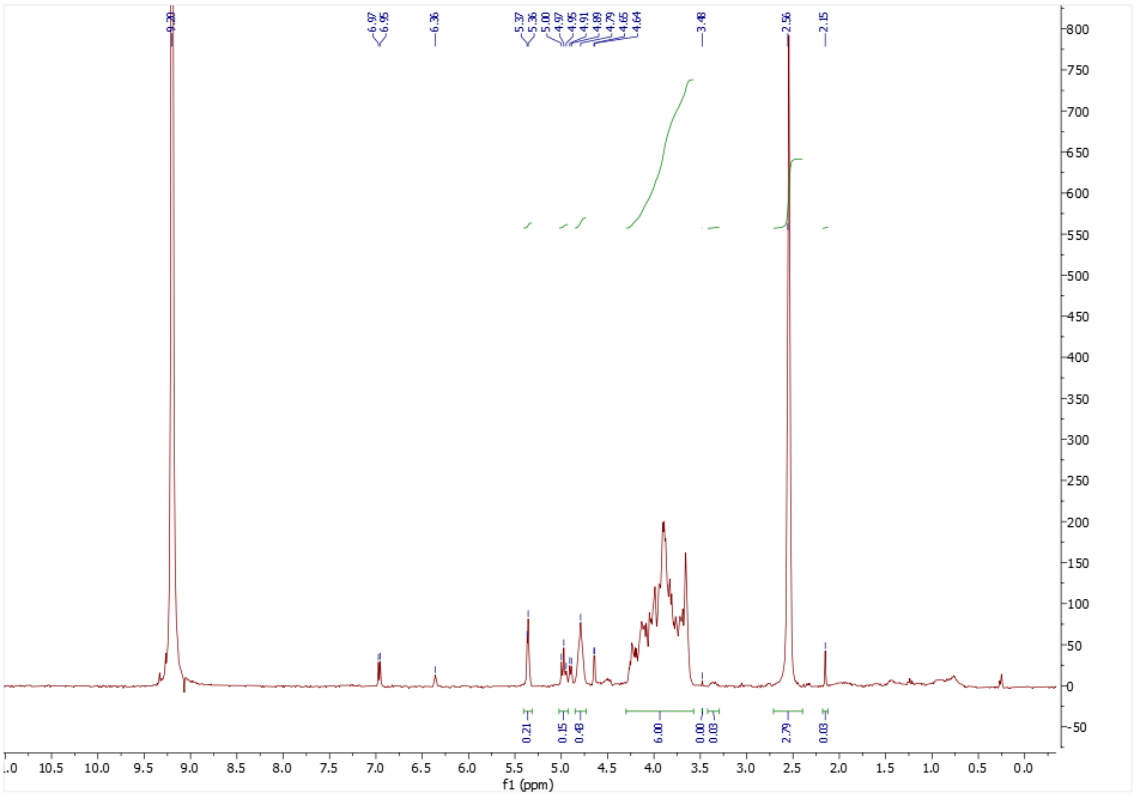

Figure 6.2.2.12: ^{1}H-NMR spectrum of chitin pulped with hydroxylammonium acetate prepared in situ in batch conditions (100 °C) by sequential addition of acid prior to base in DCl 35% in D_2O.

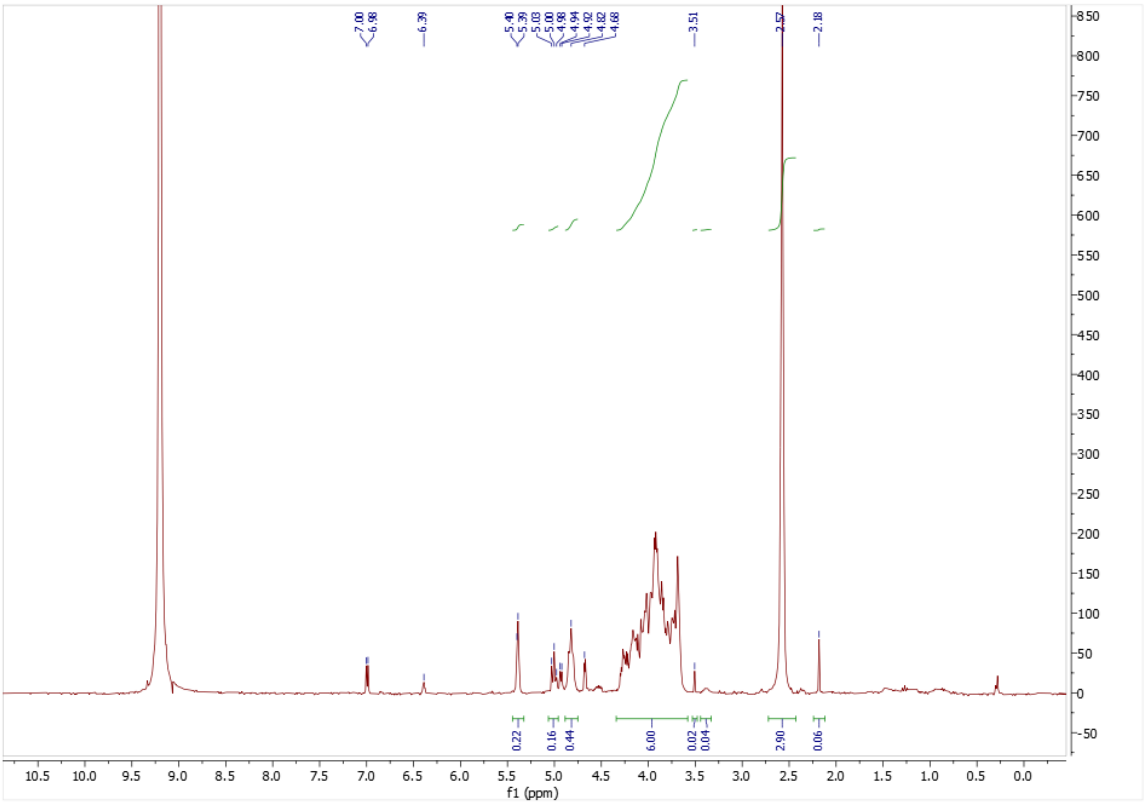

Figure 6.2.2.13: [1]H-NMR spectrum of chitin pulped with hydroxylammonium acetate prepared in situ in batch conditions (100 °C) by sequential addition of base prior to acid in DCl 35% in D_2O.

Pulping with hydroxylammonium formate

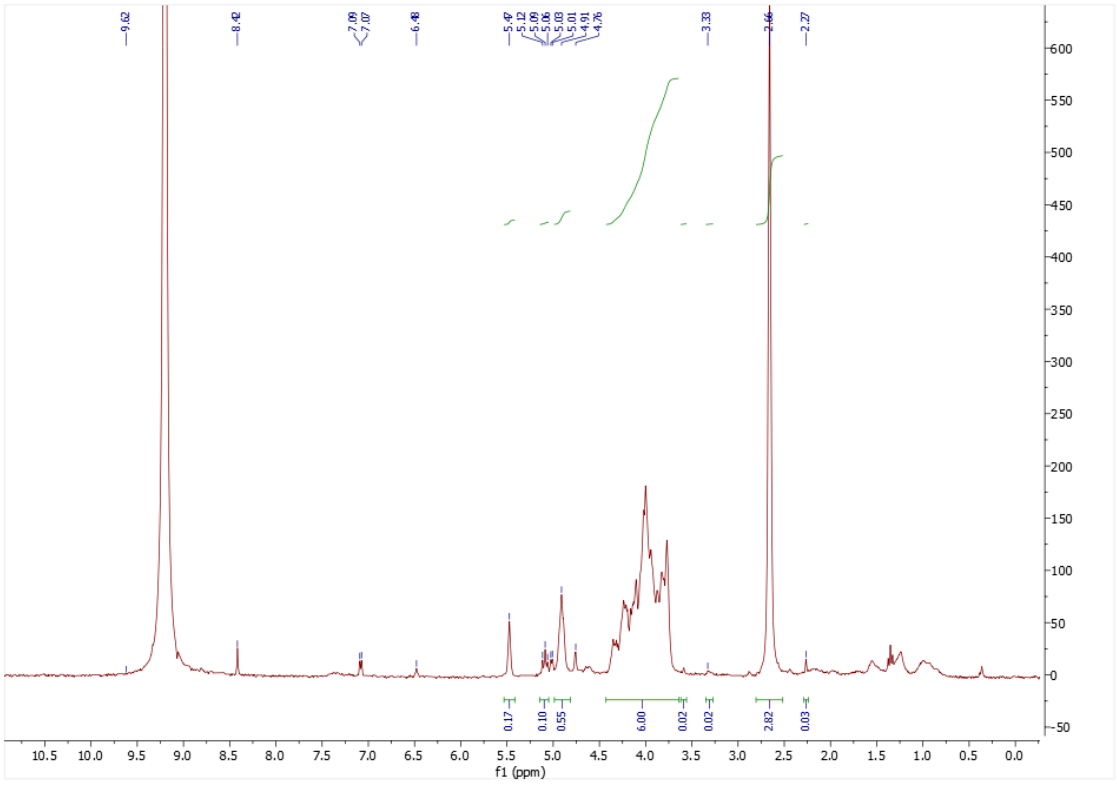

Figure 6.2.2.14: [1]-H-NMR spectrum of chitin pulped with hydroxylammonium formate solid salt in DCl 35% in D_2O.

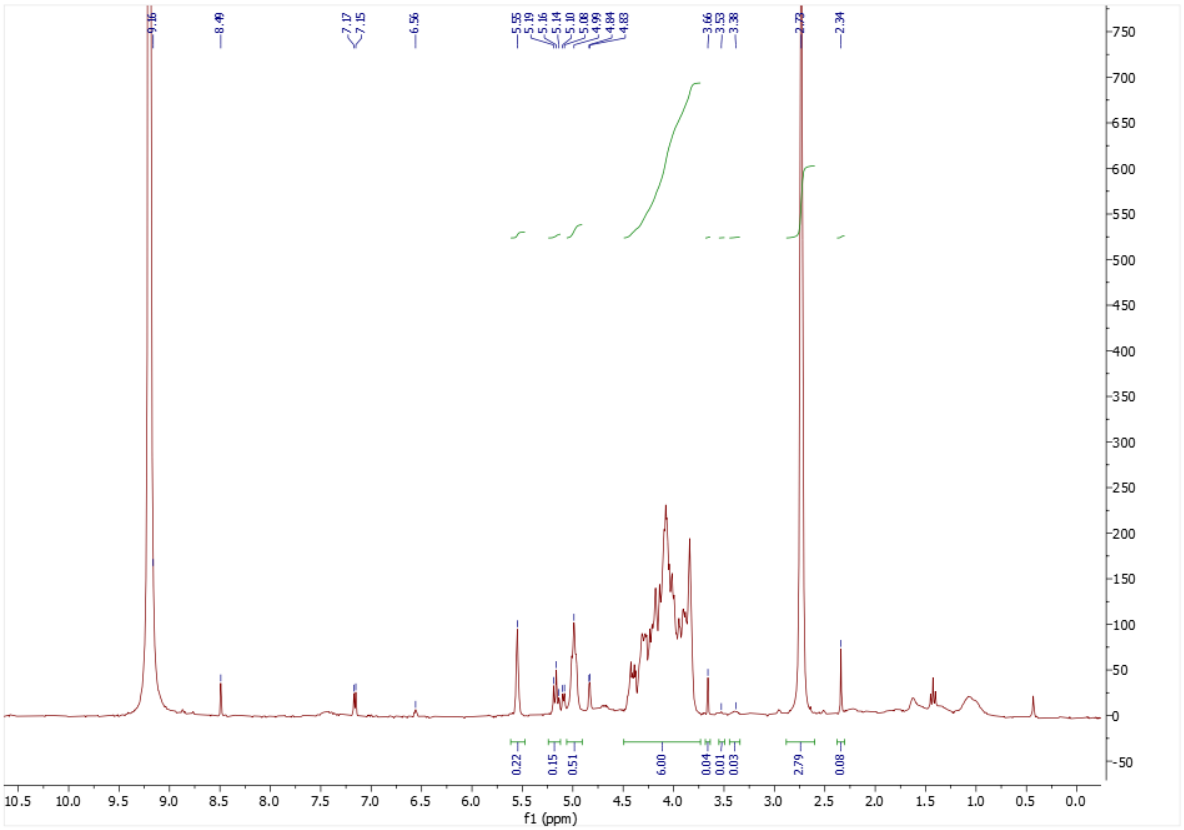

Figure 6.2.2.15: ^{1}H-NMR spectrum of chitin pulped with hydroxylammonium formate prepared in situ in batch conditions (100 °C) by sequential addition of acid prior to base in DCl 35% in D_2O.

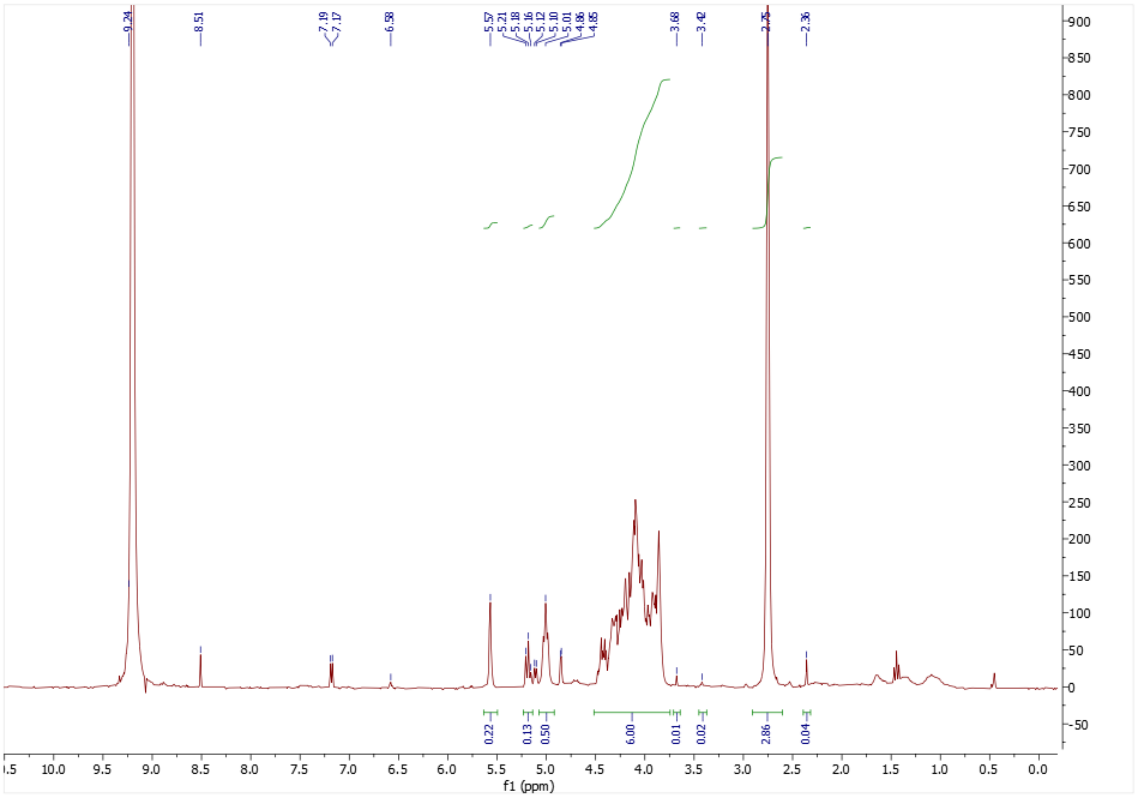

Figure 6.2.2.16: ^{1}H-NMR spectrum of chitin pulped with hydroxylammonium formate prepared in situ in batch conditions (100 °C) by sequential addition of base prior to acid in DCl 35% in D_2O.

6.2.3 FT-IR spectra

Commercial chitin

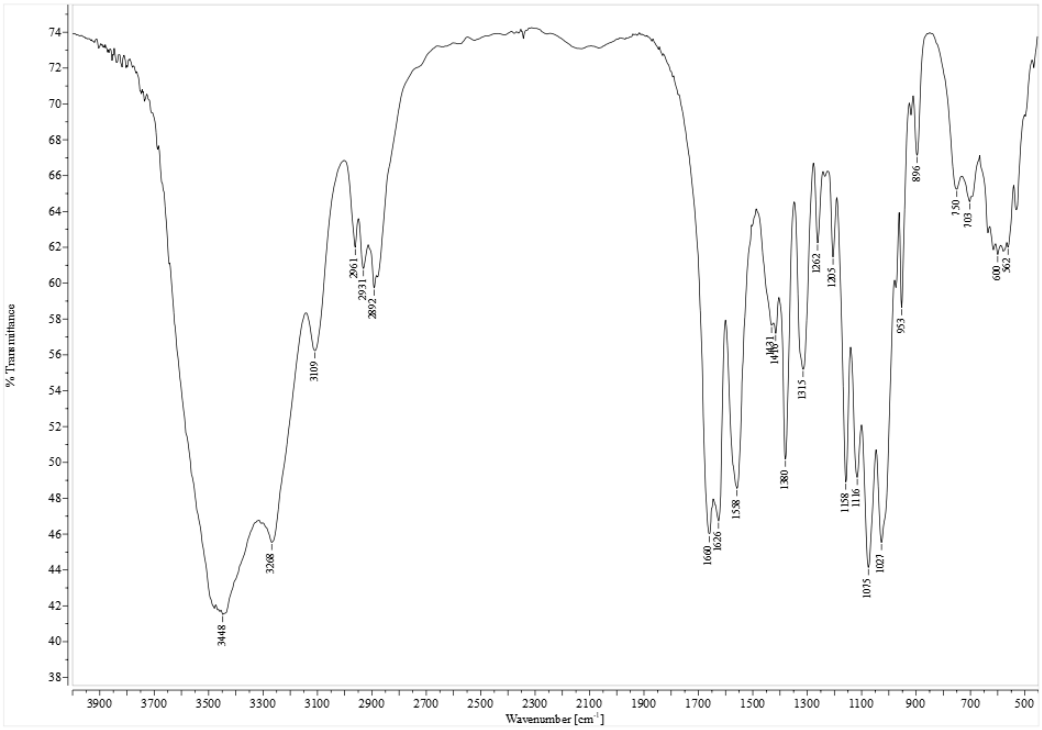

Figure 6.2.3.1: FT-IR spectrum of commercial chitin (1 mg) in KBr pellet (100 mg).

Pulping with ammonium acetate

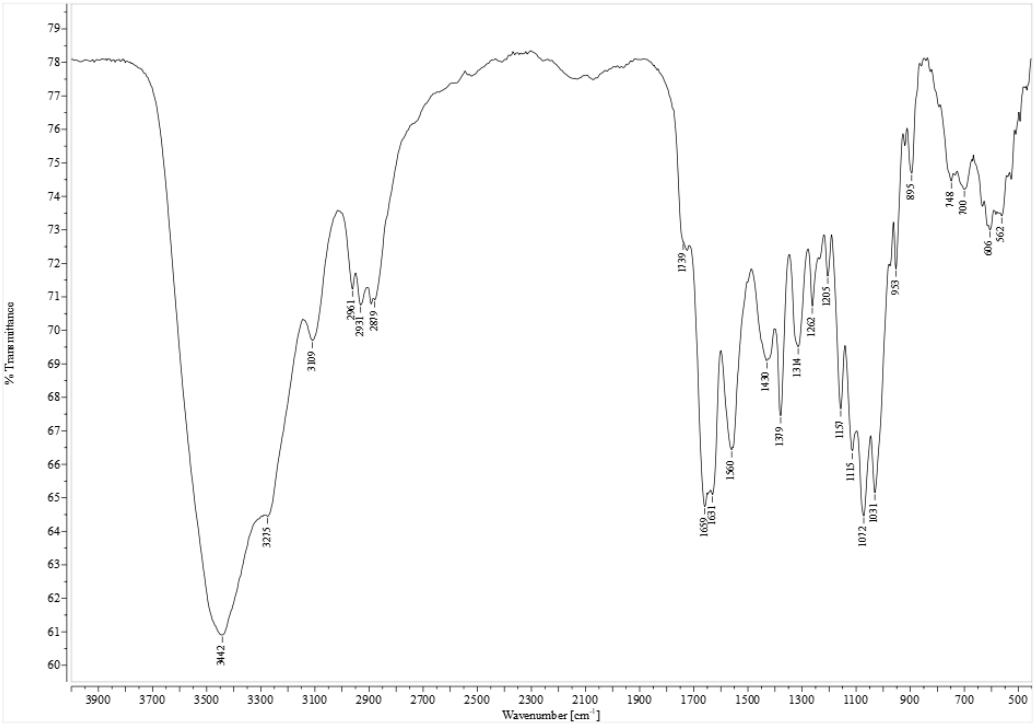

Figure 6.2.3.2: FT-IR spectrum of chitin (1 mg) pulped with ammonium acetate solid salt (145 °C) in KBr pellet (100 mg).

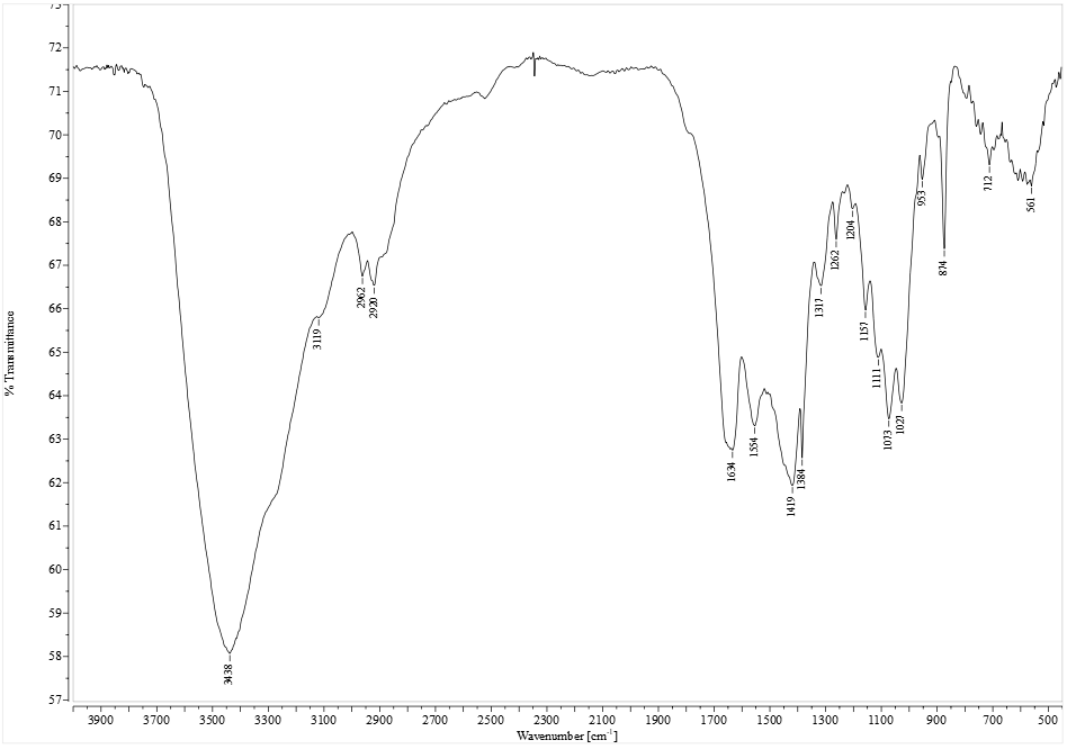

Figure 6.2.3.3: FT-IR spectrum of chitin (1 mg) pulped with ammonium acetate prepared in situ in batch conditions (100 °C) by sequential addition of acid prior to base.

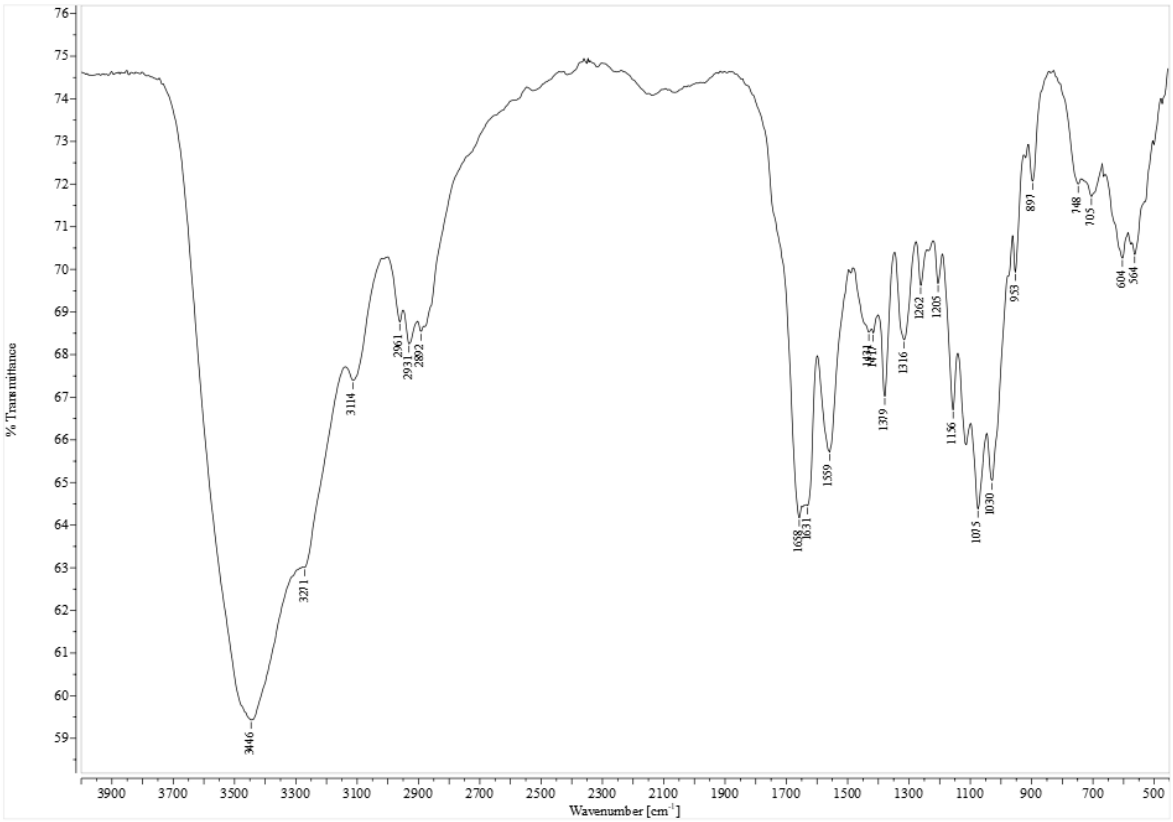

Figure 6.2.3.4: FT-IR spectrum of chitin (1 mg) pulped with ammonium acetate prepared in situ in autoclave (145 °C) by sequential addition of acid prior to base.

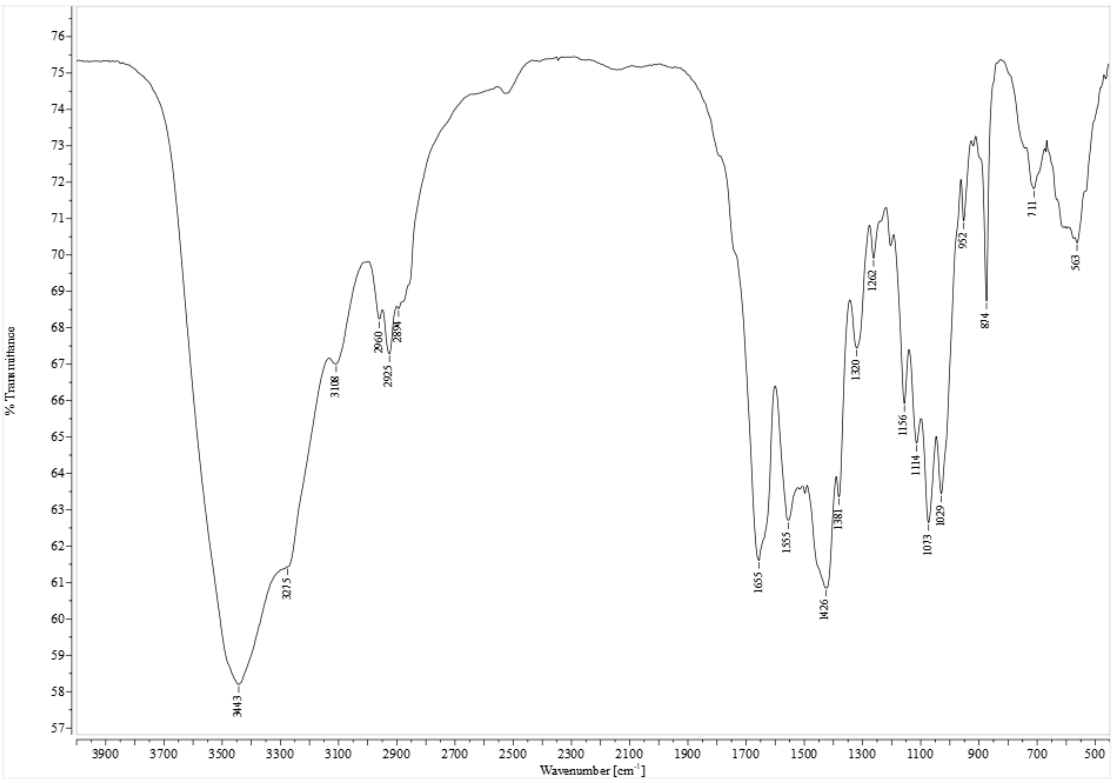

Figure 6.2.3.5: FT-IR spectrum of chitin (1 mg) pulped with ammonium acetate prepared in situ in batch conditions (100 °C) by sequential addition of base prior to acid.

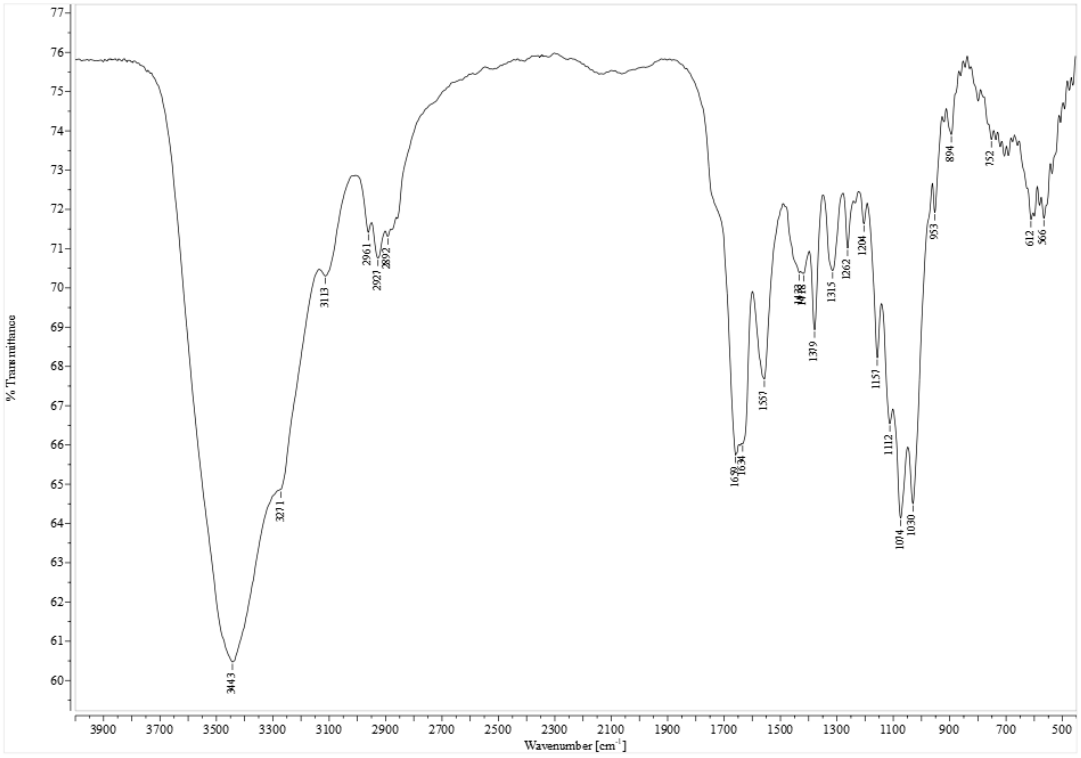

Figure 6.2.3.6: FT-IR spectrum of chitin (1 mg) pulped with ammonium acetate prepared in situ in autoclave (145 °C) by sequential addition of base prior to acid.

Pulping with ammonium formate

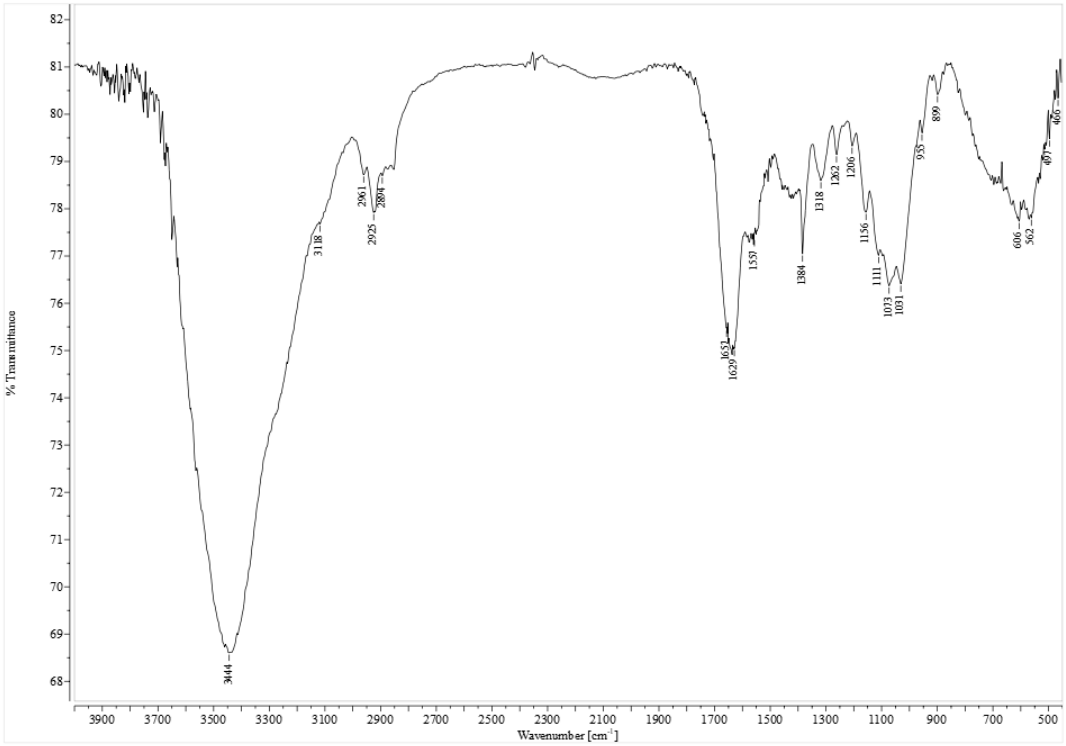

Figure 6.2.3.7: FT-IR spectrum of chitin (1 mg) pulped with ammonium formate solid salt (130 °C) in KBr pellet (100 mg).

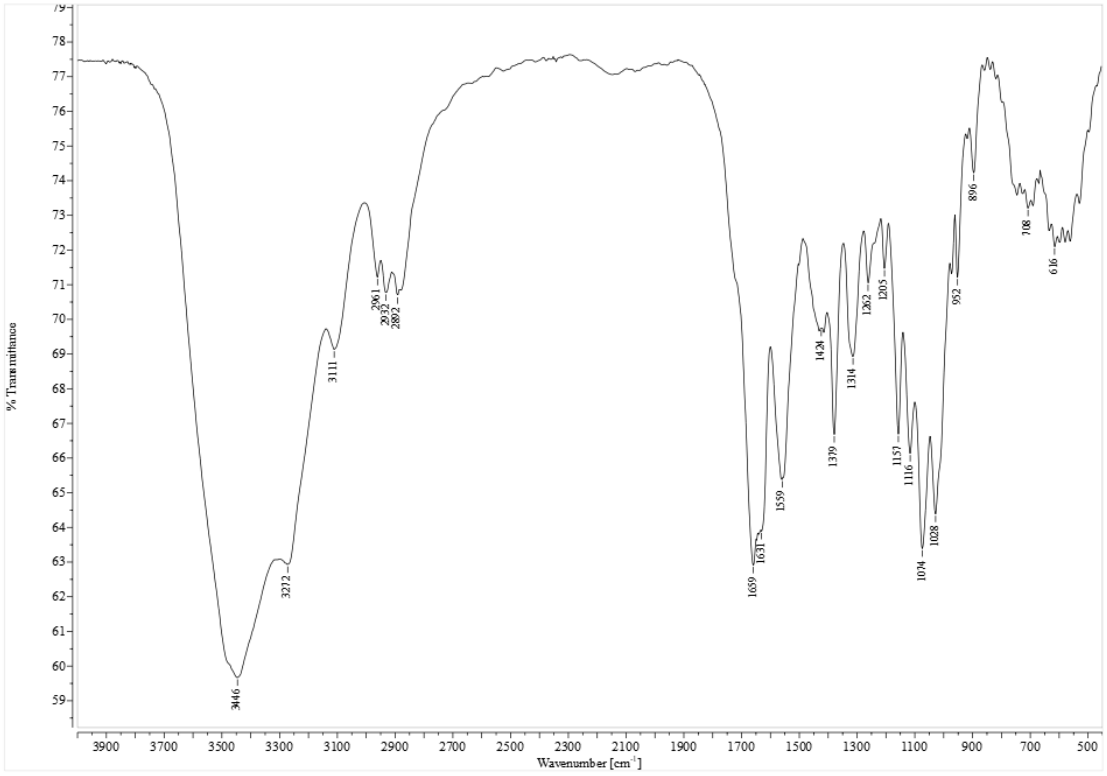

Figure 6.2.3.8: FT-IR spectrum of chitin (1 mg) pulped with ammonium formate prepared in situ in batch conditions (100 °C) by sequential addition of acid prior to base.

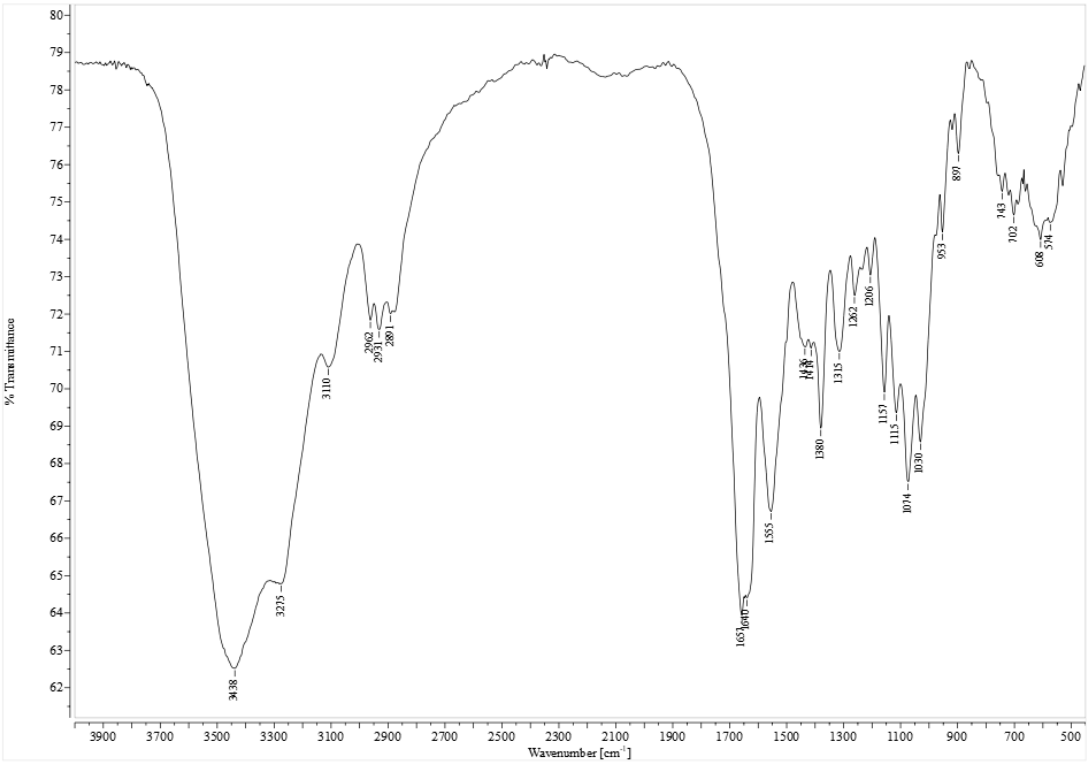

Figure 6.2.3.9: FT-IR spectrum of chitin (1 mg) pulped with ammonium acetate prepared in situ in autoclave (130 °C) by sequential addition of acid prior to base.

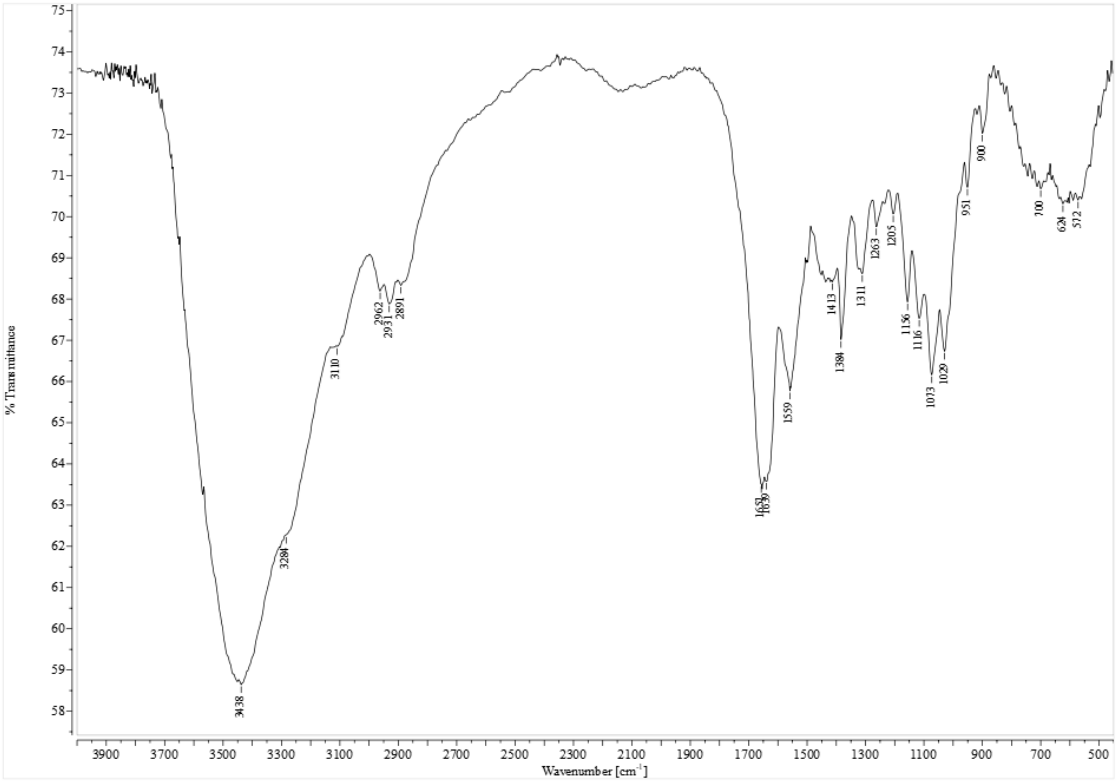

Figure 6.2.3.11: FT-IR spectrum of chitin (1 mg) pulped with ammonium formate prepared in situ in batch conditions (100 °C) by sequential addition of base prior to acid.

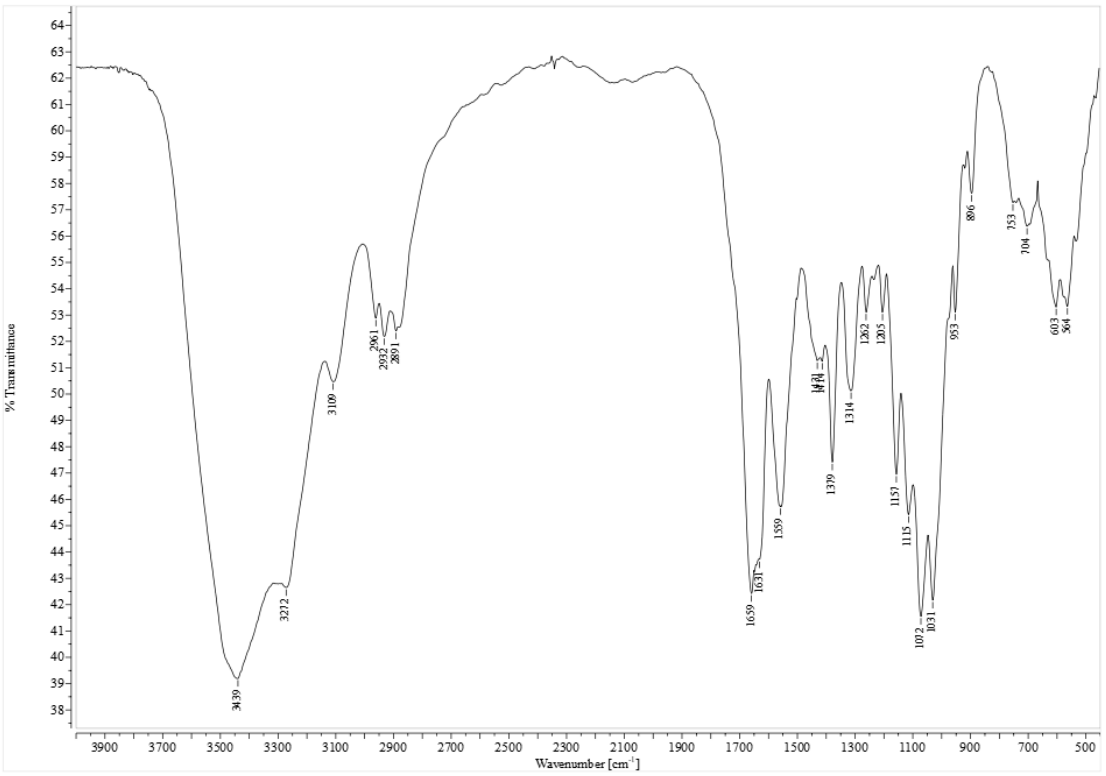

Figure 6.2.3.11: FT-IR spectrum of chitin (1 mg) pulped with ammonium formate prepared in situ in autoclave (130 °C) by sequential addition of base prior to acid.

Pulping with hydroxylammonium acetate

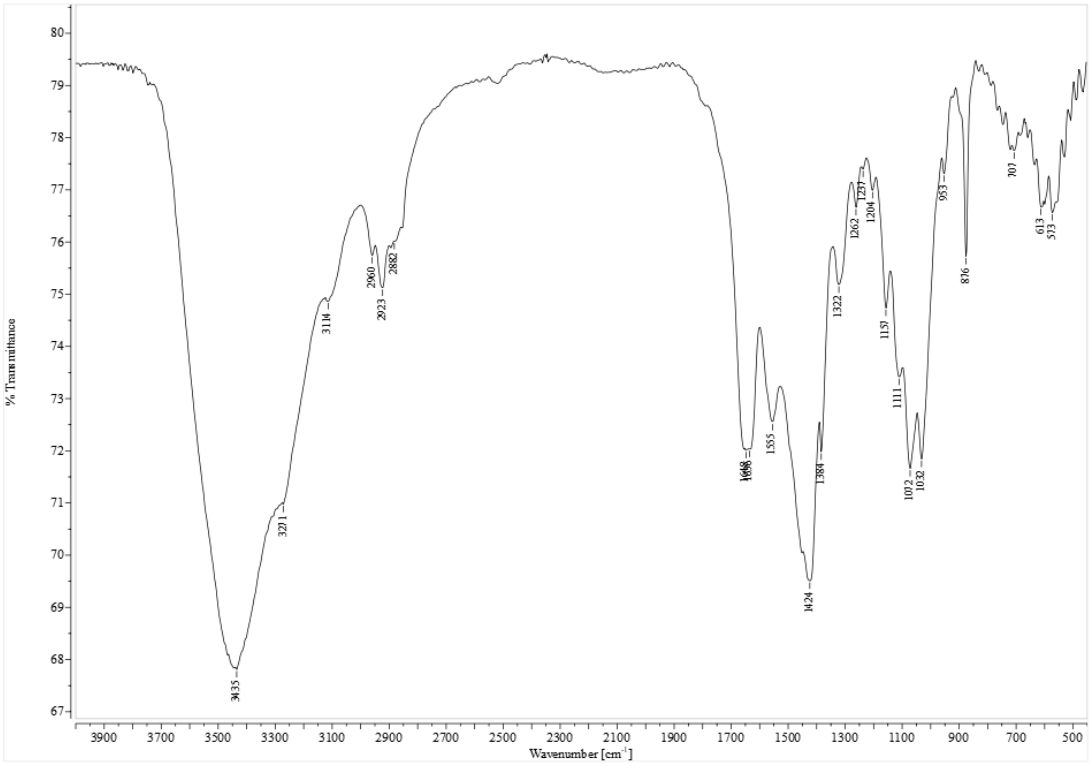

Figure 6.2.3.12: FT-IR spectrum of chitin (1 mg) pulped with hydroxylammonium acetate solid salt (100 °C) in KBr pellet (100 mg).

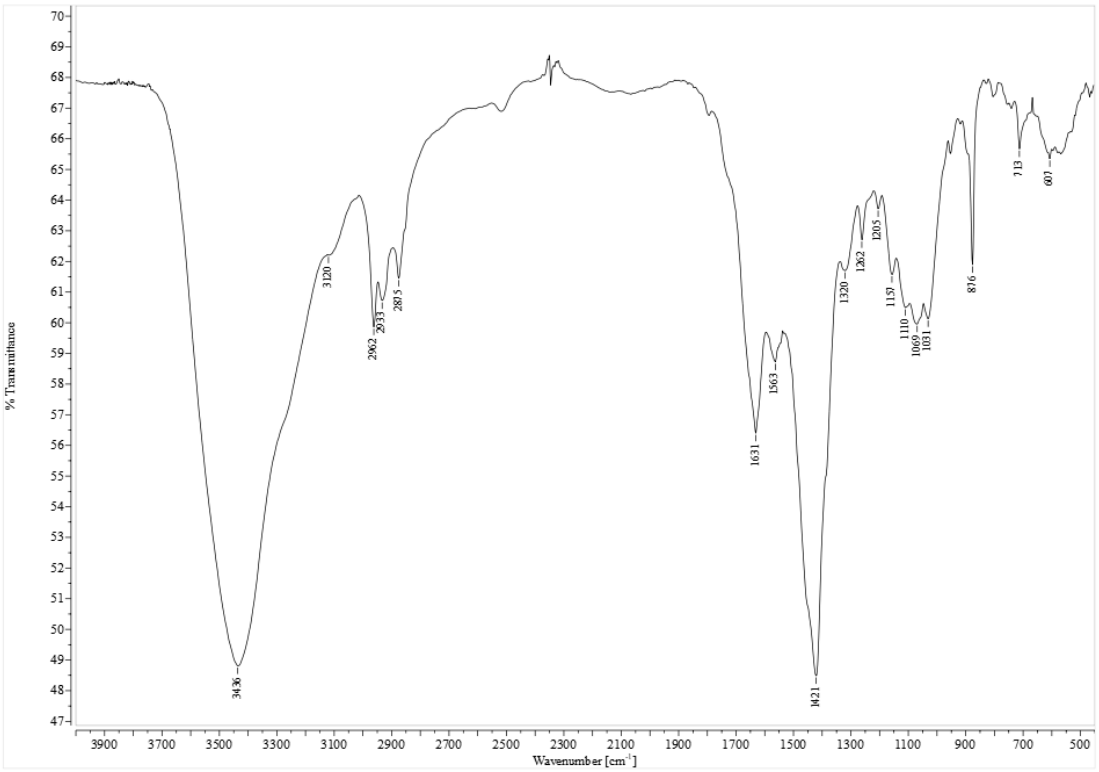

Figure 6.2.3.13: FT-IR spectrum of chitin (1 mg) pulped with hydroxylammonium acetate prepared in situ in batch conditions (100 °C) by sequential addition of acid prior to base.

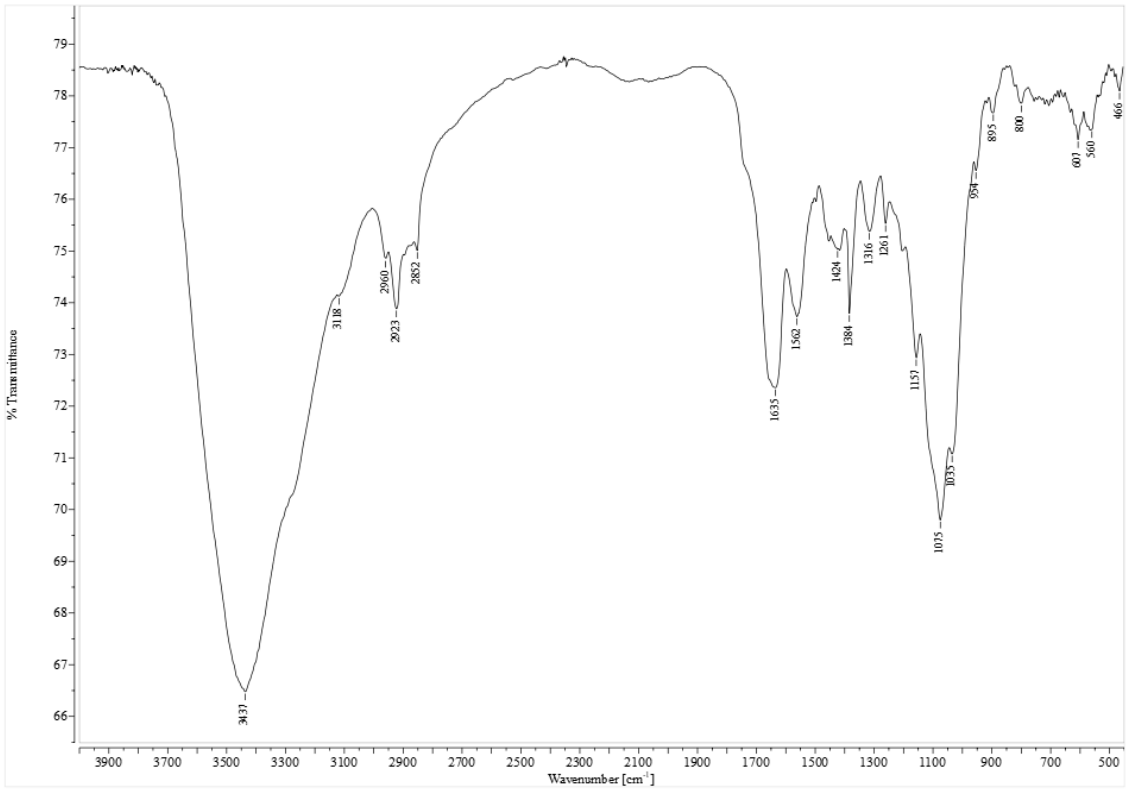

Figure 6.2.3.14: FT-IR spectrum of chitin (1 mg) pulped with hydroxylammonium acetate prepared in situ in batch conditions (100 °C) by sequential addition of base prior to acid.

Pulping with hydroxylammonium formate

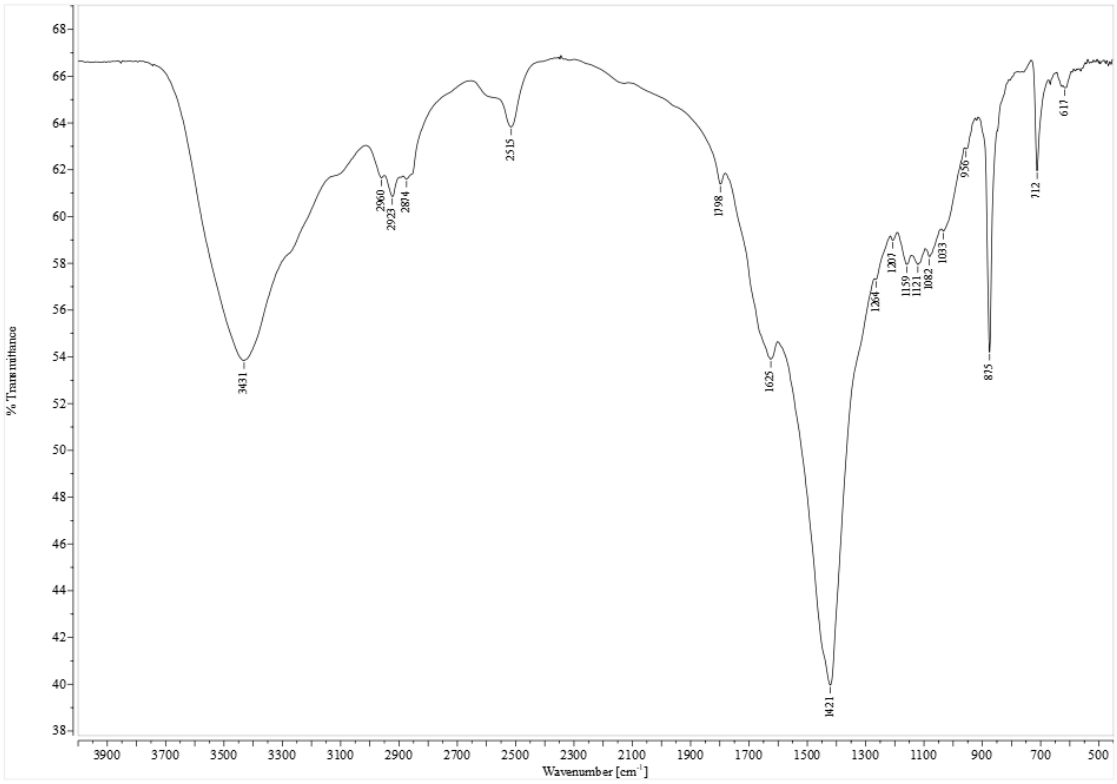

Figure 6.2.3.15: FT-IR spectrum of chitin (1 mg) pulped with hydroxylammonium formate solid salt (100 °C) in KBr pellet (100 mg).

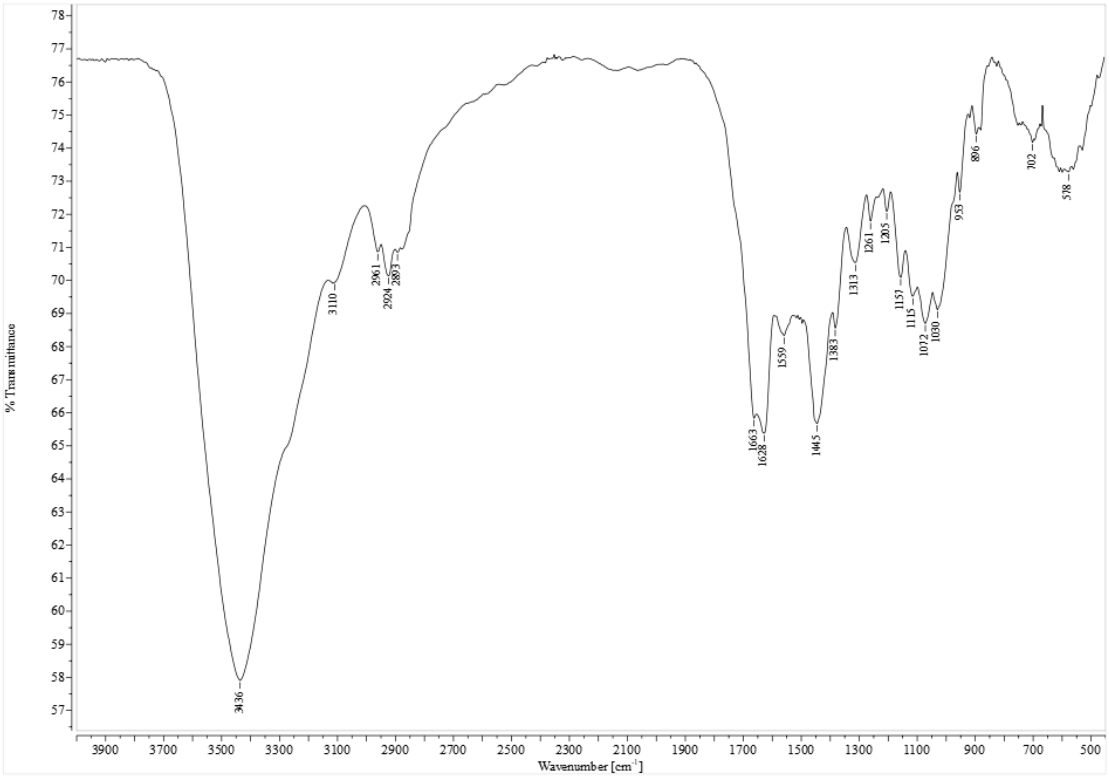

Figure 6.2.3.16: FT-IR spectrum of chitin (1 mg) pulped with hydroxylammonium formate prepared in situ in batch conditions (100 °C) by sequential addition of acid prior to base.

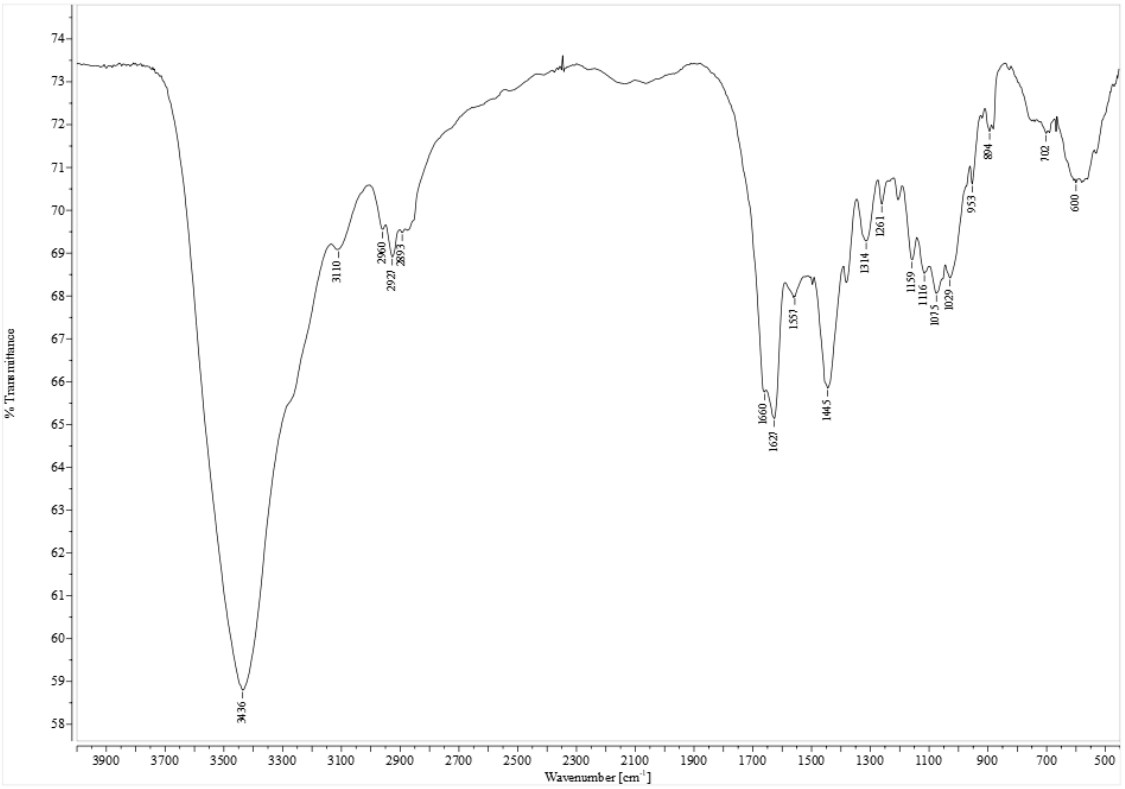

Figure 6.2.3.17: FT-IR spectrum of chitin (1 mg) pulped with hydroxylammonium acetate prepared in situ in batch conditions (100 °C) by sequential addition of base prior to acid.

6.2.4 XRD

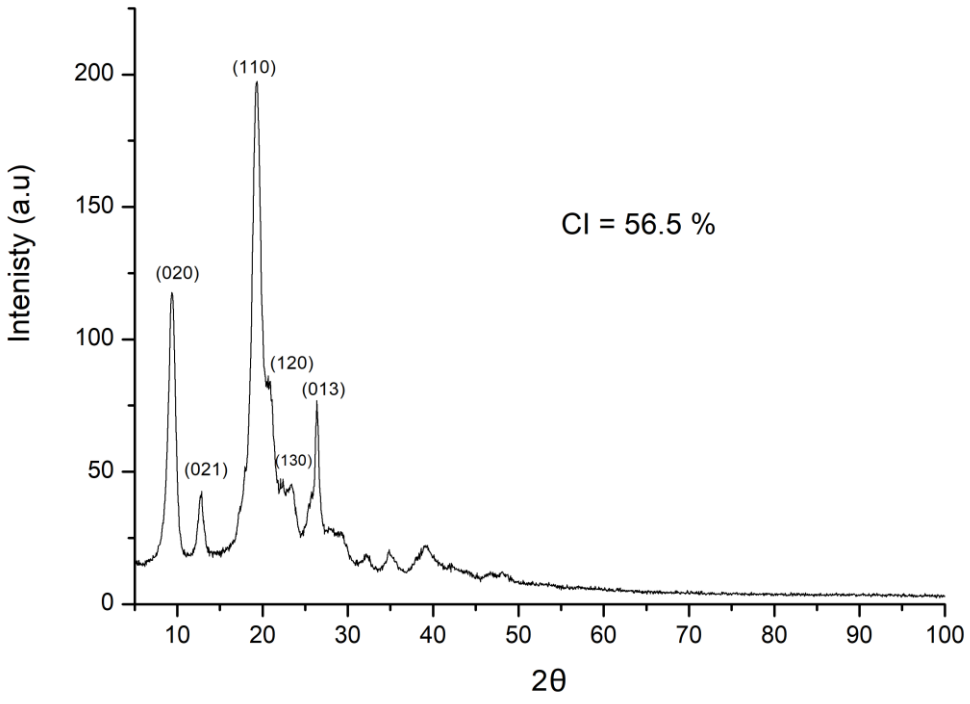

Figure 6.2.4.1: XRD diffractogram of commercial chitin.

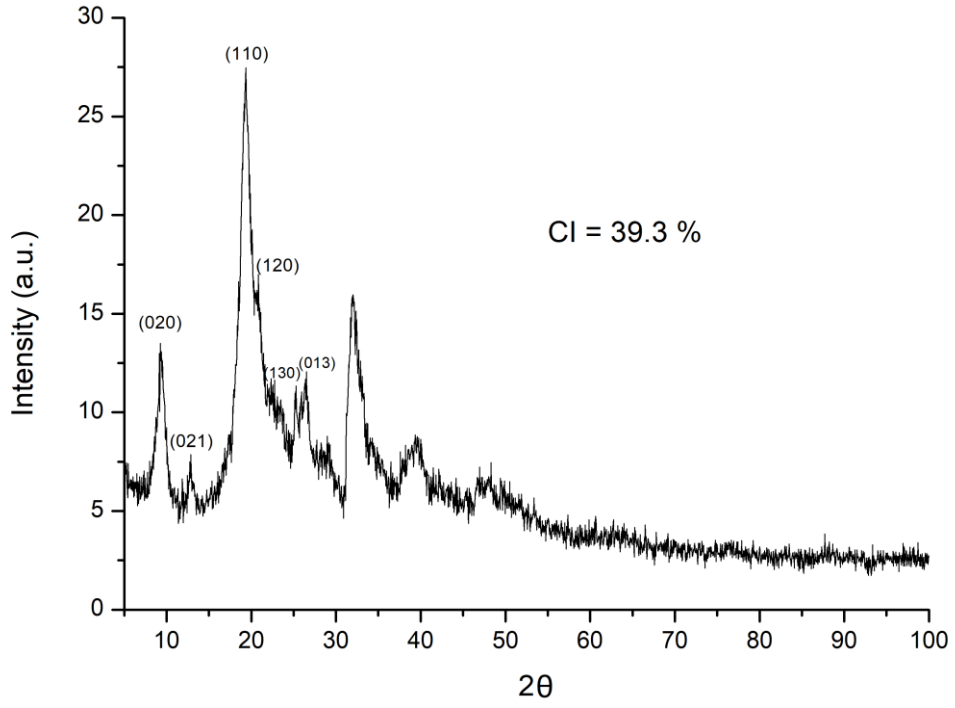

Figure 6.2.4.2: XRD diffractogram of chitin pulped with ammonium formate solid salt.

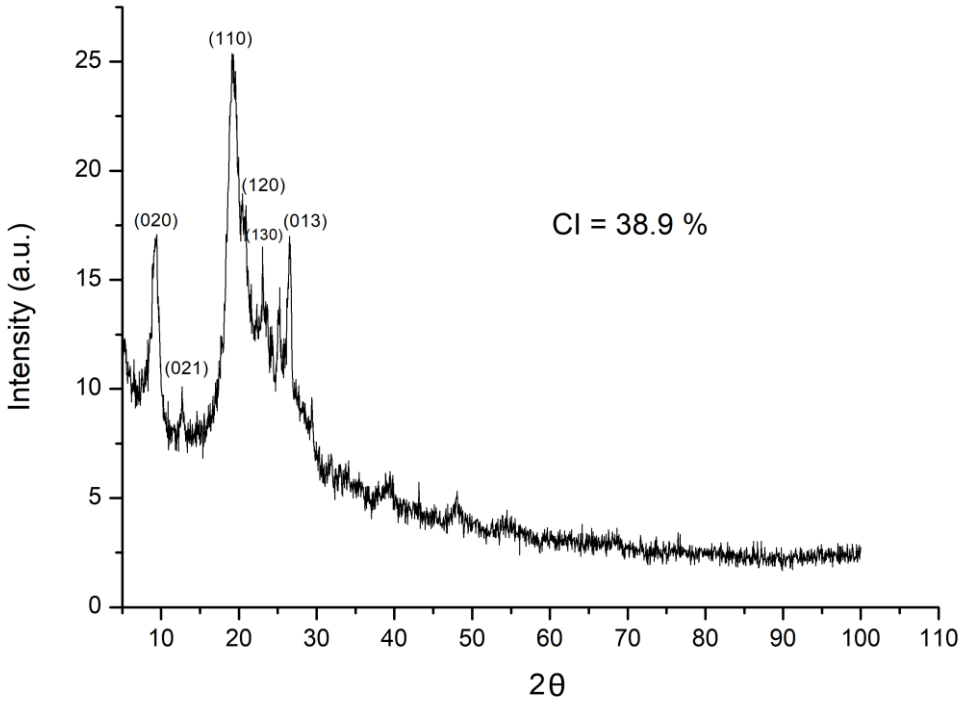

Figure 6.2.4.3: XRD diffractogram of chitin pulped with ammonium formate prepared in situ by sequential addition of acid prior to base.

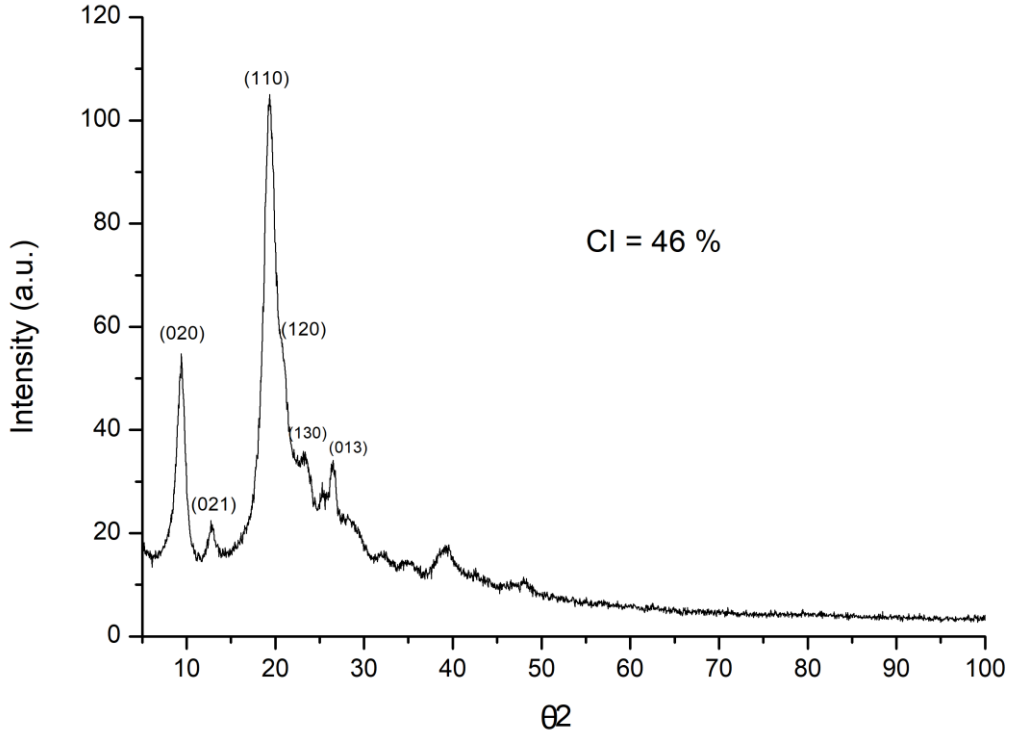

Figure 6.2.4.4: XRD diffractogram of chitin pulped with ammonium formate prepared in situ by sequential addition of base prior to acid.

6.2.5 GPC

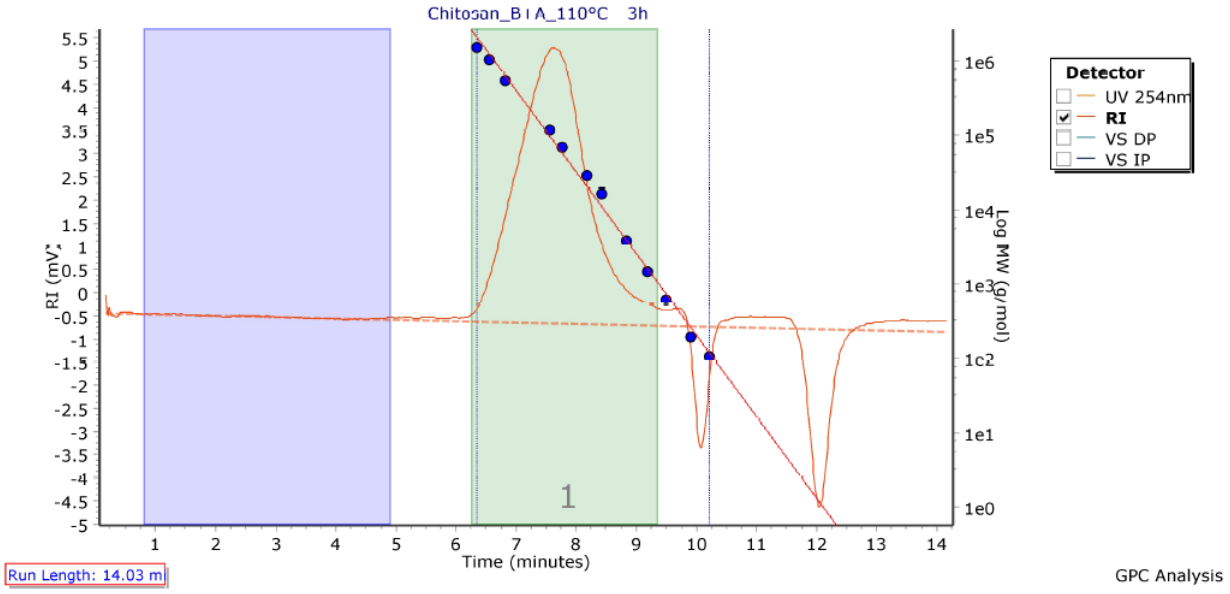

Figure 6.2.5.1: GPC representative analysis of chitosan obtained by heterogeneous alkali deacetylation of pulped chitin.

7 BIBLIOGRAPHY

1 N. V. Veríssimo, C. U. Mussagy, A. A. Oshiro, C. M. N. Mendonça, V. de C. Santos-Ebinuma, A. Pessoa, Júnior, R. P. de S. Oliveira, J. F. B. Pereira, From green to blue economy: Marine biorefineries for a sustainable ocean-based economy, *Green Chem*., 2021, **23**, 9377–9400.

2 FAO. 2020. The State of World Fisheries and Aquaculture 2020. Sustainability in action. Rome.

3 F. M. Kerton, Y. Liu, K. W. Omari, K. Hawboldt, Green chemistry and the ocean-based biorefinery, *Green Chem*., 2013, **15**, 860–871.

4 T. Maschmeyer, R. Luque, M. Selva, Upgrading of marine (fish and crustaceans) biowaste for high added-value molecules and bio(nano)-materials, *Chem. Soc. Rev*., 2020, **49**, 4527-4563.

5 AMEC, Management of Wastes from Atlantic Seafood Processing Operations, Report for Environment Canada Atlantic Region, 2003.

6 P. T. Anastas, L. G. Heine, T. C. Williamson, Green Chemical Syntheses and Processes: Introduction, *Green Chemical Syntheses and Processes*, 2000, 1-6.

7 P. T. Anastas, M.M. Kirchhoff, Origins, Current Status, and Future Challenges of Green Chemistry, *Acc. Chem. Res*., 2002, **35**, 686-694.

8 J. B. Manley, P. T. Anastas, B. W. Cue Jr, Frontiers in Green Chemistry: meeting the grand challenges for sustainability in R&D and manufacturing, *J. Clean. Prod.*, 2008, **16**, 743-750.

9 P. S. Barber, J. L. Shamshina, R. D. Rogers, A "green" industrial revolution: Using chitin towards transformative technologies, *Pure Appl. Chem*., 2013, **85**, 1693–1701.

10 Commissione europea, Direzione generale degli Affari marittimi e della pesca, Addamo, A., Calvo Santos, A., Carvalho, N., et al., The EU blue economy report 2021, Publications Office, 2021, https://data.europa.eu/doi/10.2771/5187 (accessed January 27, 2022).

11 Conservation International, "What on Earth is the 'blue economy'?", https://www.conservation.org/blog/what-onearth-is-the-blue-economy, (accessed January 26, 2022).

12 M. M. Gil, E. Pastor, J. Durán, Survival and growth of hatchery-reared Mediterranean spider crab juveniles, Maja squinado, under different rearing conditions, *Aquaculture*, 2019, **49**, 837–43.

13 M. M. Harlıoğlu, A. Farhadi, A. Suat Ateş, A review of the marine crab fisheries in the turkish seas, *Croat. J. Fish*., 2018, **76**, 159-175.

14 FAO(2018b): Fishbase report. Available on http://www.fishbase.org/report/FAO/FAOCatchList.php?c_code=&areacode=&scientific=Maja+squinado&english=&yc=00 (accessed January 27, 2022).

15 W. Fischer, M.-L. Bauchot, M. Schneider (rédacteurs), Fiches FAO d'identification desespèces pour les besoins de la pêche (Révision 1). Méditerranée et mer Noire. Zone de pêche 37. Volume I. Végétaux et Invertébrés. Publication préparée par la FAO, résultat d'un accord entre la FAO et la Commission des Communautés Européennes (Projet GCP/INT/422/EEC) financée conjointement par ces deux organisations. Rome, FAO, 1987, 1, 1-760.

16 R. A. A. Muzzarelli, J. Boudrant, D. Meyer, Nicola Manno, M. DeMarchis, M. G. Paoletti, Current views on fungal chitin/chitosan, human chitinases, food preservation, glucans, pectins and inulin: A tribute to Henri Braconnot, precursor of the carbohydrate polymers science, on the chitin bicentennial, *Carbohydr. Polym*., 2012, **87**, 995– 1012.

17 M. Yadav, P. Goswami, K. Paritosh, M. Kumar, N. Pareek, V. Vivekanand, Seafood waste: a source for preparation of commercially employable chitin/chitosan materials, *Bioresour. Bioprocess.*, 2019, **6**, 8, 1-20.

18 Y.-W. Cho, J. Jang, C. R. Park, S.-W. Ko, Preparation and Solubility in Acid and Water of Partially Deacetylated Chitins, *Biomacromolecules*, 2000, **1**, 609-614.

19 K. Y. Zhu, H. Merzendorfer, W. Zhang, J. Zhang, S. Muthukrishnan, Biosynthesis, Turnover, and Functions of Chitin in Insects, *Annu. Rev. Entomol*., 2016, **61**, 177–196.

20 C.K.S. Pillai, W. Paul, C. P. Sharma, Chitin and chitosan polymers: Chemistry, solubility and fiber formation, *Prog. Polym. Sci.*, 2009, **34**, 641–678.

21 I. Younes, M. Rinaudo, Chitin and chitosan preparation from marine sources. Structure, properties and applications,*Mar. Drugs*, 2015, **13**, 1133–1174.

22 I. Aranaz, M. Mengíbar, R. Harris, I. Paños, B. Miralles, N. Acosta, G. Galed, Á. Heras, Functional Characterization of Chitin and Chitosan, *Curr. Chem. Biol*., 2009, **3**, 203-230.

23 S. Aiba, Studies on chitosan: 4. Lysozymic hydrolysis of partially N-acetylated chitosans, *Int. J. Biol. Macromol*., 1992, **14**, 225-228.

24 G. S. Dhillon, S. Kaur, S. Kaur Brar, M. Verma, Green synthesis approach: extraction of chitosan from fungus mycelia, *Crit. Rev. Biotechnol*., 2013, **33**, 379-403.

25 J. A. Vázquez, I. Rodríguez-Amado, M. I. Montemayor, J. Fraguas, M. del Pilar González, M. A. Murado, Chondroitin Sulfate, Hyaluronic Acid and Chitin/Chitosan Production Using Marine Waste Sources: Characteristics, Applications and Eco-Friendly Processes: A Review, *Mar. Drugs*, 2013, **11**, 747-774.

26 M. Rinaudo, Chitin and chitosan: Properties and applications, *Prog. Polym. Sci*., 2006, **31**, 603–632.

27 H.-M. Cauchie, Chitin production by arthropods in the hydrosphere, *Hydrobiologia*, 2002, **470**, 63–96.

28 K. Kurita, Chitin and Chitosan: Functional Biopolymers from Marine Crustaceans, *Mar. Biotechnol.*, 2008, **8**, 203–226.

29 H. El Knidri, R. Belaabed, A. Addaou, A. Laajeb, A. Lahsini, Extraction, chemical modification and characterization of chitin and chitosan, *Int. J. Biol. Macromol*, 2018, **120**, 1181–1189.

30 K . M . Rudall, W . Kenchington, The chitin system, *Biol. Rev*., 1973, **49**, 597-636.

31 J. Blackwell, K. D. Parker, K. M. Rudall, Chitin in Pogonophore tubes, *J. Mar. Biol. Ass.* U.K., 1965, **45**, 659-661.

32 K. Kurita, Controlled functionalization of the polysaccharide chitin, *Prog. Polym. Sci*., 2001, **26**, 1921-1971.

33 R. Minke, J. Blackwell, The Structure of α-Chitin, *J.Mol. Biol*., 1978, **120**, 167-181.

34 J. C. Roy, F. Salaün, S. Giraud, and A. Ferri, "Solubility of Chitin: Solvents, Solution Behaviors and Their Related Mechanisms", in Solubility of Polysaccharides., Ed: IntechOpen London, United Kingdom, 2017 [Online]. Available: https://www.intechopen.com/chapters/57402 doi: 10.5772/intechopen.71385 (accessed February 21, 2022).

35 Einbu, Thesis for the degree of philosophiae doctor Characterisation of Chitin and a Study of its Acid-Catalysed Hydrolysis, CORE Metadata, citation and similar papers at core.ac.uk, 2007.

36 G.A.F. Roberts, Structure of chitin and chitosan. In Chitin Chemistry; Roberts, G.A.F., Ed.; Palgrave Macmillan: London, UK, 1992; 85–91.

37 P. R. Austin, Chitin solvents and solubility parameters, in “Chitin, chitosan and related enzymes”, Academic Press, Inc. (ISBN 0-12-780950-3), 1984.

38 R.C. Capozza, Solution of poly(N-acetyl-D-glucosamine), US3989535A, 1976, - expired-

39 J. Synowiecki, N. A. Al-Khateeb, Production, Properties, and Some New Applications of Chitin and Its Derivatives, *Crit Rev Food Sci Nutr*., 2003, **43**, 145–171.

40 V. Zargar, M. Asghari, A. Dashti, A Review on Chitin and Chitosan Polymers: Structure, Chemistry, Solubility, Derivatives, and Applications, *ChemBioEng Reviews*, 2015, **2**, 204–226.

41 T. Sannan, K. Kurita, Y. Iwakura, Studies on Chitin. V. Kinetics of Deacetylation Reaction, *Polym. J*., 1977, **9**, 649-651.

42 P. Broussignac, Chitosan: a natural polymer not well known by the industry, *Chim. Ind. Genie Chim.*,1968, **99**, 1241–1247.

43 K. Kurita, K. Tomita, T. Tada, S. Ishii, S.-I. Nishimura, K. Shimoda, Squid Chitin as a Potential Alternative Chitin Source: Deacetylation Behaviour and Characteristic Properties, *J. Polym. Sci.*, 1993, **31**, 485-491.

44 M. Rhazi, J. Desbrières, A. Tolaimate, A. Alagui, P. Vottero, Investigation of different natural sources of chitin: influence of the source and deacetylation process on the physicochemical characteristics of chitosan, *Polym. Int.*, 2000, **49**, 337-344.

45 C.V. Lusena, R.C. Rose, Preparation and Viscosity of Chitosans, *J.Fish. Res. Bd. Can*., 1953, **10**, 521-522.

46 C. Chatelet, O. Damour and A. Domard, Influence of the degree of acetylation on some biological properties of chitosan films, *Biomaterials*, 2001, **22**, 261–268.

47 H. M. Ibrahim, and E. E. Zairy, Chitosan as a Biomaterial — Structure, Properties, and Electrospun Nanofibers, in Concepts, Compounds and the Alternatives of Antibacterials., Ed. IntechOpen. London, United Kingdom, 2015 [Online]. Available: https://www.intechopen.com/chapters/49246 doi: 10.5772/61300 (accessed February 21, 2022).

48 L. R. Berger and R. S. Weiser, The β-glucosaminidase activity of egg-white lysozyme, *Biochim. Biophys. Acta*, 1957, **26**, 517–521.

49 Y. Shigemasa, K. Saito, H. Sashiwa and H. Saimoto, Enzymatic degradation of chitins and partially deacetylated chitins, *Int. J. Biol. Macromol*., 1994, **16**, 43–49.

50 Y. Okamoto, K. Kawakami, K. Miyatake, M. Morimoto, Y. Shigemasa and S. Minami, Analgesic effects of chitin and chitosan, *Carbohydr. Polym*., 2002, **49**, 249–252.

51 S. B. Rao and C. P. Sharma, Use of chitosan as a biomaterial: Studies on its safety and hemostatic potential, *J. Biomed. Mater. Res*., 1997, **34**, 21–28.

52 I.M. Helander, E.-L. Nurmiaho-Lassila, R. Ahvenainen, J. Rhoades, S. Roller, Chitosan disrupts the barrier properties of the outer membrane of Gram-negative bacteria, *Int. J. Food Microbiol*., 2001, **71**, 235–244.

53 X. F. Liu, Y. L. Guan, D. Z. Yang, Z. Li, K. De Yao, Antibacterial Action of Chitosan and Carboxymethylated Chitosan, *J. Appl. Polym. Sci*., 2001, **79**, 1324–1335.

54 C. Pires, A. Marques, M. L. Carvalho, I. Batista, Chemical Characterization of *Cancer Pagurus*, *Maja Squinado*, *Necora Puber* and *Carcinus Maenas* Shells, *Poult. Fish Wildl. Sci*., 2017, **5**, 1, 1-6.

55 J. Li, J.-F. Revol, R. H. Marchessault, Effect of Degree of Deacetylation of Chitin on the Properties of Chitin Crystallites, *J. Appl. Polym. Sci*., 1997, **65**, 373-380.

56 H. Ehrlich, Chitin and collagen as universal and alternative templates in biomineralization, *Int. Geol. Rev.*, 2010, **52**, 661–699.

57 A. Percot, C. Viton, A. Domard, Optimization of Chitin Extraction from Shrimp Shells, *Biomacromolecules*, 2003, **4**, 12-18.

58 E. S. Abdou, K. S.A. Nagy, M. Z. Elsabee, Extraction and characterization of chitin and chitosan from local sources, *Bioresour. Technol*., 2008, **99**, 1359–1367.

59 F.A. Al Sagheer, M.A. Al-Sughayer, S. Muslim, M.Z. Elsabee, Extraction and characterization of

chitin and chitosan from marine sources in Arabian Gulf, *Carbohydr. Polym.*, 2009, **77**, 410–419.

60 E. Khor,Chapter 5 - The Sources and Production of Chitin, E. Khor,Chitin, Ed. Elsevier Science Ltd, 2001, 63-72.

61 A. Wasko, P. Bulak, M. Polak-Berecka, K. Nowak, C. Polakowski, A. Bieganowski, The first report of the physicochemical structure of chitin isolated from *Hermetia illucens*, *Int. J. Biol. Macromol*, 2016, **92**, 316–320.

62 Tolaimate, J. Desbrieres, M. Rhazi, A. Alagui, Contribution to the preparation of chitins and chitosans with controlled physico-chemical properties, *Polymer,* 2003, **44**, 7939–7952.

63 M. H. Mohammed, P. A. Williams, O. Tverezovskaya, Extraction of chitin from prawn shells and conversion to low molecular mass chitosan, *Food Hydrocoll.*, 2013, **31**, 166-171.

64 M. Kaya, I. Sargin, K. O. Tozak, T. Baran, S. Erdogan, G. Sezen, Chitin extraction and characterization from *Daphnia magna* resting eggs, *Int. J. Biol. Macromol*, 2013, **61**, 459– 464.

65 S. Kaur, G. S. Dhillon, Recent trends in biological extraction of chitin from marine shell wastes: a review, *Crit. Rev. Biotechnol*., 2015, **35**, 44–61.

66 A. Khanafari, R. Marandi, Sh. Sanatei, Recovery of chitin and chitosan from shrimp waste by chemical and microbial methods, *Iran. J. Environ. Health. Sci. Eng*., 2008, **5**, 19-24.

67 G. T. Kjartansson, S. Zivanovic, K. Kristbergsson, J. Weiss, Sonication-Assisted Extraction of Chitin from North Atlantic Shrimps (*Pandalus borealis*), *J. Agric. Food Chem.,* 2006, **54**, 5894−5902.

68 J. L. Shamshina, P. S. Barber, G. Gurau, C. S. Griggs, R. D. Rogers, Pulping of Crustacean Waste Using Ionic Liquids: To Extract or Not To Extract, *ACS Sustain. Chem. Eng*., 2016, **4**, 6072–6081.

69 L. D. Tolesa, B. S. Gupta, M.-J. Lee, Chitin and chitosan production from shrimp shells using ammonium-based ionic liquids, *Int. J. Biol. Macromol*, 2019, **130**, 818–826.

70 M. R. Kasaai, Determination of the degree ofN-acetylation for chitin and chitosan by various NMR spectroscopy techniques: A review, *Carbohydr. Polym*., 2010, **79**, 801-810.

71 J.R. Dean, Practical Inductively Coupled Plasma Spectroscopy, Ed. Wiley, New York, 2005.

72 J. Kumirska, M. Czerwicka, Z. Kaczyński, A. Bychowska, K. Brzozowski, J. Thöming, P. Stepnowski, Application of Spectroscopic Methods for Structural Analysis of Chitin and Chitosan, *Mar. Drugs*, 2010, **8**, 1567-1636.

73 A. Einbu, K. M. Vårum, Characterization of Chitin and Its Hydrolysis to GlcNAc and GlcN, *Biomacromolecules*, 2008, **9**, 1870–1875.

74 C. Bosso, J. Defaye, A. Domard, A. Gadelle, The behaviour of chitin towards anhydrous hydrogen fluoride. Preparation of β-(1-4) linked 2-acetamido-2-deoxy-D-glucopyranosyl oligosaccharides, *Carbohydr. Res.,* 1986, **156**, 57-68.

75 M. Vincendon, Regenerated chitin from phosphoric acid solutions, *Carbohydr. Polym.*, 1997, **32**, 233–237.

76 A. Einbu and K. M. Vårum, Depolymerization and De-N-acetylation of Chitin Oligomers in Hydrochloric Acid, *Biomacromolecules*, 2007, **8**, 309–314.

77 Galo Cárdenas, G. Cabrera, E. Taboada, S. P. Miranda, Chitin Characterization by SEM, FTIR, XRD, and 13C Cross Polarization/Mass Angle Spinning NMR, *J. Appl. Polym. Sci.*, 2004, **93**, 1876-1885.

78 M. R. Kasaai, A review of several reported procedures to determine the degree of N-acetylation for chitin and chitosan using infrared spectroscopy, *Carbohydr. Polym.*, 2008, **71**, 497-508.

79 G. L. Clark, A. F. Smith, X-ray diffraction studies of chitin, chitosan and derivatives, *J. Phys. Chem*.,

1936, **40**, 863-879.

80 Y. Zhang, C. Xue, Y.Xue, R. Gaoa, X. Zhang, Determination of the degree of deacetylation of chitin and chitosan by X-ray powder diffraction, *Carbohydr. Res*., 2005, **340**, 1914-1917.

81 B. Focher, Chitosans from *Euphausia superba*. 2: Characterization of solid state structure, *Carbohydr. Polym.*, 1992, **18**, 43-49.

82 A.B. Vishu Kumar, M.C. Varadaraj, R.G. Lalitha, R.N. Tharanathan, Low molecular weight chitosans: preparation with the aid of papain and characterization, *Biochim. Biophys. Acta*, 2004, **1670**, 137-146.

83 M. Ioelovich, Crystallinity and Hydrophility of Chitin and Chitosan, *RRJC*, 2014, **3**, 7-14.

84 A. Nzihou, Handbook on characterization of biomass, biowaste and related by-products, Springer Nature Switzerland AG, 2020.

85 K. Zielinskaa, A. G. Shostenko, S. Truszkowski, Analysis of Chitosan by Gel Permeation Chromatography, *High Energy Chem*., 2014, **48**, 72-75.

86 M. Terbojevich, C. Carraro, A. Cosani, Solution studies of the chitin-lithium chloride-N-N-dimethylacetamide system, *Carbohydr. Res*., 1988, **180**, 73-86.

87 G. Galed, E. Diaz, F. M. Goycoolea, A. Heras, Influence of N-Deacetylation Conditions on Chitosan Production from α-Chitin, *Nat. Prod. Commun*. 2008, **3**, 543-550.